

„Immune Modulation by Zinc-induced Regulatory T Cells“

Von der Fakultät für Mathematik, Informatik und Naturwissenschaften der RWTH-Aachen University zur Erlangung des akademischen Grades einer Doktorin der Naturwissenschaften genehmigte Dissertation

vorgelegt von

Diplom-Biologin

Eva Rosenkranz

aus Düren

Berichter: Universitätsprofessor Dr.rer.nat. Lothar Rink

Universitätsprofessor Dr.rer.nat. Jürgen Bernhagen

Tag der mündlichen Prüfung: 11.04.2013

Diese Dissertation ist auf den Internetseiten der Hochschulbibliothek online verfügbar

List of Contents

I	Introduction.....	1
1.1	The Immune System	1
1.2	Regulatory T Cells	2
1.3	Mechanisms of Treg-Mediated Suppression.....	3
1.4	Foxp3	4
1.5	Epigenetic Regulation of Foxp3 Expression.....	4
1.6	Interaction of Histone-Deacetylase (HDAC) Sirt-1 and Foxp3	5
1.7	The Allergic Immune Response.....	7
1.8	Graft-Versus-Host-Disease (GVHD).....	8
1.8.1	The Mixed Lymphocyte Culture as In Vitro Model for GVHD	9
1.9	Autoimmune Diseases.....	9
1.9.1	Multiple Sclerosis (MS)	10
1.9.2	EAE as Animal Model for MS.....	10
1.10	Zinc and the Human Body	11
1.11	Zinc and the Immune System.....	12
II	Scope of the Study	14
III	Materials and Methods.....	15
3.1	Materials	15
3.1.1	Equipment	15
3.1.2	Laboratory Supplies	16
3.1.3	Cell Culture Media and Additives.....	16
3.1.4	Immunological Reagents.....	17
3.1.5	Miscellaneous Reagents	17
3.1.6	Commercially Available Kits.....	19
3.2	Methods.....	20
3.2.1	Preparation of Zinc Solutions	20
3.2.2	Cell Cultures	20
3.2.3	Peripheral Blood Mononuclear Cell (PBMC) Isolation.....	21
3.2.4	Lysis of Erythrocytes	21
3.2.5	Generation and Stimulation of Two-Way Mixed Lymphocyte Cultures (MLC).....	22
3.2.6	Human Zinc-Supplementation Study.....	23
3.2.7	Allergy Assay.....	23
3.2.8	V β -Assay	24
3.2.9	Murine Splenocyte Isolation	24
3.2.10	Generation and Stimulation of Murine MLCs	25
3.2.11	Animal Treatment and Induction of EAE	26
3.2.12	Clinical Evaluation of EAE.....	27
3.2.13	Tissue Sample Harvesting.....	27
3.2.14	Transcardial Perfusion of Mice.....	27
3.2.15	Paraffin-Embedding of Mice Tissue Samples.....	28
3.2.16	Immunohistochemistry (IHC)	29
3.2.17	Enzymed-Linked Immunosorbent Assay (ELISA)	30
3.2.18	Fluorescence-Activated Cell Sorting (FACS).....	31
3.2.19	Calculating the Protein Concentration	33
3.2.20	Generation of Cell Lysates.....	34
3.2.21	Immunoprecipitation.....	34
3.2.22	Sodium Dodecyl Sulfate Discontinuous Polyacrylamid Gelelectrophoresis (SDS- PAGE)	36
3.2.23	Western Blot	37
3.2.24	Membrane Reprobing	38
3.2.25	RNA Isolation from PBMC	39
3.2.26	DNA Isolation of PBMCs.....	40

3.2.27	Spectrophotometric Determination of RNA or DNA Concentration.....	40
3.2.28	Reverse Transcription	41
3.2.29	Methyl Screen Assay	41
3.2.30	Quantitative Real time Polymerase Chain Reaction (Q-PCR).....	42
3.2.31	[³ H] Thymidine Proliferation Assay	45
3.2.32	Sirtuin 1 (Sirt-1) Assay	46
3.2.33	Detection of Labile Zinc	46
3.2.34	Statistical Significance and Program Analysis	48
IV	Results.....	49
4.1	Zinc Attenuates the Allogeneic Immune Reaction	49
4.1.1	Modulated Cytokine Production by Zinc	49
4.1.2	Attenuated Proliferation in Zinc-Supplemented MLCs	51
4.2	Zinc-Induced Treg Upregulation in the MLC.....	52
4.2.1	Zinc Upregulates Expression of the Treg-Associated Molecules Foxp3 and CTLA-4	52
4.2.2	Zinc-Induced Upregulation of Tregs Occurs in Allogene-Activated Blast.....	53
4.2.3	Zinc Upregulates the Expression of Foxp3-Associated Molecules CD25 and CTLA-4	54
4.2.4	Zinc Upregulates Expression of Activation-Marker CD69 in T Cells.....	59
4.2.5	Zinc Enhances PPAR- γ mRNA Expression.....	60
4.3	Investigation of Molecular Zinc-targets in Tregs.....	62
4.3.1	Analysis of Foxp3 Promoter Methylation Pattern	62
4.3.2	Zinc-Associated Inhibition of the HDAC Sirt-1	63
4.3.3	Sirt-1 Inhibition Enhances Foxp3-Acetylation	65
4.3.4	Sirt-1 Inhibitor Ex-527 Mirrors Zinc Effects in MLCs.....	66
4.4	<i>In Vivo</i> Zinc-Supplementation Upregulates Tregs in <i>In Vitro</i> Generated MLCs.....	68
4.5	Zinc-Induced Tregs Attenuate the Allergen-Induced Immune Response	70
4.6	Zinc Ameliorates Murine EAE Disease Course.....	76
4.6.1	Zinc Upregulates Tregs in Murine MLCs	76
4.6.2	Zinc-Supplementation Affects Treg-Levels <i>In Vivo</i>	77
4.6.3	Zinc-Induced Tregs Attenuate EAE Disease	79
V	Discussion.....	86
VI	Conclusion	98
VII	References.....	99
VIII	List of Abbreviations	111
	Danksagung.....	113
	CURRICULUM VITAE.....	114
	Publications.....	115
	Zusammenfassung (deutsch).....	116

I. Introduction

1.1 The Immune System

The immune system evolved to protect the body against potentially harmful substances. Antigen-recognition and subsequent immune responses towards pathogens are the main functions of the immune system, which comprises various tissues, cells, and proteins. The immune system can be roughly subdivided into the innate and the adaptive immune system. The innate immune system provides the first line of defense and consists of cellular components (monocytes/macrophages, granulocytes, dendritic cells, mast cells and natural killer cells) as well as countless soluble proteins (complement proteins, acute phase proteins, cytokines, and chemokines). Cells of the innate immune system perform non-specific immune responses based on the recognition of pathogen-associated molecular patterns (PAMPs) via pattern-recognition receptors (PRR). Thus triggered immune responses are fast while lacking immunological memory. Moreover, they build the most important host defense, found in most organisms (Litman et al. 2005). Since cells and soluble components of the innate immune system activate and participate in adaptive immune responses, they form an intricate association between the innate and the adaptive immune systems.

The adaptive immune system comprises the two main lymphocyte subsets, B and T cells, which in contrast to innate immune cells, express specific receptors directed against certain target structures, and establish immunological memory. The diversity of these antigen-specific receptors originates in their development that include random recombination of variable receptor gene segments and pairing of different variable chains (Janeway 2008). This diversity, as consequence of more rapid and specific recognition and elimination of upcoming antigens, warrants efficient immune responses and long-lasting protection. Upon specific antigen-recognition, clonal expansion of a small subset of selectively activated lymphocytes initiates the subsequent adaptive immune response. Activated B cells differentiate into Ig-secreting plasma cells, contributing to the humoral immunity. Activated T cells affect other cells, either by regulating the activity of immune cells or by killing transformed or infected cells. Based on their co-receptor expression, mature T cells can be divided into different subgroups: CD8⁺ cytotoxic T lymphocytes (CTLs) mediate cell-death of virus-infected and tumor cells via direct cell-cell interaction. CD4⁺ T helper cells (Th) modulate the activation of further immune cells. Naïve Th cells can differentiate into at least four effector subtypes: Th1, Th2, Th17, and regulatory T cells (Tregs). Th1 cell-secreted cytokines, such as interferon (IFN)- γ and interleukin (IL)-2 are mainly involved in the activation of macrophages and CTLs (cell-mediated responses). Th2 cytokines, in contrast, including IL-4 and IL-5, are generally known to promote antibody production by stimulating B cell (humoral) responses. Th17 cells produce several pro-inflammatory cytokines, particularly IL-17A. Tregs,

conversely, suppress immune reactions via cytokine production and cell-cell contact-dependent suppression mechanisms, thus, maintaining tolerance. Dysregulation of immune functions causes inadequate, excessive, or absent immune responses, leading to immune disorders. Disturbed immune responses provoke manifestation of allergic diseases, hypersensitivity, autoimmune diseases, graft-versus-host disease (GVHD), and immunodeficiency (Parkin and Cohen 2001). Consequently, several control mechanisms have evolved to control immune homeostasis.

1.2 Regulatory T Cells

One major problem concerning the body's immune defense involves the discrimination between "self" and "non-self" or foreign antigens. Mechanisms have evolved that allow for effective immune responses against microbial antigens, while preventing autoimmune responses. Strategies for immunological self-tolerance include physical elimination of autoreactive immune cells (known as "clonal deletion") or their functional inactivation (known as "anergy") (Ramsdell and Fowlkes 1990). In addition, a subpopulation of T cells emerged with the capacity to suppress CD4⁺ effector T cells, CD8⁺ T cells, antigen presenting cells (APCs), natural killer cells (NKs) and B cells. Based on their function they were named regulatory T cells (Tregs). In 1995, Sakaguchi and colleagues were the first to observe the existence of Tregs by illustrating that the transfer of purified CD4⁺CD25⁺ cells inhibited naïve CD4 T cell-mediated autoimmunity in lymphopenic mice (Sakaguchi et al. 1995). The significance of Tregs for proper immune function becomes evident when Tregs are dysfunctional and/or deficient as this is associated with high incidences of autoimmune diseases, inflammatory bowel disease (IBD), allergies and alleviated GVHD (Robinson 2004; DeJaco et al. 2006; Pilat et al. 2010).

In both, humans and mice, CD4⁺ Tregs are defined by their expression of Treg marker molecules, including CD25 (the IL-2 receptor α -chain), the transcription factor Foxp3 (forkhead box p3), CTLA-4 (Cytotoxic T-Lymphocyte Antigen 4, also known as CD152), and GITR (glucocorticoid-induced TNFR-related protein). Furthermore, Tregs are characterized by their scarce production of the cytokines IL-2, IFN- γ , IL-4 and IL-17, as well as their hypoproliferative condition upon T cell receptor (TCR)-activation (Sakaguchi 2005). Two main groups of Tregs can be distinguished; naturally occurring CD4⁺CD25^{hi}Foxp3⁺ Tregs (nTregs) arise intrathymically from CD4 single positive precursor cells and account for approximately 10% of all peripheral CD4⁺ T cells (Baecher-Allan et al. 2002). Induced Tregs (iTregs) on the other hand derive extrathymically from CD4⁺CD25⁻ naïve T cells following antigen exposure and TCR activation in adequate environments. Induction of the transcription factor Foxp3 provides a crucial step in the progression of iTreg conversion. An interaction between both, nTregs and iTregs, is crucial to the mediation of dominant tolerance toward "self", and for controlling ongoing immune reactions, as their distinct origins reveal divergent Tregs functions (Haribhai et al. 2011). Due to their

intrathymically development, nTregs express specific $\alpha\beta$ TCR against self-antigens, whereas iTregs are specific for self- and foreign antigens encountered in the periphery.

The differentiation of peripheral iTregs depends on successful antigen presentation via APCs in the presence of IL-2 and transforming growth factor (TGF) $-\beta$, which was demonstrated in various *in vivo* scenarios (Zheng et al. 2007). While TGF- β is crucial for Treg induction, IL-2 is indispensable for Treg survival and expansion. Furthermore, TCR signals and Foxp3 need to synergize in order to generate functional Tregs (Marson et al. 2007). Suboptimal antigen stimulation (e.g. constant ingestion of proteins in the gut) results in iTreg induction, leading to oral tolerance. Furthermore, preceding inflammatory diseases induce the generation of iTregs, which in turn hamper exacerbated immune responses to prevent fatal acute inflammation (Curotto de Lafaille et al. 2008). Preceding inflammatory diseases include autoimmune diseases such as multiple sclerosis and allergic diseases such as allergic rhinitis. In addition, induction of iTregs was also observed following allogeneic transplantations, and enhanced amounts of iTregs may ameliorate transplantation outcomes by preventing allograft rejection (see mixed lymphocyte culture (MLC)) (Neto et al. 2000). In these scenarios, activated effector T cells (Teffs) are generated concomitantly with iTregs and the balance between Teffs and Tregs determines the clinical outcome. Therefore, generation and increase of iTregs is a promising step in the ablation of various adverse immune responses.

1.3 Mechanisms of Treg-Mediated Suppression

Overall, two types of suppression can be defined: Treg-dependent deprivation of Teff activation signals, and direct Treg-mediated inactivation and killing of Teffs and APCs. Incorporated in the first group is a CTLA-4-dependent suppression mechanism, revealed by the development of fatal lymphoproliferation and autoimmune diseases in Treg-specific CTLA-4-deficient mice (Waterhouse et al. 1995). The co-inhibitory molecule CTLA-4 is constitutively expressed by Tregs, contrary to its activation-induced upregulation by Teffs. CTLA-4 presents higher affinity towards CD80/86 than its co-stimulatory homologue CD28. Thus, CD28 signaling, which is indispensable for T cell activation, is inhibited by CTLA-4 expression. This is because Treg-CTLA-4 prevents Teff-CD28-mediated co-stimulation by outcompeting CD28 for CD80/86 in the immunological synapse. The deprivation of CD28 signaling is further supported by down-regulation of CD80/86 on APCs in a CTLA-4-dependent manner (Qureshi et al. 2011). Additionally, CTLA-4 interaction with DCs induces expression of the tryptophan catabolizing enzyme indoleamine 2,3-dioxygenase (IDO) which contributes to T cell suppression (Mellor et al. 2004).

Moreover, an IL-2-dependent mechanism of suppression was discovered that depends on both, the unique Treg-associated features including IL-2 hypoproduction and the constitutive

expression of the IL-2 high affinity receptor. These conditions result in strong exogenous IL-2-dependence for Treg cell survival, as demonstrated by reduced Treg numbers and lymphoproliferative/autoimmune diseases in IL-2- or IL-2 receptor-deficient animals (Nelson 2004). Increased IL-2 high-affinity receptor expression on Tregs results in local IL-2 absorption. In turn, antigen-reactive Teffs are inhibited or eliminated by undergoing apoptosis. Activation and expansion of Tregs and Teffs can be modulated by IL-2 supplementation, because the survival of Tregs firmly relies on IL-2, whereas concomitantly Tregs abrogate IL-2 production in Teffs. Additionally, Treg-mediated suppression is achieved by cytokine production (e.g. IL-10 and TGF- β) and the expression of cytotoxic and immunomodulatory molecules.

As “master control gene” responsible for these suppressive functions *foxp* was validated (Fontenot et al. 2003).

1.4 Foxp3

The transcription factor Foxp3 belongs to the forkhead/winged-helix family of transcriptional regulators. Foxp3 is considered as the Treg key transcription factor relevant for Treg function, stability, and differentiation. Foxp3 regulates the expression of various genes through the formation of oligomeric complexes with other proteins. Among the regulated genes are the Foxp3-repressed genes *il-2*, *il-17* and the Foxp3-activated genes *ctla-4*, *cd25*, as well as *foxp3* itself (Hu et al. 2007). Its importance is best illustrated in Foxp3- deficient mice (scurfy mice) and humans suffering from IPEX (immune dysregulation, polyendocrinopathy, enteropathy, X-linked syndrome) with mutations or deletions in the *foxp3* gene (Bennett et al. 2001). Consequently missing Treg formation results in fatal autoimmune diseases, inflammatory bowel disease, severe allergies, and infections. In addition, the relevance of Foxp3 for Treg function is also demonstrated by Foxp3 transfection studies, which demonstrate induction of Treg phenotypes in conventional T cells, including the upregulation of Treg-associated molecules like CD25, CTLA-4 and GITR (Hori et al. 2003). Additionally, the adoptive transfer of polyclonal wild-type T cells transduced with an inducible form of Foxp3 was shown to suppress immune responses (Andersen et al. 2008). Correspondingly, mixed bone-marrow chimeras consisting of both wild-type and Foxp3^{-/-} cells demonstrated that Foxp3^{-/-} cells are incapable of generating suppressive CD4⁺CD25⁺ T cells (Fontenot et al. 2003). Therefore, Foxp3 establishes Tregs as a functionally distinct T cell lineage.

1.5 Epigenetic Regulation of Foxp3 Expression

The *Foxp3* locus is located on the p-arm of the X chromosome and comprises a conserved promoter sequence upstream of the transcription start site. This promoter sequence includes

common eukaryotic promoter features, such as GC, TATA and CAAT boxes, known to bind the transcription-factors AP1, NF-AT, Sp1 and Sp3 (Mantel et al. 2006).

Foxp3 expression levels are regulated by transcriptional and post-transcriptional mechanisms. Epigenetic modifications play a key role in the control of Foxp3 expression. Epigenetics is defined by heritable changes in phenotype or gene expression without altering the DNA sequence of the genome (Slatkin 2009). These gene modifications involve methylation of DNA-included CpG dinucleotides, or covalent posttranslational modification of histones, since specific amino acids of histone N-tails form targets for enzyme-mediated modifications. Several epigenetic markers, such as histone acetylation and cytosine residue methylation in CpG islands, were described for the *Foxp3* locus, which contains three conserved intrinsic non-coding sequences (CNS) with discrete function in Treg differentiation and maintenance. These *cis*-regulatory elements, CNS1 and CNS2, are located upstream of exon 1, whereas CNS3 resides in intron 1 (Zheng et al. 2010). CNS1 contributes to peripheral Foxp3 induction. CNS3 is considered to play an essential role in *de novo* induction of Foxp3 expression in the thymus and in the periphery making it indispensable for nTreg and iTreg generation. CNS2, also referred to as Treg-specific demethylated region (TSDR), contains a CpG island. In nTregs this TSDR is demethylated resulting in stable Foxp3 expression. In contrast, this site shows residual methylation in iTregs, concomitantly with instable Foxp3 expression. Hence, CNS2, which recruits the Foxp3-Runx/CBF β complex in a CpG demethylation-dependent manner, controls Treg lineage commitment by controlling the heritable maintenance of Foxp3 expression (Zheng et al. 2010). In addition to CNS2, another TSDR resides in the first intron of *Foxp3*. This TSDR is fully demethylated in nTregs, but is methylated in naïve CD4⁺ T cells (Polansky et al. 2008). Moreover, the methylation pattern influences the commitment to Treg lineage; as iTregs with transient Foxp3 expression, induced by TCR activation, can be converted into nTregs by demethylating agents, which induce high stable Foxp3 expression required for the induction of a functional Treg suppressor phenotype.

1.6 Interaction of Histone-Deacetylase (HDAC) Sirt-1 and Foxp3

Enzymes of the group HDACs catalyze deacetylation from ϵ -amino-acetylated lysine residues of histones and non-histone proteins. Four classes of HDACs are distinguished. Classes I, II and IV are zinc-dependent enzymes, whereas class III members, named Sirtuins (silent mating type information regulation 2 homolog) require NAD⁺ (nicotinamide adenine dinucleotide) as a cofactor. In mammals, seven closely related Sirtuin enzymes (Sirt-1 – Sirt-7) were described, all sharing a characteristic ~30 kDa core deacetylase domain. During Sirtuin-mediated deacetylation, the hydrolysis of every molecule of NAD⁺ produces one molecule of nicotinamide, the

deacetylated substrate, and one molecule of 2'3'-O-acetyl-ADP-ribose (O-AADPr) (Landry et al. 2000).

Among the Sirtuins, Sirt-1 is the most extensively studied enzyme, revealing important roles in many aspects of physiological processes ranging from aging, to metabolism, to neurological development (Kong et al. 2009). Sirt-1 possesses two nuclear localization signals at the N-terminus supporting its presence in the nucleus and a coiled-coil domain C-terminus of the core domain (Frye 1999). Endogenous substrates for Sirt-1 are plentiful and include p53, p65, c-Jun, and c-Myc.

Notably, Sirt1 is also expressed in T cells following TCR-mediated signaling (Beier et al. 2011). Interaction of Sirt-1 with various transcription factors involved in the production of inflammatory cytokines and leucocyte activation was demonstrated and suggests a modulating role of Sirt-1 in innate and adaptive immune responses. By repressing the proinflammatory activity of NF κ B and AP-1, Sirt1 functions as a negative regulator of CD4⁺ T cells (Zhang et al. 2009). Conversely, CD4-specific deletion of Sirt-1 was demonstrated to reduce cardiac allograft rejection, which was likewise achieved by treatment with Sirt-1 inhibitors (Beier et al. 2011). The mechanism enabling prolonged allograft survival was verified to include increased Treg function, as Sirt-1 targeting in Tregs promotes Foxp3 expression. Alongside, van Loosdregt et al. proved Foxp3 as Sirt-1 substrate because cotransfection of Foxp3 and Sirt-1 into HEK 293 cancer cells resulted in Foxp3 deacetylation (van Loosdregt et al. 2010).

Whereas deacetylated Foxp3 proteins possess a short life-time, Foxp3-acetylation prevents its own proteasomal degradation, thus inducing increased Foxp3 levels. Accordingly, inhibition of Sirt-1-activity enhances Foxp3 levels in murine and human primary T cells, revealing an increased amount of Tregs with improved suppressive capacity. As molecular mechanism, an acetylation/ubiquitinylation switch in Foxp3 was proposed, where lysine acetylation and polyubiquitination are mutually exclusive (see Fig. 1) (van Loosdregt et al. 2011). Acetylation out-competes polyubiquitination hence prevents protein degradation. Recently, three Foxp3 acetylation sites were identified which regulate suppressive capacity of Tregs. In mice these include K31, K262, and K267. The corresponding sites in human Foxp3 are K31, K263, and K268 (Kwon et al. 2012). Foxp3 acetylation is mainly regulated by the histone acetyl transferase (HAT) p300 (van Loosdregt et al. 2010).

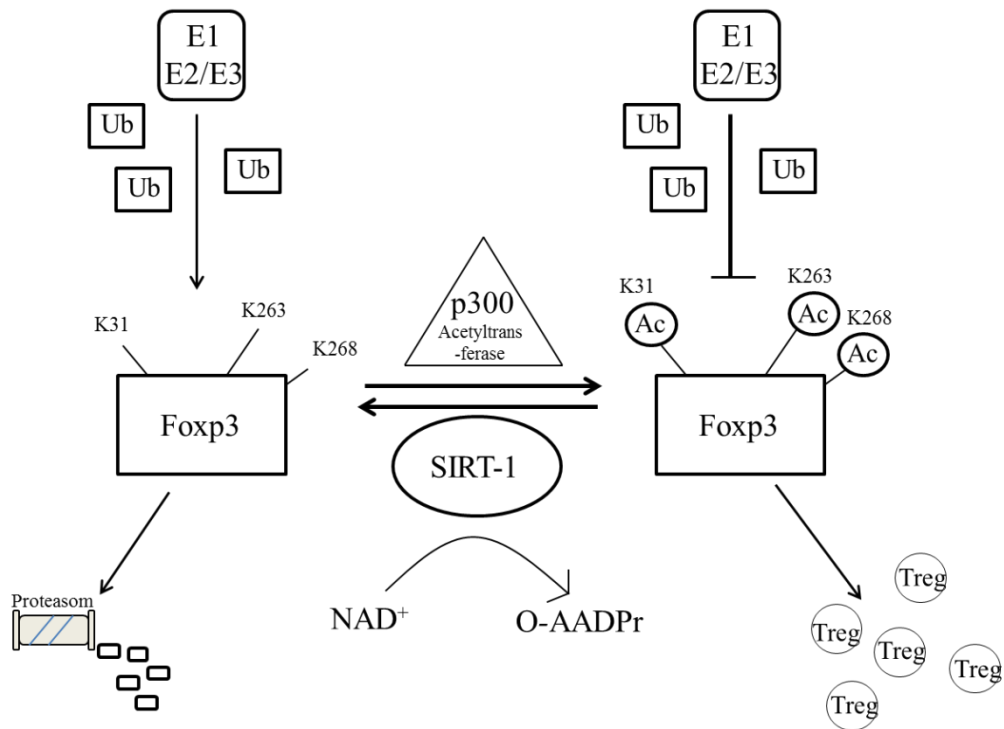


Fig. 1 Influence of Sirt-1 on Foxp3-stabilization. Foxp3 protein is acetylated by the acetyltransferase p300 and deacetylated by the HDAC Sirt-1. Deacetylated lysine residues are vacant to be ubiquitinated by the E1, E2/E3 complex leading to proteasomal degradation of Foxp3 protein. Inhibition of Sirt-1 therefore results in decreased Foxp3 degradation and increased amounts of Tregs. In human, the Foxp3 lysine acetylation sites K31, K263, and K268 were discovered. Foxp3-deacetylation by Sirt-1 consumes NAD^+ and produces 2'3'-O-acetyl-ADP-ribose (O-AADPr) (Landry et al. 2000; van Loosdregt et al. 2010; Beier et al. 2011; Kwon et al. 2012).

1.7 The Allergic Immune Response

Allergies occur as a consequence of hypersensitive immune reactions towards harmless environmental antigens and precede under the control of IL-4 and IL-5 producing Th2 cells. Th2 cytokines and co-stimulatory signals stimulate B cells to produce IgE antibodies, which bind to high affinity FcεRI receptors on the surface of mast cells, basophils, and activated basophils. Antigen cross-linking of FcεRI-bound IgE activates the release of inflammatory mediators. Once IgE is produced in response to allergen exposure, reexposure to the same allergen triggers an allergic response.

Two classes of mediators released by activated mast cells are distinguished. The first class comprises pre-formed mediators such as histamine, which are stored in granules and secreted rapidly after mast cell activation. The second class of mediators includes cytokines and chemokines, which become newly synthesized upon mast cell activation and are therefore secreted with a delay. The immediate allergic reaction caused by mast cell degranulation is followed by the late-phase response, which involves the recruitment of other effector cells, including eosinophils, basophils, and Th2 cells. Since mast cell activation occurs at the site of

allergen exposure the immunopathology of allergic IgE-mediated reactions depends on the allergens route of entry.

Seasonal allergic rhinoconjunctivitis, also commonly known as hay fever, is induced by the inhalation of pollen and is associated with intense nasal itching, sneezing, and rhinorrhea (excess nasal secretion) (Zuberbier et al. 2010). In addition, the airborne pollen induce allergic conjunctivitis in the majority of hay fever patients (Katelaris and Bielory 2008). Hay fever is the most common allergic disease affecting approximately 400 million people worldwide (Pawankar et al. 2011) and is generally caused by environmental antigens with seasonal prevalence. These allergens comprise specific weed, tree, and grass pollen, e.g. timothy grass (*Phleum pratense*)-derived pollen. Grass pollen exposure is one of the major causes of allergic rhinitis in many parts of the world (D'Amato et al. 2007; Burbach et al. 2009).

T lymphocytes are among the principal factors that regulate and co-ordinate immune responses in allergic diseases. Studies reported decreased expression of Foxp3 in asthma and allergic rhinitis (Provoost et al. 2009). Clinical improvement after allergen immunotherapy in allergic diseases such as rhinitis and asthma is associated with the induction of IL-10 and TGF- β producing Tr-1 cells, a Treg subpopulation, as well as Foxp3 (Nouri-Aria 2009).

1.8 Graft-Versus-Host-Disease (GVHD)

Following allogeneic hematopoietic cell transplantation (HCT) about 35-50% of patients develop acute graft-versus-host disease (GVHD) (Jacobsohn and Vogelsang 2007). This systemic inflammatory disorder represents a significant threat of morbidity and mortality and is based on the presence of graft-derived immunocompetent cells, which are not eliminated by the immunocompromised recipient. These alloreactive donor-derived T cells consider recipient-derived tissue as foreign, due to disparities within alloantigens, namely minor histocompatibility molecules, and major histocompatibility molecules (MHC). In humans, MHC antigens are encoded in the human leucocyte antigen (HLA) loci, reaching nearly 1600 alleles due to polymorphism and polygenesis (Tinckam and Chandraker 2006). Therefore, the likelihood for MHC mismatches between unrelated individuals is immense. In addition, the non-MHC proteins mHAGs, first described by Barth and colleagues in 1956, are polymorphic expressed molecules (Barth et al. 1956). In fact, every polymorphic protein can function as mHAG and induce GVHD, even in the presence of identical MHC molecules. Until today the role of mHAGs is not entirely elucidate.

Alloantigen recognition by donor-derived lymphocytes induces excessive immune activation resulting in tissue damage, including skin, gastrointestinal tract and liver destruction. The occurrence of acute GVHD was historically limited to 100 days following HCT (Pidala 2011).

Moreover, chronic GVHD arises in up to 60%-80% of patients, who survived the first 100 days. related clinical observations suggest that alloreactive T cells play a substantial role in the pathobiology of chronic GVHD (Group. 2005).

1.8.1 The Mixed Lymphocyte Culture as *In Vitro* Model for GVHD

As early as 1964, independent studies from Bain et al. and Bach and Hirschhorn reported development of blastoid cells in a multiple-day mixed culture of PBMC (peripheral blood mononuclear cells) from unrelated donors (Bach and Hirschhorn 1964; Bain et al. 1964). Likewise, a mixed culture of PBMC derived from monozygotic twins showed no blastoid cells. Nowadays, mixed lymphocyte cultures (MLC) comprising PBMC from a potential donor, mixed with irradiated lymphocytes from the potential recipient, are primarily generated to detect the presence of alloreactive T cells by measuring proliferation of activated donor cells. The described procedure is named one-way MLC and provides insight into which potential donor shows the least alloreactivity towards the recipient.

Concomitantly, in a two-way MLC untreated PBMC of two persons are mixed. In this MLC lymphocyte proliferation and cytokine production cannot be assigned to the respective individuals. However, this is of no importance when MLC generation serves as *in vitro* research model for GVHD (Maclaurin 1965; Segall and Bach 1976). Alongside, the Th1 cytokine IFN- γ production was identified as a sensitive lymphocyte activation parameter, revealing IFN- γ as a marker for direct T cell activation (Danzer et al. 1996). Faber et al. used IFN- γ detection in two-way MLCs to investigate the specificity of MHC mismatches. Interestingly, permissive mismatches did not induce an allogeneic immune response in the MLC (Faber 2004).

Notably, Treg number and chronic GVHD are inversely associated (Miura et al. 2004), supporting the assumption that Treg therapy may be beneficial to patients with GVHD. Two broad strategies for Treg therapy are applied in humans: firstly, induction of Tregs from naïve precursors *in vivo* using targeted delivery of alloantigen under appropriate tolerizing conditions (Dhodapkar et al. 2001). The second approach is the infusion of *ex vivo* expanded autologous Tregs derived from peripheral blood (Hoffmann et al. 2004). Preclinical models show that the adoptive transfer of Tregs ameliorated GVHD, but the clinical approach has been challenging (Cohen et al. 2002).

1.9 Autoimmune Diseases

The loss of self-tolerance and expansion of auto-reactive lymphocytes results in autoimmune disorders, in which the body's tissues are attacked by its own immune system. Until now, research on autoimmune diseases has not completely unraveled the mechanism underlying

autoimmune responses. One important aspect is the genetic predisposition of certain individuals to develop autoimmune diseases (Thorsby and Lie 2005). The combination with other risk factors including drugs or microorganisms, triggers the immune system to be directed against itself.

Autoimmune diseases affect various body tissues. Prevalent autoimmune diseases include *systemic* lupus erythematosus (SLE), Diabetes mellitus type 1 (IDDM) (*endocrinological*), Crohn's Disease (*gastrointestinal*), and multiple sclerosis (MS) (*neurological*).

1.9.1 Multiple Sclerosis (MS)

MS is an inflammatory autoimmune disorder affecting the central nervous system (CNS). This disease results from myelin-reactive T lymphocytes and their mediators, which initiate inflammation, demyelination of axons, and neurodegeneration, leading to sensory deficits, cerebellar or brainstem dysfunction, and cognitive impairment. Active MS lesions reveal pronounced inflammatory infiltrate, composed mainly of lymphocytes, macrophages, and activated microglia. Autoantigen-specific T cells belong to the key players in the induction of CNS-concentrated autoimmunity. CD8⁺ T lymphocytes predominate in MS lesions and are supposed to directly attack neurons (Babbe et al. 2000). In addition, a role of CD4⁺ T helper cells is well recognized in the pathogenic T cell response, including prominent roles for IFN- γ -producing Th1 cells and IL-17 producing Th17 cells (Chu et al. 2000; Hofstetter et al. 2009). In accordance with these findings, Tregs of patients with MS exhibit impaired function and reduced Foxp3 expression, implying Tregs as a promising therapeutic target (Venken et al. 2008). Around 120,000 - 140,000 patients are diagnosed with MS worldwide, making it the most common chronic-inflammatory disease of the CNS (Friedrich 2008; Sellner et al. 2011). In order to gain a better understanding of MS, various animal models have been established. In particular the model of experimental autoimmune encephalomyelitis (EAE) has become widely accepted as an MS animal model.

1.9.2 EAE as Animal Model for MS

The experimental autoimmune encephalomyelitis is induced by injecting animals with various CNS-derived protein-antigens such as myelin-antigens. The administered proteins are emulsified in an adjuvant to generate an enhanced immune response. In addition, the animals are injected with pertussis toxin, which allows the crossing of the blood-brain barrier. That way, the animal's immune system becomes sensitized towards its own myelin tissue, resulting in spontaneous CNS inflammation closely resembling MS in man. Symptoms involve sensory loss, muscle weakness, ataxia, and spasms. Comparable to MS, Th1 and Th17 T cells were established as the key immunopathogenetic mediators in EAE. The immense production of IL-17A promotes inflammatory cell infiltration, the formation of extensive spinal cord lesions, and clinical

dysfunction (Aranami and Yamamura 2008). Counteracting Tregs were found to ameliorate EAE progression (McGeachy et al. 2005).

Two types of EAE were identified, which can be specifically induced by certain auto-antigens: chronic EAE and relapsing-remitting EAE. Whereas chronic EAE shows progressive pathogenic lesions in the CNS and increasing paralysis of the nervous system, the symptoms of relapsing-remitting EAE animals display a disease peak about 2 weeks after EAE induction followed by a relapse-remitting course (Zhang et al. 2004). It has to be taken into account that although the EAE model is useful for studying specific aspects of MS pathology and pathogenesis, it does not mirror the complex pathology of human MS.

1.10 Zinc and the Human Body

Zinc is an essential trace element with various functions in all cell and organ systems (Prasad 2009). The human body contains a total amount of 2-3g zinc (Haase and Rink 2010) and its distribution differs considerably between the various tissues, spanning from 10 µg/g dry weight in the brain (1.5% of the total body zinc) up to 100 µg/g in the bone (29% of the total body zinc). In contrast, plasma zinc concentrations merely reaches 10-18 µM, equaling to around 1 µg/g (0.1 % of the total body zinc) (Mills 1989). Plasma zinc is abundantly bound to albumin (60%) with low affinity; to α₂-macroglobulin (30%), and with high affinity to transferrin (10%) (Rink and Gabriel 2000). Cellular zinc is distributed between nucleus (30-40%), cytoplasm, organelles, and vesicles (50%) (Vallee and Falchuk 1993), including zinc-specific vesicles called “zincosomes” (Beyersmann and Haase 2001). The remaining zinc is associated with the cell membrane. Like serum zinc, the vast majority of cellular zinc is bound to proteins leaving only a minor loosely-bound or unbound part of intracellular zinc, which is referred to as “free zinc” and contributes to the regulation of cellular processes. The intracellular protein methallothionein (MT) contains over 20 cysteine residues, representing nearly 30% of its amino acid residues (Sutherland and Stillman 2011) and binds 5-20% of cellular zinc (Andrews 2001). Thus, MT protects against metal-toxicity and oxidative stress. Its expression is regulated in a zinc-dependent way by the transcription-factor MTF-1 (metal-response element-binding transcription-factor). In addition, MTF-1 induces expression of further regulatory genes involved in the complex control of zinc homeostasis (Andrews 2001). Zinc uptake into cells and its intracellular homeostasis are regulated by members of the zinc transporter family, including 14 Zip proteins (Zrt- and Irt-like protein, SLC39), responsible for zinc transport into the cytosol, and 10 zinc transporter (ZnT, solute linked carrier, SLC30) family proteins that export zinc from the cytosol (Lichten and Cousins 2009).

The importance of zinc is apparent in its function as a cofactor in more than 300 enzymes and an even higher amount of proteins attaching zinc (Vallee and Falchuk 1993). Based on a search for

known zinc-binding sequences, it was estimated that up to 10% of the proteins encoded in the human genome may contain zinc (Andreini et al. 2006). Based on this estimate, zinc influences the regulation of virtually all cellular processes, including signal transduction (Haase et al. 2008), transcription (Vallee and Falchuk 1993), DNA replication (Wu and Wu 1987), enzymatic catalysis (Auld 2001), redox regulation (Maret 2006), cell proliferation (MacDonald 2000), cell differentiation (Chesters and Petrie 1999) and apoptosis (Sunderman, 1995; Truong-Tran et al., 2001b).

The recommended daily allowance (RDA) suggested by the World Health Organization (WHO) recommends a supply of 11 mg for men and 8 mg for women. Since the body has only limited zinc storage capacity, frequent zinc intake is necessary to replenish the total body zinc. Dietary zinc refills about 0.1 % of the total body zinc-content in humans (Maret and Sandstead 2006). This is accomplished by two well-balanced systems: the absorption from the intestine on the one hand, and the endogenous loss via pancreatic and other intestinal secretion systems on the other hand (Liuzzi et al. 2004).

Zinc deficiency poses an immense risk factor for human health and accounts for one of the life-threatening factors especially in developing countries (World Health Organization. The World Health Report, 2002). Zinc deficiency manifests itself on different levels and can be subdivided into either severe zinc deficiency or into marginal zinc deficiency. Severe zinc deficiency is provoked by the zinc uptake-affecting metabolic disorder *Acrodermatitis enteropathica* as well as by other causes such as total parenteral nutrition without zinc, excessive use of alcohol, or following penicillamine therapy (Prasad 2008). Marginal zinc deficiency may be caused by nutritional zinc deficiency due to high consumption levels of zinc-chelating phosphates, lignins, and phytates which counteract zinc absorption; by the malabsorption syndrome, or by sickle cell anemia (Lonnerdal 2000; Prasad 2002). It also occurs frequently in the elderly, during pregnancy and lactation, due to rapid growth, in vegetarians, or persons with renal insufficiency (Brieger and Rink 2010; Haase and Rink 2010). In comparison, increased zinc levels may result in low copper status, altered iron function, and metabolism disorders (Fosmire 1990). However, only extremely high zinc levels as obtained by excessive use of denture fixative with high zinc content (17-32 mg/g) were observed to act poisonous, leading to hematologic and neurologic abnormalities linked to copper deficiency (Barton et al. 2011). Overall, when moderately supplied (≤ 50 mg/day), zinc is a comparatively nontoxic nutrient.

1.11 Zinc and the Immune System

The importance of zinc for proper immune function is most obvious in zinc-deficient individuals. Disturbances in the zinc homeostasis affect multiple aspects of the immune system, including hematopoiesis, the innate immunity, the adaptive immune response, and immune-regulating

molecules. Regarding innate immunity, increased basal production of proinflammatory cytokines and ROS (reactive oxygen species) is observed in zinc-deficient individuals (Fagiolo et al. 1993; Kahmann et al. 2008), resulting from modulated signal transduction via NF κ B or p38 MAPK signaling (Haase et al. 2008; Prasad 2008). The influence of zinc on T cell immunobiology is prominent, because zinc deficiency results in various T cell defects manifested in thymus atrophy and lymphopenia (King et al. 2005). Additionally, altered T cell function and disturbed polarization of mature T cells occur. Zinc deprivation inhibits the polarization into Th1 cells and hence changes the Th1/Th2 ratio towards Th2 cells, leading to unbalanced cell-mediated immune responses (Prasad 2000). Accordingly, the risk for infections and Th2-driven allergies is increased. Furthermore, the functional impairment of T cell-mediated responses, during zinc-deficiency, favors the development of autoimmune diseases (Honscheid et al. 2009).

Consistently, both zinc deficiency, and also increasing zinc levels influence T cell function. Increasing zinc levels during T cell activation were postulated to calibrate TCR signaling, leading to T cell responses following suboptimal stimuli (Yu et al. 2011). In contrast, physiological zinc-level-exceeding zinc concentrations (50-100 μ M) inhibit T cells as demonstrated by suppressed IL-1 β -stimulated IFN- γ expression (Wellinghausen et al. 1997), and reduced IFN- γ production in zinc supplemented MLCs (Campo et al. 2001). Therefore, a concentration-conditioned zinc effect promotes T cell activation in lower concentration while hampering T cell activity in higher concentration, notably without affecting cell viability.

Important molecular zinc targets responsible for the above mentioned zinc effects comprise receptor proteins, kinases, phosphatases, caspases, and transcription factors, which can be activated or inactivated by zinc (Haase and Rink 2009). Furthermore, its function as a second messenger involved in signal transduction contributes to its immunomodulating capacity (Haase et al. 2008).

II. Scope of the Study

Although zinc supplementation already has been reported to suppress immune function the mechanism underneath has not been revealed sufficiently, yet. The importance of immunosuppression becomes obvious in the context of various adverse immune reactions, which are aimed to be attenuated. These adverse reactions comprise widespread allergic reactions, frequently appearing autoimmune diseases, and transplantation-associated allogeneic immune reactions. Until now, a major medical goal is the induction of tolerance against allergens, autoantigens, and alloantigens. Concomitantly, the immune response towards hazardous antigens must persist in a protective manner. Therefore, complete immunosuppression as generally applied in transplanted patients is important for the prevention of acute and chronic transplant rejection, but concurrently compromises the patient's health. An interesting target for modulating adverse immune reactions is the induction or the enrichment of regulatory T cells, due to their immunosuppressive function. Enhanced amounts of Tregs directed against allergens, auto-, or alloantigens suppress these adverse immune reactions, but allows for a sustained immune-mediated protection.

Among other various functions, the essential micronutrient zinc is involved in immune regulation. Pharmacological zinc doses inhibit allogeneic immune reactions effectively. As molecular mechanism behind the immunosuppressive effect a zinc-induced upregulation of Tregs is reasonable. The scope of this thesis is to reveal the capacity of zinc to enhance protective Tregs and its possible attenuating effect regarding the allergic-, auto-, and allogeneic immune reaction. In this study, the allergic reaction is represented by timothy grass allergen supplementation to isolated PBMCs. The autoimmune disease MS is simulated by induction of experimental autoimmune encephalomyelitis in mice, and the allogeneic immune response is induced in the mixed lymphocyte culture. The impact of zinc regarding diverse parameters is investigated.

Moreover, it is of interest to further analyse the probable induction of Tregs by zinc. Since zinc plays an important role in various enzymes, a potential molecular target for zinc involved in the induction of Tregs is explored in this work. By revealing a molecular mechanism of the zinc-induced immunosuppressive effect, the role of zinc in modulating the adverse immune responses achieves further importance. The relevance of this study is provided in the fact that zinc administered in physiological concentrations lacks toxic effects for the human body. In addition, although the enrichment of Tregs is a major goal in transplantation medicine, until today there is no applicable method reported to reach adequate tolerance by Treg-induction. Therefore, it is of great interest to investigate the immunomodulatory role of zinc. This is even reinforced by the ubiquity and inexpensiveness of zinc, which makes it a favourable candidate for the treatment of adverse immune reactions.

III. Materials and Methods

3.1 Materials

3.1.1 Equipment

- Analytical scales, 770/GS/GJ (Kern, Balingen-Frommern)
- Blot transfer chamber, Mini-trans (Bio-Rad, München)
- Cell Counter, Casy 1 TT (Scharfe System, Reutlingen)
- CO₂ incubator, MCO-17AIC (Sanyo, Gunma, Japan)
- Electrophoresis chamber for polyacrylamide gels, Mini-Protean 3 Electrophoresis Module Assembly (Bio-Rad, München)
- Electrophoresis chamber for polyacrylamide gels, Protean II xi (Bio-Rad, München)
- Electrophoresis net, EPS 3500 XL (Amersham Pharmacia Biotech, Uppsala, Sweden)
- Electrophoresis power supply, Power Pac 300 (Bio-Rad, München)
- Electrophoresis power supply, Power Pac 1000 (Bio-Rad, München)
- ELISA Reader, Magellan (Tecan, Crailsheim)
- ELISA Washer, Atlantis (Asys Hitech, Eugendorf)
- Flow cytometer, FACScan and FACSCalibur (Becton Dickinson, Heidelberg)
- Floor centrifuge, Varifuge 3.0 RS (Heraeus Christ, Osterode)
- Floor centrifuge, Z 400 K (Hermle, Wehingen)
- Freezer, -20°C (Bosch, München)
- Freezer, -80°C, MDF-U71V (Sanyo, Gunma, Japan)
- Heat sealer, Polystar 100 (Rische and Herfurth, Hamburg)
- Laboratory scales, 1265 MP (Sartorius, Göttingen)
- Liquid Scintillation β Counter 1219 Rackbeta (LBK, Wallace, Freiburg)
- Luminescent image analyzer, LAS-3000 (Fujifilm, Düsseldorf)
- Magnet stirring bar retriever, MR3001 (Heidolph, Schwabach)
- Microscope, SM-LUX (Leitz, Wetzlar)
- Multipipetter, Multipette plus (Eppendorf, Hamburg)
- Multiplate Reader, Ultra 384 (Tecan, Crailsheim)
- pH measuring device, HI 9321 (Hanna Instruments, Kehl am Rhein)
- Photometer, BioPhotometer (Eppendorf, Hamburg)
- Pipetter, pipetus-akku (Hirschmann, Eberstadt)
- Pipettes, 0.5-10 μ l, 10-100 μ l an 100-1000 μ l, Research (Eppendorf, Hamburg)
- Refrigerator (Bosch, München)
- Shaker, HS 250 basic (IKA Labortechnik, Staufen)
- Sonicator, Vibra Cell (Sonics & Materials, Danbury, CT, USA)
- Sterile working station, KR-130 and KR-210 (Kojair, Vilppula, Finland)
- Table top centrifuge, 5417 (Eppendorf, Hamburg)
- Table top centrifuge, Biofuge A (Heraeus, Osterode)
- Taqman PCR-Gerat, Sequence Detection System ABI Prism 7000 (Life Technologies Corporation, Carlsbad, CA, USA)
- Thermomixer, comfort and compact (Eppendorf, Hamburg)
- Video Graphik Printer, UP-895CE (Sony, Tokyo, Japan)
- Vortexer, Reax (Heidolph, Schwabach)
- Weighing scales, 1265 MP (Sartorius, Göttingen)

- Western Blot chamber, Mini-Protean 3 Electrophoresis Module Assembly (Bio-Rad, München)

3.1.2 Laboratory Supplies

- Bürker counting chamber (Brand, Wertheim)
- Casy-Cups (Scharfe System, Reutlingen)
- Cell culture flasks, T25 and T75 (Nunc, Roskilde, Denmark)
- Cell culture 6-well, 12-well, 24-well plates (Becton Dickinson, Heidelberg)
- Centrifuge tubes, Sorvall GS3 (Kendro, Langenselbold)
- Centrifuge tubes, Sorvall SA-600 (Kendro, Langenselbold)
- FACS tubes (Sarstedt, Nümbrecht)
- Film cassette, 20 x 25 cm (Bio-Rad, München)
- Gel blotting paper GB003 (Schleicher and Schuell, Dassel)
- Glass pipettes (Brand, Wertheim)
- Glass plates, outer glass PLT W/1.5 mm, M-P 3 (Bio-Rad, München)
- Glass plates, short plates, M-P 3 (Bio-Rad, München)
- Glass plates, outer plates 16 x 20 cm (Bio-Rad, München)
- Latex gloves (Kimberly-Clark, Zaventem, Belgium)
- Microcentrifuge tubes, 1.5 ml (Sarstedt, Nümbrecht)
- Nitrocellulose membrane Trans-blot transfer medium, pure (Bio-Rad, München)
- One-way pipettes, 5 ml, 10 ml and 25 ml (Grenier, Nürtingen)
- Optical Tubes 8er Stripes ABI PRISM (Applied Biosystems, Foster City, USA)
- Optical Caps 8er Stripes ABI PRISM (Applied Biosystems, Foster City, USA)
- Pipette Combitips, 1 ml, 2.5 ml, 5 ml and 10 ml (Eppendorf, Hamburg)
- Pipette tips, 1-10 µl and 10-1000 µl (Sarstedt, Nümbrecht)
- Pipette tips, 100-1000 µl (Eppendorf, Hamburg)
- Plastic tubes with tops, 15 ml and 50 ml (Falcon, Heidelberg)
- Plastic wrap (RUF, Bremen)
- Polystyrene tubes with tops, 13 ml (Sarstedt, Nümbrecht)
- Sponges, 8 x 11 cm (BioRad Laboratories, München)
- Szintillation tubes (PerkinElmer, Rodgau)
- Syringes, 1 ml, 10 ml and 20 ml (Braun, Melsungen)
- UV-cuvette, UVette (Eppendorf Hamburg)
- Vacuum filter, Stericup 0.22 µm GP ExpressPlus (Millipore, Schwalbach)

3.1.3 Cell Culture Media and Additives

- Culture medium RPMI 1640 (Lonza, Verviers, Belgium)
- Fetal calf serum (PAA, Cölbe)
- L-glutamine, 200 mM (Lonza, Verviers, Belgium)
- Non-essential amino acids (Lonza, Verviers, Belgium)
- Penicillin/Streptomycin, 10,000 U/ml + 10,000 µg/ml (Lonza, Verviers, Belgium)
- Phosphate Buffered Saline (PBS) without Ca²⁺ and Mg²⁺ (Lonza, Verviers, Belgium)
- Sodium chloride (KMF, Leipzig)
- Sodium pyruvate (Lonza, Verviers, Belgium)
- Ultra Doma (Lonza, Verviers, Belgium)

3.1.4 Immunological Reagents

3.1.4.1 Antibodies used for Immunoprecipitation/Western-blot

- Goat anti-biotin conjugated HRP (Cell Signaling, Beverly, MA, USA)
- Goat anti-rabbit conjugated HRP (Cell Signaling, Beverly, MA, USA)
- Horse anti-mouse conjugated HRP (Cell Signaling, Beverly, MA, USA)
- Mouse anti-human Foxp3 (Abcam, Cambridge, UK)
- Rabbit anti-human β -Actin (Cell Signaling, Beverly, MA, USA)
- Goat anti-Foxp3 (Santa Cruz Biotechnology, Santa Cruz, CA, USA)
- Rabbit anti-human AcK31-Foxp3 (kindly provided by Dr. Melanie Ott (J. David Gladstone Institute of Virology and Immunology, San Francisco, CA, USA)

3.1.4.2 Antibodies used for Flow-Cytometry

- Mouse anti-human CD4 conjugated FITC (Becton Dickinson, Heidelberg)
- Mouse anti-human CD25 conjugated FITC (Becton Dickinson, Heidelberg)
- Mouse anti-human CD25 conjugated PE (Becton Dickinson, Heidelberg)
- Mouse anti-human CD69 conjugated PE (Becton Dickinson, Heidelberg)
- Mouse anti-human CD152 conjugated PE (Becton Dickinson, Heidelberg)
- Mouse anti-human CD152 conjugated PE-Cy5 (Becton Dickinson, Heidelberg)
- Mouse anti-human Foxp3 conjugated PE (Becton Dickinson, Heidelberg)
- Mouse anti-human/mouse ROR γ T/RORC2 conjugated PE (R&D Systems, Minneapolis, MN, USA)
- Rat anti-mouse CD4 conjugated APC (eBiosciences, San Diego, CA, USA)
- Rat anti-mouse Foxp3 conjugated PE (Becton Dickinson, Heidelberg)

3.1.4.3 Isotype-control Antibodies used for Flow-Cytometry

- Mouse IgG1, k conjugated FITC isotype (Becton Dickinson, Heidelberg)
- Mouse IgG2a, k conjugated FITC isotype (Becton Dickinson, Heidelberg)
- Mouse IgG1, k conjugated PE isotype (Becton Dickinson, Heidelberg)
- Mouse IgG2a, k conjugated PE isotype (Becton Dickinson, Heidelberg)
- Mouse IgG2a, k conjugated PE-Cy5 isotype (Becton Dickinson, Heidelberg)
- Mouse IgG2b, k conjugated PE isotype (Becton Dickinson, Heidelberg)
- Rat IgG2b conjugated APC isotype (eBiosciences, San Diego, CA, USA)
- Rat IgG2b, k conjugated PE isotype (Becton Dickinson, Heidelberg)

3.1.4.4 Antibodies used for Immunohistochemistry

- Rabbit anti-mouse CD3 (Abcam, Cambridge, UK)
- Rabbit anti-mouse Foxp3 (Abcam, Cambridge, UK)
- Horse anti-rabbit biotinylated secondary antibody (Vector Labs BA 2000, Burlingame, CA, USA)

3.1.5 Miscellaneous Reagents

- Acetic acid, 100 % (Merck, Darmstadt)
- Acylamide/bisacrylamide, 30 % (Serva, Heidelberg)

- Agarose (Gibco, Karlsruhe)
- Aqua ad iniectabilia (Braun, Melsungen)
- Aqua irrigation solution (Delta Select, Pfulingen)
- 5-Aza-2-deoxycytidine (Sigma-Aldrich, Steinheim)
- Ammonium persulfate (BioRad Laboratories, München)
- Aminoethyl carbazole (Invitrogen, Germany)
- Biocoll, Ficoll 1.077 g/ml (Biochrom, Berlin)
- Brilliant SYBR Green QPCR Mastermix (Life Technologies Corporation, Carlsbad, CA, USA)
- Bromphenol blue (Riedel-de-Haën, Hannover)
- Bovine serum albumin (Fluka, Buchs, Switzerland)
- Calcium aspartate, capsule (RWTH University Hospital, Aachen)
- Casy-Ton (Scharfe System, Reutlingen)
- Chloroform (RWTH University Hospital, Aachen)
- Clexane (Sanofi-aventis, Frankfurt)
- Cyclosporin A (Alexis Corporation, Lausen, Switzerland)
- Dimethylsulfoxide (DMSO) (Carl-Roth, Karlsruhe)
- Di-Natriumhydrogenphosphat-Dodecahydrat (Carl-Roth, Karlsruhe)
- Dithiothreitol (DTT) (Sigma-Aldrich, Steinheim)
- Ethanol, absolut (RWTH University Hospital, Aachen)
- Ethanol, 70 %, denatured (RWTH University Hospital, Aachen)
- Ethylenediaminetetraacetic acid (Carl-Roth, Karlsruhe)
- EX-527 (Sigma-Aldrich, Steinheim)
- Fat-free milk powder Sucofin (Trade Service International, Zeven)
- Fluozin-3 (Life-Technologies, Darmstadt)
- Glycerine (Merck, Darmstadt)
- Glycine (Sigma-Aldrich, Steinheim)
- H-89 (Sigma-Aldrich, Steinheim)
- Heparin sodium, 5000 (Ratiopharm, Ulm)
- Hha I (New England Biolabs, Ipswich, MA, USA)
- Histo-Clear (Biozym, Hessisch-Oldendorf)
- IBMX, Isobutyl-1-methylxanthin (Sigma-Aldrich, Steinheim)
- Hydrochloric acid, 32 % (Merck, Darmstadt)
- Hydrogen peroxide (Carl-Roth, Karlsruhe)
- Lipoluma Plus (Lumac LSC B.V., Groningen, Niederlande)
- Loading dye solution, O`Range 6x (MBI Fermentas, St. Leon-Rot)
- LumiGLO reagent and peroxide (Cell Signaling, Beverly, MA, USA)
- N, N, N', N' – Tetermethylethylenediamine (Sigma-Aldrich, Steinheim)
- Na₃VO₄ Protease Inhibitor Cocktail (Sigma-Aldrich, Steinheim)
- McrBC (500U) (New England Biolabs, Ipswich, MA, USA)
- Methanol (RWTH University Hospital, Aachen)
- Methyl-[3H]-Thymidine (Amersham Biosciences, Buckinghamshire, UK)
- Natriumdihydrogenphosphat-Monohydrat (Carl-Roth, Karlsruhe)
- β-Mercaptoethanol (Merck, Darmstadt)
- Paraformaldehyde (Sigma-Aldrich, Steinheim)
- Phytohemagglutinin (PHA) (Becton Dickinson, Heidelberg)
- Ponceau S (Fluka, Buchs, Schweiz)
- Propidium Iodide, Minimum 95% (HPLC) (Sigma-Aldrich, Steinheim)

- Protein A/G agarose beads (Santa Cruz Biotechnology, Santa Cruz, CA, USA)
- Protein marker, biotinylated (Cell Signaling, Beverly, MA, USA)
- Recombinant human IL-2 (Peprotech Inc., NY, USA)
- Sodium azide (Merck, Darmstadt)
- Sodium chloride (Merck, Darmstadt)
- Sodium chloride 0,9% solution (Braun, Melsungen)
- Sodium citrate dehydrate (Sigma-Aldrich, Steinheim)
- Sodium dodecyl sulfate (Merck, Darmstadt)
- Sulphuric acid 95-97% (Merck, Darmstadt)
- Timothy grass pollen-extract (Artu biological, Hamburg; provided by Prof. Dr. Petersen from the Leibnitz-Center for Medicine and Biosciences, Borstel)
- Tris-(hydroxymethyl)-aminomethane (Tris Base) (Merck, Darmstadt)
- Trizol Reagent (Ambion, Austin, TX, USA)
- TSST superantigen (produced as described in (Gross et al. 2006)
- Tween-20 (Merck, Darmstadt)
- Zinc apartate, solution (Unizink®) (Köhler Pharma GmbH, Alsbach-Hähnlein)
- Zinc aspartate, capsule (Unizink®) (Köhler Pharma GmbH, Alsbach-Hähnlein)
- ZinPyr-1 (NeuroBioTex,)
- ZnSO₄ x 7 H₂O (Merck, Darmstadt)

3.1.6 Commercially Available Kits

- Fluorogenic SIRT1 (Sir2) Assay Kit (BPS Biosciences, San Diego, CA, USA)
- Human ELISA Component-Set for IL-2, IL-10, IFN- γ and TNF- α detection (BD Biosciences Pharmingen, Heidelberg)
- Hooke kits for induction of EAE (Hooke Laboratories, Lawrence, MA, USA)
- Human Foxp3 buffer set (Becton Dickinson, Heidelberg)
- Mouse Foxp3 buffer set (Becton Dickinson, Heidelberg)
- NucleoSpin RNA® II Kit (Macherey-Nagel, Dueren)
- Qia Amp DNA Mini Kit (Qiagen, Hilden)
- Q-Script cDNA Synthesis Kit (Quanta, Gaithersberg, MD, USA)
- VECTASTAIN® ABC (peroxidase) system (Vector Labs, Burlingame, CA, USA)

3.2 Methods

3.2.1 Preparation of Zinc Solutions

Zinc sulphate was dissolved in Aqua ad iniectabilia to a stock solution of 100mM. The zinc solution was sterile filtered with bacteria filters (pore size 0.2µm). Subsequently, the stock solution was diluted in Aqua ad iniectabilia and further in protein-free medium (Ultradoma) providing a 2mM zinc sulphate solution.

Zinc-aspartate (Unizink®, 0.6mg/ml) was diluted in NaCl (0.9%) to concentrations of either 0.03 mg/ml or 0.006 mg/ml, respectively.

3.2.2 Cell Cultures

The different cell lines listed in table 1 were cultured in CO₂-incubators maintained at 37°C, 5% CO₂, and saturated air humidity. The cells were examined under a microscope twice a week and transferred into fresh medium (1ml cells + 10ml medium). Fetal calf serum (FCS) was inactivated at 56°C for 30 min. Freshly isolated primary cells were used depending on the respective experiment settings.

Table 1. Cell lines and corresponding culture medium

Cell line	Media	Supplements
Jurkat ¹	RPMI 1640	10 % heat-inactivated FCS 1 % L-Glutamin 1 % Penicillin/Streptomycin 1 % Natriumpyruvat 1 % NEAA
Molt-4 ¹ , Hut-78 ¹ , Raji ¹ , RAW264.7 ²	RPMI 1640	10 % heat-inactivated FCS 1 % L-Glutamin 1 % Penicillin/Streptomycin
primary cells	RPMI 1640	10 % heat-inactivated FCS 1 % L-Glutamin 1 % Penicillin/Streptomycin
Vβ ³	IMDM	10 % heat-inactivated FCS 1 % L-Glutamin 1 % Penicillin/Streptomycin 1 ml G418

¹ from DSMZ (Deutsche Sammlung von Mikroorganismen und Zellkulturen)

² from American Type Culture Collection (Manassas, USA)

³ kindly provided from Prof. B. Fleischer, Bernhard-Nocht-Institut Hamburg

3.2.3 Peripheral Blood Mononuclear Cell (PBMC) Isolation

Background:

Peripheral blood mononuclear cells (PBMC) comprise blood leukocytes carrying a round shaped nucleus, including lymphocytes, monocytes, and NK cells. Compared to granulocytes and erythrocytes they maintain a lower density, which simplifies their isolation by Ficoll-density-gradient. Ficoll is composed of high molecular polysaccharides and epichlorohydrin, a reactive organic compound. After centrifugation, erythrocytes and granulocytes settle to the bottom of the gradient, whereas low density cells like thrombocytes remain in the upper phase. Due to their density, PBMCs accumulate in an interphase above the Ficoll solution and can be removed selectively. Isolated PBMCs are washed twice with PBS before culturing in medium.

Reagents:

- Heparin (25,000 U/ml)
- PBS 1x
- Ficoll with density 1.077 g/ml
- Whole blood

Procedure:

1. 50ml whole blood containing 2500U heparin was diluted 1:1 with PBS
2. 25ml of the blood/PBS mixture was slowly pipetted onto 25ml Ficoll (4x50ml tubes)
3. The Ficoll gradient was centrifuged for 20 min at 600g and RmT
4. The PBMC-containing interphase was carefully removed and placed in a new 50 ml Falcon tube, which was then filled to the top with PBS
5. The PBMCs were centrifuged for 10 min at 300g and RmT
6. The pellets were washed twice with PBS

3.2.4 Lysis of Erythrocytes

Background:

Contaminating erythrocytes, which occur during the isolation of PBMC, are removed through hypotonic lysis. This procedure comprises the brief resuspension of PBMC in sterile water to induce erythrocyte lysis. Subsequently, the addition of the same volume of 2 times concentrated PBS recreates isotonic conditions. Acaryotic erythrocytes respond more sensitive to hypotonic solutions and can therefore be eliminated specifically.

Reagents:

- Aqua irrigation solution
- PBS (2x und 1x)
- RPMI medium containing 10% heat-inactivated FCS, 1% L-glutamine and 1% penicillin/streptomycin

Procedure:

1. The PBMCs were washed with PBS
2. The pellets were briefly resuspended in 10ml Aqua irrigation solution and rapidly 10ml 2xPBS was added
3. The PBMCs were centrifuged for 10 min at 300g and RmT
4. The pellets were resuspended in 50ml 1xPBS and centrifuged for 10 min at 300g and RmT
5. The cell concentration was adjusted with RPMI medium

The isolated PBMC were used for further stimulation as indicated, the generation of MLCs (see 3.2.5) and in the allergy assay (see 3.2.7)

3.2.5 Generation and Stimulation of Two-Way Mixed Lymphocyte Cultures (MLC)

In the MLC equal amounts of different donors' PBMCs are mixed and incubated. After incubation over an experiment-dependent time-period, various parameters, such as protein expression or proliferation, were analyzed.

Reagents:

- RPMI medium containing 10% heat-inactivated FCS, 1% L-glutamine and 1% penicillin/streptomycin
- ZnSO₄ (2mM)
- CsA (1 mg/ml)

Procedure:

1. The PBMCs were adjusted to a concentration of 2×10^6 /ml
2. The PBMCs were incubated in T25 cell-culture flasks with either RPMI medium, or ZnSO₄ (50μM), or CsA (1 μg/ml), for 15 min at 37°C and 5% CO₂
3. The same volume of PBMC of two donors (with the same stimulation) were mixed and dispersed into a 24-well plate (1 ml/well)
4. The MLCs were incubated at 37°C and 5% CO₂. Supernatants were collected for the analysis of cytokine expression by ELISA (3.2.17); pellets were used for FACS analysis (3.2.18), western blot (3.2.23) and real-time PCR (3.2.30). FACS analysis included the detection of surface molecule expression (3.2.18.1), and the expression of intracellular proteins (3.2.18.2). Furthermore, the MLC was analyzed in the [³H]-thymidine proliferation assay (see 3.2.31).

3.2.6 Human Zinc-Supplementation Study

A group of 9 healthy male subjects were orally administered with 10 mg/day zinc in form of Zn-DL-Aspartate for a time period of 10 days. Prior to the first zinc intake, peripheral blood samples were obtained (t=0d). The serum zinc-concentration was determined by Atomic Absorption Spectrophotometry (AAS). Furthermore, peripheral blood mononuclear cells (PBMC) were isolated (compare 3.2.3) and MLCs were generated (compare 3.2.5). The MLCs were incubated for 8 days at 37°C and 5% CO₂ and supernatants along with cells were used for the analysis of different parameters. After 10 days of zinc-intake (t=10), peripheral blood samples were repeatedly taken and processed as described above (t=0). As control group a group of 7 healthy male subjects were supplemented with placebo for 10 days and samples were analyzed equivalently. Placebo capsules contained filling material likewise used in the zinc-containing capsules. Both were produced under pharmacological law in the hospital pharmacy in the RWTH hospital pharmacy. The study was approved by the local ethical committee Nr. AZ 016/09 „Vergleich der Bioverfügbarkeit verschiedener Präparate zur Nahrungsergänzung mit Zink (BioVZn)“. (Comparing the bioavailability of diverse compounds used for nutritional zinc supplementation)

3.2.7 Allergy Assay

In the allergy assay, PBMCs were incubated with timothy-grass pollen extract prior to the investigation of various relevant parameters. PBMCs were obtained from allergic donors immunoreacting to the exposure of timothy grass (responder). Timothy grass allergen-insensitive donor-derived PBMCs served as control (non-responder). The experiments were conducted during hay fever season to guarantee pre-activation and high-responsiveness of allergen-responsive immune cells in the timothy-grass allergic subjects.

Reagents:

- RPMI medium containing 10 % heat-inactivated FCS, 1 % L-glutamine and 1 % penicillin/streptomycin
- ZnSO₄ (2mM)
- Timothy-grass pollen extract dissolved in PBS (1 mg/ml)

Procedure:

1. The PBMCs were adjusted to a concentration of 2×10^6 /ml
2. The PBMCs were incubated in T25 cell-culture flasks with either PBS or ZnSO₄ (50µM) for 15 min at 37°C and 5% CO₂
3. 1 ml of pre-incubated PBMCs was dispersed in each well of a 48 well plate prior to addition of either PBS or timothy grass pollen extract (2.5 µg/ml)
4. The cells were incubated at 37°C and 5% CO₂ for 5 days at the most. Supernatants were collected for the analysis of cytokine expression by ELISA (3.2.17); pellets were used for

analysis by FACS (3.2.18), western blot (3.2.23) and real-time PCR (3.2.30). FACS analysis included the detection of surface molecule expression (3.2.18.1) and the expression of intracellular proteins (3.2.18.2). Furthermore, the proliferation was measured by [³H]-thymidine proliferation assay (3.2.31).

3.2.8 V β -Assay

Background:

The V β -assay serves as a stimulation assay for murine T cells, which were transfected with either a human V β 2 element or with a V β 6.5 element of the T cell receptor. In the presence of antigen presenting cells (Raji B cell line) V β T cells can be activated by the addition of the superantigens TSST-1 (toxic shock syndrome toxin 1) or SEA (staphylococcal enterotoxin A).

Reagents:

- IMDM-Medium containing 10% heat-inactivated FCS, 100 U/ml Penicillin, 100 μ g/ml Streptomycin, 2mM L-Glutamine, and 1ml G418
- V β cells
- Raji cells
- PFA (3%)
- TSST-1 (20 μ g/ml)
- ZnSO₄ (2mM)
- PHA (1 mg/ml)

Procedure:

1. The Raji cells were adjusted to 2.5×10^5 cells per ml and fixated with PFA for 10 min at 37°C.
2. The V β cells were adjusted to 5×10^5 cells/ml
3. 500 μ l of both cell lines were then mixed in a 24 well plate and preincubated with or without zinc (50 μ M) for 15 min at 37°C and 5% CO₂
4. The preincubated cells were stimulated with PHA (10 μ g/ml) or TSST-1 (250 ng/ml) for 24h at 37°C and 5% CO₂
5. The supernatants were collected and analyzed by mIL-2 ELISA (3.2.17)

3.2.9 Murine Splenocyte Isolation

Reagents:

- RPMI medium containing 10% heat-inactivated FCS, 1% L-glutamine and 1% penicillin/streptomycin
- 70% ethanol
- Sterile H₂O

- PBS (1x)
- PBS (2x)

Procedure:

1. 5 ml RPMI medium were added to a petri dish
2. Double-layered gauze was mounted on a 50 ml centrifuge tube
3. The sacrificed mouse was washed with 70% ethanol
4. The spleen was removed:
 - a. The fur along the left side of the mouse was cut away, about half-way between the front and back legs
 - b. The body cavity was cut open
 - c. The spleen was removed using sterile forceps
5. The spleen was homogenized with the plunger end of the syringe
6. The cells were transferred through the gauze into the 50 ml tube (the gauze served as a cell strainer)
7. 5 ml RPMI medium were used to wash the petri dish and transfer of the remaining splenocytes through the gauze into the tube
8. The cells were centrifuged at 300g for 10 min
9. The supernatant was discarded and the pellet was resuspended in 5 ml H₂O, followed by rapid administration of 5 ml PBS (2x) (lysis of erythrocytes)
10. The tubes were filled up with PBS (1x) and centrifuged at 300g for 10 min
11. The supernatant was discarded and the pellet was resuspended in 25ml RPMI medium and centrifuged at 300g for 10 min
12. The pellet was resuspended in 20 ml RPMI medium and the cells were counted
13. The splenocyte concentration was adjusted to 1×10^6 /ml

3.2.10 Generation and Stimulation of Murine MLCs

Background:

Isolated murine splenocytes were allogeneic stimulated with cells of the murine leukemic monocyte macrophage cell-line RAW264.7. The splenocytes were obtained from wild-type C57BL/6 mice, carrying the H2^b haplotype, whereas the Balb/c strain-derived RAW264.7 cells express the H2^d haplotype. Due to different MHC haplotypes, the splenocytes are activated by the MHC-expressing RAW264.7 cells, resulting in allogeneic immune reaction.

Reagents:

- ZnSO₄ (2mM)
- RPMI medium containing 10% heat-inactivated FCS, 1% L-glutamine and 1% penicillin/streptomycin

Procedure:

1. The RAW cells were adjusted to a concentration of 2.5×10^5 cells/ml and seeded into a 24 well plate 24 h prior to MLC generation
2. 1×10^6 splenocytes/ml were preincubated with or without $50 \mu\text{M}$ zinc for 15 min at 37°C and 5% CO_2
3. 1 ml of the splenocyte suspension was added to each well of the adherent RAW cells in the 24 well plate
4. The MLCs were incubated for 5 and 8 days, the cells were used for FACS analysis (3.2.18), western blot (3.2.23) and the supernatant was collected

3.2.11 Animal Treatment and Induction of Experimental Autoimmune Encephalomyelitis (EAE)

Female C 57BL/6 mice 10 weeks old were obtained from JANVIER (le Genest-St-Isle, France) and maintained in the animal facilities of the Medical Faculty of the RWTH Aachen University. Animals underwent routine cage maintenance once a week and microbiological monitoring according to the Federation of European Laboratory Animal Science Associations recommendations. All procedures were in accordance with the Review Board for the Care of Animal Subjects of the district government (North Rhine-Westfalia, Germany) and performed according to international guidelines on the use of laboratory animals. The animal testing number was 10612G1.

Mice were immunized subcutaneously (s.c.) on the upper back and at the lower back with $200 \mu\text{g}$ of myelin oligodendrocyte glycoprotein peptide (MOG)₃₅₋₅₅ emulsified in Complete Freund's Adjuvant (CFA) containing 2 mg/ml of *Mycobacterium tuberculosis* H37Ra. Pertussis toxin ($1 \mu\text{g}$), a potent ancillary adjuvant necessary for EAE induction, was injected intraperitoneally (i.p.) at day 0 and 2.

The animals were divided into the 5 different groups I-V (compare Table 2). Groups I and II did not receive EAE induction, but either NaCl or high dose zinc treatment, respectively. Groups IV-V were injected (i.p.) daily with $6 \mu\text{g/day}$ ($100 \mu\text{l}$ of 0.006 mg/ml solution) or $30 \mu\text{g/day}$ ($100 \mu\text{l}$ of 0.03 mg/ml solution) zinc aspartate, respectively, starting two days before EAE immunization. Group III was injected with $100 \mu\text{l}$ NaCl (0.9%) serving as control.

Mice were sacrificed after 19 days following EAE induction. Animal scarification was performed two days after the mice reached the peak of disease (acute EAE).

Table 2. Experimental set-up

Group	Treatment	Number of mice
I	NaCl only	4
II	Zn-Aspartate only (30 µg/day)	4
III	NaCl and EAE	11 (12)*
IV	Zn-Aspartate and EAE (6 µg/day)	12
V	Zn-Aspartate and EAE (30 µg/day)	12

* one animal died before start of experiment

3.2.12 Clinical Evaluation of EAE

Mice were monitored daily for clinical signs of EAE and neurological impairment was scored according to the following increasing severity scale:

0. → no disease
1. → limp tail (tail plegia)
2. → limp tail and weakness of hind legs
3. → limp tail and complete paralysis of hind legs or paralysis of one front and one hind leg
4. → complete hind leg and partial front leg paralysis
5. → complete hind and complete front leg paralysis or mouse is found dead due to paralysis

Mice scoring level 4 for 2 days were euthanized and then listed as score 5.

3.2.13 Tissue Sample Harvesting

For FACS analysis, blood and spleen were collected from the animals. After animal anaesthesia, blood was taken from the Orbital Sinus by using small glass capillaries. The blood was immediately filled into 1.5ml reaction tubes containing 2µl heparin (25,000 U/ml).

Subsequently, the spleen was removed and processed for FACS analysis as described in 3.2.18.

For histological/immunohistochemical analysis, mice were transcardially perfused with 2% paraformaldehyde containing 1.5% saturated picric acid as described in 3.2.14.

3.2.14 Transcardial Perfusion of Mice

Background:

Transcardial perfusion accomplishes the fixation of whole animals, which enables histological/immunohistochemical tissue analysis.

Reagents:

- RPMI medium containing 10% heat-inactivated FCS, 1% L-glutamine and 1% penicillin/streptomycin
- Perfusion solution (NaH₂PO₄ 3g, Na₂HPO₄ 45g, paraformaldehyde 20g, saturated picric acid 100ml, in 1000ml, pH 7.4)
- Clexane (40mg)
- PBS
- Isofluran (5%)

Procedure:

1. 10µl Clexane (40mg) was applied 30 min prior to the start by intraperitoneal injection
2. Animals were deeply anaesthetized with Isofluran (5%)
3. Animals were fixed, the thorax was opened by using forceps and scissors, and a small opening was cut into the right heart atrium
4. A small needle was inserted into the left heart ventricle prior to perfusion of 50 ml ice-cold perfusion solution
5. The head and the trunk were cut
6. The brain/spinal cord was dissected and stored in 1:5 diluted (in PBS) perfusion solution at 4°C until used

3.2.15 Paraffin-Embedding of Mice Tissue Samples**Background:**

Paraffin is immiscible with water, which necessitates tissue dehydration by ethanol baths with progressively increasing ethanol concentration. This is followed by a clearing agent, usually xylene or Histo-clear. Finally, tissue samples are put into molten paraffin wax (60°C). The wax is changed 3 times eliminate xylene residues.

Reagents:

- Ethanol (abs., 96%, 70%)
- Histo-Clear
- Paraffin

Procedure:

1. The tissue samples were embedded in paraffin by immersing them under gentle agitation as described in Table 3

Table 3. Treatment of tissue samples

70% ethanol	3x30 min
96% ethanol	3x30 min
100% ethanol	3x30 min
Histo-Clear	3 x 60 min
paraffin	3 x 120 min and then overnight at 60°C

3.2.16 Immunohistochemistry (IHC)

Background:

After transcatheter perfusion (3.2.14) and overnight postfixation in the same fixative, spinal cords were dissected for further analysis by IHC. IHC comprises detection of antigens expressed in cells of tissue sections. Antibodies directed against the target protein are used and visualising of the antigen-antibody complex is achieved by conjugation of antibody to an enzyme, which can catalyse a colour-producing reaction.

Reagents:

- Blocking solution: PBS containing 2% normal horse serum
- Antibodies
- PBS
- Biotinylated secondary antibody
- Peroxidase-coupled avidin-biotincomplex
- Kaiser's glycerine gelatin
- Aminoethyl carbazole
- Sodium citrate buffer (10mM citric acid, 0.05% Tween 20, pH 6.0)
- Tris/EDTA buffer (10mM Tris Base, 1mM EDTA Solution, 0.05% Tween 20, pH 9.0)
- Xylol
- Hydrogen peroxide 0.3%
- Ethanol (absolute, 96%, 70%)
- H₂O dest.

Procedure:

1. 5 µm-thick sections were placed on superfrost glass and deparaffinised in 4 x 5 min xylol, rinsed in 3 x 5 min 100% ethanol and 2 x 5 min 96% ethanol and 1 x 5 min 70% ethanol and 1 x 5 min in PBS

2. Heat-mediated antigen retrieval was performed by boiling slides in the desired buffer, sodium citrate buffer for 20 min, followed by cooling-down of the slides
3. The slides were washed 3x in PBS (5 min)
4. Unspecific binding of the secondary antibodies was blocked by incubating the slides in PBS containing 2% normal horse serum for 1 h at RmT
5. The blocking solution was decanted and primary antibody was applied diluted 1:1000 (Foxp3) or 1:500 (CD3) in blocking solution and incubated overnight at 4°C
6. The primary antibody was decanted and the slides were washed 2x with PBS (2 min)
7. The endogenous peroxidase activity was blocked by incubating slides for 30 min in 0.3% hydrogen peroxide diluted in PBS in the dark
8. The slides were washed 2x in PBS (2 min)
9. VECTASTAIN® ABC (peroxidase) system was used to label primary antibody-antigen conjugates following the manufacturer`s recommendation.
10. The slides were washed 2x in PBS (2 min)
11. The slides were incubated in aminoethyl carbazole for up to 30 min at RmT to visualize antibody-antigen conjugates
12. The slides were counterstained with the nuclear dye hematoxylin for 5 min and then rinsed with water
13. The the slides were mounted in Kaiser`s glycerine gelatine
14. CD3⁺ and Foxp3⁺ cells were counted by 3 blinded independent individuals

3.2.17 Enzymed-Linked Immunosorbent Assay (ELISA)

Background:

Sandwich ELISAs are commonly used for determining the amount of secreted molecules such as cytokines. The sandwich ELISA starts with the immobilization of an antigen-specific antibody (“capture antibody”) in a 96-well plate. The plate is then blocked with BSA to prevent unspecific binding. Subsequently, titrated standard and diluted samples, most commonly cell supernatant, are added to the appropriate wells. After incubation of the samples/standards, excess cytokines are aspirated and a biotinylated antibody specific for a different epitope of the investigated cytokine (detection antibody) is provided. Finally, the enzyme reagent consisting of avidin-horseradish peroxidase conjugate is added. After further wash steps to remove excessive antibodies, the substrate (p-Nitrophenyl phosphate) is added and a chemical reaction proceeds, which induces a change in colour corresponding to the amount of present antibody. This reaction is stopped by sulphuric acid, which induces a further change of the developed colour. The adsorption can now be measured by a well-plate reader.

Reagents:

- Carbonate buffer: 29mM sodium carbonate, 22mM sodium hydrogen carbonate, pH 9.6
- Coating buffer: Carbonate buffer + 1% BSA
- Assay diluent: PBS + 10% FCS
- Wash buffer: 2000mL PBS + 1ml Tween 20
- Capture antibodies (monoclonal anti-human IFN- γ , IL-10, IL-2, TNF- α)
- Biotinylated detection antibodies (monoclonal anti-human IFN- γ , IL-10, IL-2, TNF- α)
- Standard solutions (Recombinant human IFN- γ , IL-10, IL-2, TNF- α)
- Substrate solution: Tetramethylbenzidine (TMB) and Hydrogen Peroxide (1:1)
- Stop solution (1M H₂SO₄)

Procedure:

1. Coating of the micro titre plates and assay procedure were performed in accordance with the producers' instructions

3.2.18 Fluorescence-Activated Cell Sorting (FACS)**Background:**

Due to its multifunctionality, the technique of flow cytometry is of increasing relevance for various research issues. Among other functions it allows the accession of cell surface marker expression, sorting of cells according to particular characteristics, performance of intracellular staining, visualizing of apoptotic cells, and determination of cell cycle progression. Despite its name not every FACS machine is capable of cell sorting and they are often used for cell analysis only.

Through a nozzle the cell suspension flows into a stream of sheath fluid leading to cell scattering before entering into a laser path. At an interrogation point the cells are then analyzed for reflection, diffraction, or refraction of light or fluorescence. A photodiode measures forward-angle scatter (FSC) light whilst photodetectors sense emitted side scatter light (SSC). Combination of both detectors reports the size and granularity of the investigated cells. Fluorescence-labelled cells emit light, which is separated into characteristic wavelength and whose intensity is measured by photodetectors equipped with coloured filters. As light passes through the photodetectors, the light signals are transformed into electrical signals. Each photodetector can be adjusted by changing its voltage and amplifier gain.

Specific binding of fluorochrome-conjugated antibodies is controlled by using isotype controls. Isotype controls are antibodies bearing the identical isotype but lacking specificity towards antigens in the investigated organism. Herewith, unspecific binding as, for example arising by antibody-binding to Fc-receptors, can be distinguished from specific binding to the desired antigen.

Flow-cytometry was applied for the following procedures and methods:

- cell-surface marker analysis → MLC, allergy assay, EAE, PBMC
- intracellular staining → MLC, allergy assay, EAE
- detection of intracellular zinc levels (see 3.2.33) → PBMC

3.2.18.1 Cell-Surface Marker Analysis

Immune cells express cell-specific surface marker. By using antibodies directed against these molecules, the molecule's expression level per cell can be analyzed as well as the total and relative amount of cells expressing the molecule.

Reagents:

- PBS 1x
- PBS/FCS (1%)
- Lysing solution 10x: magnesium chloride (1.5M ammonium chloride, 100mM sodium bicarbonate, H₂O, pH 7.4)
- antibodies

Procedure:

1. The cells were adjusted to a concentration of 1×10^6 /ml in PBS/1 % FCS
2. 100 μ l whole blood or 1 ml of 1×10^6 /ml cells were transferred into each FACS tube
3. The tubes were centrifuged for 10 min at 300g and RmT, and the supernatants were discarded
4. For erythrocyte-lysis in murine whole blood (3.2.4) the cells were incubated for 10 min at 4°C in the dark with 2 ml lysing solution (1x) and washed twice in 2 ml PBS
5. The pellets were resuspended and 100 μ l PBS/1%FCS was added to each tube
6. Direct fluorescent-labelled antibodies were added and incubated with cells for 20 min at RmT in the dark
7. Step 3 was repeated
8. The supernatants were discarded, and the pellets were resuspended in 500 μ l PBS/1% FCS
9. The samples were analyzed by using FACS-Calibur or FACS-Scan

FACS analysis was performed with CellQuest software (Becton Dickinson, Heidelberg).

3.2.18.2 Intracellular Staining

Intracellular staining is applied if the desired antigen is present within the cell. This is the case for molecules such as transcription factors or cytokines. In order to stain intracellular antigens with the fluorescence-associated antibodies, cells need to be permeabilized and fixated.

Reagents:

- PBS 1x

- Staining buffer: PBS 1x, heat-inactivated FCS (2%), sodium azide (0.1%)
- Fixation solution
- Permeabilization solution
- Antibodies

Procedure:

Steps 1-7 were performed analogous to cell surface marker analysis

Intracellular staining was performed as instructed by the manufacturer and analyzed by using FACS-Calibur or FACS-Scan.

3.2.18.3 PI (Propidium Iodine) Staining

The fluorochrome propidium iodine (PI) is not capable of entering living cells through the intact plasma membrane. Therefore, it is used for the staining of dead cells.

Reagents:

- Propidium iodine (1 mg/ml)
- PBS/FCS (1%)

Procedure:

1. Cells were adjusted to 1×10^6 /ml in 1ml PBS/1% FCS
2. 10 μ g/ml PI was added and the cells were incubated at 4°C in the dark for 10 min
3. Flow cytometric analysis was performed by using FACS-Scan or FACS-Calibur

3.2.19 Calculating the Protein Concentration

Background:

The Bradford protein assay functions as protein concentration determination assay. Bradford reagent is a solution based on the acidic dye called Coomassie Brilliant Blue G, which complexes with proteins. Proteins in the presence of an acidic milieu alter the absorption maximum of this dye from 465 nm to 595 nm. The Coomassie dye binds to basic and aromatic amino acid residues, particularly arginine. A protein standard curve, using BSA, is established before the actual samples are measured. Its variation coefficient should not exceed 10%. The micro-Bradford assay was performed detecting proteins in a concentration range from 1 to 25 μ g/ml.

Reagents:

- Bradford reagent
- Bovine serum albumin (BSA) (1 mg/ml) dissolved in Aqua ad iniectabilia
- Aqua irrigation solution

Procedure:

1. The standards were generated according to Table 4

Table 4. Standards for the Micro Bradford Assay

CONCENTRATION	AQUA	BSA
1 µg/ml	799 µl	1 µl
2.5 µg/ml	797.5 µl	2.5 µl
5 µg/ml	795 µl	5 µl
10 µg/ml	790 µl	10 µl
15 µg/ml	785 µl	15 µl
25 µg/ml	775 µl	25 µl

2. 200µl Bradford reagent was added to blank, standards, and samples
3. Standards, blank, and samples were incubated for at least 5 min
4. The absorption was measured at 595 nm with a photometer

3.2.20 Generation of Cell Lysates

Background:

For the detection of non-secreted intracellular proteins, the cells need to be disrupted prior to SDS-PAGE procedure and western blot analysis (3.2.23). Cell lysates are generated in sample buffer containing sodium-orthovanadate in order to inhibit protein tyrosine phosphatases and alkaline phosphatases from removing phosphate groups. This is important when phosphorylated proteins are investigated.

Reagents:

- Sample buffer: 65mM Tris-HCl, 25% glycerine, 10% SDS, 1mM sodium orthovanadate, pH 6.8

Procedure:

1. Samples were centrifuged in microcentrifuge tubes for 1 minute at 20,000g
2. The supernatants were removed, and the pellets were resuspended in 100µl sample buffer
3. The samples were sonificated on ice (Intensity 3, Output control 5, duty cycle 50%, 10 sec)
4. The sonificated samples were boiled at 95°C for 5 min
5. The samples were stored at -20°C

3.2.21 Immunoprecipitation

Background:

In order to concentrate distinct proteins from whole cell lysates immunoprecipitation is performed. Whole cell lysates are incubated with an antibody directed against the desired protein in the presence of agarose-beads coupled to protein A/G. Incubation allows binding of the antibody to its target antigen and binding of the Fc fragment to protein A/G-coupled beads. Isolation of the protein/antibody/beads complex is achieved by centrifugation, resuspension in 2x

sample buffer and 5 min boiling. Immunoprecipitation-efficiency is detected by the collection of supernatant before the addition of the antibody and after incubation with the beads. Sample analysis is performed by SDS-PAGE (3.2.22) and western blot (3.2.23).

Reagents:

- RIPA-lysis buffer: 20mM Tris HCl, pH 7.5, 150mM NaCl, 10mM EDTA, 1% (vol/vol) Triton X-100, 1% (wt/vol) Desoxycholate
- Phenylmethanesulfonylfluorid (PMSF) 100mM
- Aprotinin (1000 Kallikrein-inhibitor units/ml)
- Sodiumbutyrate 0.9M (deacetylase inhibitor)
- Anti-Foxp3 antibody (Santa Cruz)
- Protein A/G agarose beads
- 2 x Sample buffer (130 mM Tris-HCl, 50% glycerine, 20% SDS, 200 mM sodium orthovanadate, 2% β -mercaptoethanol, 5% bromphenol blue, pH 6.8)

Procedure:

1. 1×10^7 cells were lysed in 500 μ l RIPA-lysis buffer provided with freshly added protease inhibitors: PMSF (1mM), aprotinin (100 KIU/ml) and sodiumbutyrate (20mM)
2. The lysates were incubated on ice for 10 min and sonificated on ice (Intensity 3, Output control 5, duty cycle 50%, 10 sec)
3. The lysate was incubated on ice for 30 min and centrifuged at 4°C for 10 min at 10000g
4. The supernatants were transferred into a new reaction tube and the protein concentration was determined by Bradford protein assay (3.2.19)
5. 100-500 μ g total protein per sample was incubated with 1.5 μ l anti-Foxp3 antibody at 4°C for 1 h with constant agitation
6. 20 μ l Protein A/G agarose beads per sample were washed in PBS, resuspended in RIPA buffer and added to the lysate/antibody mixture
7. The lysates were incubated over night at 4°C with constant agitation
8. Immunoprecipitates were collected by centrifugation at 4°C, 3000rpm for 5 min
9. The supernatants were removed carefully and the beads were washed four times with 1ml RIPA buffer to diminish unspecific bound proteins
10. The supernatants were removed and the pellets resuspended in 40 μ l 2x sample buffer and boiled at 95°C for 5 min to ensure antibody-complex destruction
11. SDS-Page was loaded with 6-10 μ l per sample and western blots were performed

3.2.22 Sodium Dodecyl Sulfate Discontinuous Polyacrylamid Gelelectrophoresis (SDS-PAGE)

Background:

The SDS-PAGE functions to separate proteins according to their electrophoretic mobility. The anionic detergent sodium dodecyl sulfate (SDS) covers protein charges, providing uniformly negatively charged proteins. Addition of β -mercaptoethanol-containing sample buffer disrupts disulfide bridges within polypeptides. Furthermore, secondary and tertiary structures are dislocated by 5 minutes of protein-boiling. Thus, the polypeptides are present in their primary, linear structure and negatively charged, which allows for fractionation by approximate size during electrophoresis.

By using discontinuous SDS-PAGEs more concentrated bands develop that simplify the identification of the investigated protein. For this purpose two different buffer sets are used. The stacking gel concentrates the proteins, which are then separated according to their molecular weight by the resolving gel.

Reagents:

- Sample buffer (65mM Tris-HCl, 25% glycerine, 10% SDS, 100mM sodium orthovanadate, pH 6.8)
- Distilled water
- Ammonium persulfate (APS) (10%)
- Bromphenol blue
- β -mercaptoethanol
- Stacking gel buffer: Tris-HCl (1.5M, pH 8.8)
- Resolving gel buffer: Tris-HCl (0.5M, pH 6.8)
- Electrophoresis buffer (5x): 0.12M Tris base, 0.96M glycine, 30 ml 10% SDS, 600ml, pH 8.3
- Acrylamide:Bisacrylamide 29:1 (30%)
- N,N,N',N'-tetramethylethylenediamine (TEMED)
- Biotinylated molecular marker

Procedure:

1. The glass gel plates were rinsed with 70% ethanol, wiped clean with tissues, and then placed in the gel holders
2. The reagents for the 10% resolving gel were mixed according to Table 5, pipetted between the glass plates, layered with distilled water, and left for 20 min of polymerization

Table 5. Gel Reagents for SDS-PAGE

SUBSTANCES	8,5% RESOLVING GEL	SUBSTANCES	4% STACKING GEL
H ₂ O	4.11 ml	H ₂ O	2.08 ml
1.5 M TrisHCL pH 8.8	2.34 ml	0.5 M TrisHCL pH 6.8	910 µl
Acrylamide/ bisacrylamide, 30%	2.55 ml	Acrylamide/ bisacrylamide, 30%	467 µl
APS, 10%	90 µl	APS, 10%	35 µl
TEMED	20 µl	TEMED	7.8 µl
Total volume	9 ml	Total volume	3.5 ml

3. The water was removed, the 4% stacking gel was prepared as shown in Table 5, the combs were placed in the gel, and the stacking gel was allowed to polymerize for 20 minutes
4. The gel comb was removed and the glass plates containing the polymerized gel were placed into the electrophoresis chamber
5. The chamber was filled with 1x electrophoresis buffer
6. The samples and the molecular weight marker were mixed with bromphenol blue and 1% β-mercaptoethanol and were heated at 95°C for 5 minutes prior to pipetting into the gel slots
7. The electrophoresis was conducted at 150V for 90 min on ice

3.2.23 Western Blot

Background:

Western Blot includes the transfer of by SDS-PAGE separated proteins from polyacrylamide matrices onto nitrocellulose membranes utilizing electrical fields. The protein pattern remains conserved during protein transfer. Protein-bound SDS is washed out in this procedure so that the proteins regain their original secondary, and to some extent tertiary structure. Proteins can hence be recognized by epitope-directed antibodies, enabling the detection of specific target proteins within a homogenized culture sample.

In order to prevent non-specific antibody-binding to the nitrocellulose membrane, potential binding sites are blocked with protein solutions containing BSA or fat-free milk powder. Detection of high-affinity antibodies bound to protein epitopes is achieved by using species-specific secondary antibodies conjugated to the horseradish peroxidase enzyme (HRP). This enzyme converts substrate (LumiGLO solution) into its oxidized form, which then emits light detected by a digital biomolecular imager.

Reagents:

- Transfer buffer: 25mM Tris base, 0.2M glycine, 20 % methanol, pH 8.5
- Ponceau S-solution

- TBS-buffer (10x): 0.2M Tris base, 2.28M NaCl, pH 7.6
- TBS/T buffer (1x): TBS, 0.1% Tween 20
- Blocking buffer: 2.5g fat-free milk powder dissolved in 50ml TBS/T buffer
- Primary antibody: 10ml TBS-T, 5% fat-free milk powder, and primary antibody (diluted 1:1000)
- Secondary antibody: 10ml TBS-T, 5% fat-free milk powder, secondary antibody (diluted 1:2000), and HRP-conjugated anti-biotin antibody (diluted 1:1000)
- Detection solution: 250µl LumiGLO reagent (20 x), 250µl LumiGLO peroxide (20 x), and 4.5ml distilled water for each gel

Procedure:

1. The nitrocellulose membrane and gel blotting paper were cut to fit the size of the gel
2. The membrane, gel blotting paper, and sponges were equilibrated in transfer buffer
3. The blot sandwich was assembled and then placed in the blot module with the gel facing the cathode side and the membrane facing the anode side
4. The cooling element was placed next to the blot module and the module was filled with transfer buffer
5. The blotting process was performed for about 90 min at 100 V
6. The proteins were visualized by placing the membrane in Ponceau S solution and then washed with distilled water to ensure proper blotting
7. The Ponceau S solution was completely removed by transfer buffer and the membrane was rinsed with distilled water
8. The membrane was incubated with 25 ml blocking buffer for 1 h at RmT followed by incubation with the primary antibody at 4°C overnight
9. The membrane was washed 3 x with TBS/T buffer
10. The membrane was incubated with the secondary antibody for 1 h at RmT
11. Step 10 was repeated
12. The membrane was covered with 5 ml detection solution for 1 minute
13. Chemiluminescence was detected by LAS-3000 imager

3.2.24 Membrane Reprobing

Background:

Membrane stripping is useful when more than one protein is investigated on the same membrane. Previously antibody-incubated nitrocellulose membranes derived from western blot analysis (3.2.23) can be reused for further analysis by using a β -mercaptoethanol-containing buffer. The stripped nitrocellulose membrane is reusable following blocking in fat-free milk powder for incubation with further antibodies.

Reagents:

- Stripping buffer (0.06M Tris base, 0.7% β -mercaptoethanol, 0.07M SDS, pH 6.8)
- TBS/T buffer (1 x): TBS, 0.1% Tween 20

Procedure:

1. The membrane was washed 4 x with TBS/T buffer
2. The membrane was incubated with stripping buffer for 30 min at 70°C
3. The membrane was washed 6 x with TBS/T buffer
4. The washed membrane entered the western blot procedure at step 8 (3.2.23)

3.2.25 RNA Isolation from PBMCs**Background:**

RNA isolation was performed using the NucleoSpin RNA® II Kit (Macherey-Nagel), which allows RNA isolation of fragments larger than about 200 bp thereby preventing the isolation of small RNA molecules such as 5.8S rRNA, 5S rRNA and tRNA. First, cells are lysed by a solution containing large amounts of chaotropic ions that inactivate interfering RNases. In the presence of ethanol intact RNA binds to a silica membrane. Washing steps with different buffers remove salts, metabolites and macromolecular cellular components. Finally, pure RNA is eluted under low ionic strength conditions with RNase-free H₂O.

Reagents:

- β -Mercaptoethanol
- Ethanol (70%)
- RNase-free water
- Lysis Buffer RA1
- Wash Buffer RA2
- Wash Buffer RA3
- Membrane Desalting Buffer MDB
- Reaction Buffer for rDNase
- rDNase

Procedure:

1. RNA isolation was performed exactly as described in the manual
2. Isolated RNA was stored at -80°C after determination of the RNA concentration

3.2.26 DNA Isolation of PBMCs

Background:

The QiaAmp DNA Mini Kit from Qiagen enables the isolation of genomic DNA. Following cell lysis, the genomic DNA binds to a silica membrane in the presence of ethanol. Finally, the elution is achieved with H₂O.

Reagents:

- Proteinase K
- AL-buffer
- Ethanol, absolute
- AW1 buffer
- AW2 buffer
- Aqua ad iniectabilia

Procedure:

1. DNA isolation was performed exactly as described in the manual
2. Isolated DNA was stored at -20°C after determination of the DNA concentration

3.2.27 Spectrophotometric Determination of RNA or DNA Concentration

Background:

A method for determining nucleic acid concentration and purity is spectrophotometry. Absorbance at wavelength of 260nm and 280nm is detected. Whereas the absorption peak of proteins takes place at 280nm, the absorption peak of nucleic acids is at 260nm. The ratio A_{260}/A_{280} provides information about the purity of isolated RNA or DNA. Pure preparations of DNA and RNA have A_{260}/A_{280} ratios of 1.8 to 2.0. Ratios significantly lower indicate protein or phenol contamination (high A_{280}) while higher ratios indicate salt contamination (high A_{260}).

Reagents:

- Aqua ad iniectabilia

Procedure:

1. RNA was diluted 1:50 and DNA was diluted 1:10 in Aqua ad iniectabilia
2. The photometer was blanked with aqua ad iniectabilia
3. The RNA concentration was calculated as follows:

Concentration ($\mu\text{g/ml}$) = dilution factor x 40 x extinction at 260nm

The DNA concentration was calculated as follows:

Concentration ($\mu\text{g/ml}$) = dilution factor x 50 x extinction at 260nm

3.2.28 Reverse Transcription

Background:

For reverse transcription of isolated RNA into cDNA (complementary DNA) the qScript cDNA-Synthesis Kit (Quantas) was used. This kit provides oligo-dT primer (complementary to the poly-A-tail at the 3' end of the mRNA) and random hexamer primers. Primer annealing to mRNA results in double-strand DNA/RNA molecules serving as a starting point for DNA synthesis by reverse transcriptase enzymes.

Reagents:

- Aqua ad iniectabilia
- 1 µg RNA template
- qScript Reaction Mix (5x)
- qScript Reverse Transcriptase

Procedure:

1. 1 µg RNA was diluted with 15 µl Aqua ad iniectabilia in a 1.5 reaction tube
2. 4 µl Reaction Mix (5x) and 1 µl Reverse transcriptase were added
3. Tubes were mixed gently and heated in a thermomixer as described in table 6

Table 6. Temperature conditions

Time	Temperature
5 min	25°C
60 min	42°C
5 min	85°C

3.2.29 Methyl Screen Assay

Background:

In order to identify genomic DNA methylation patterns the methyl screen assay provides an efficient and sensitive alternative to the else used bisulfite-sequencing method. The Methyl screen assay utilizes combined restriction from both methylation-sensitive restriction enzymes (MSRE, e.g. HhaI) and methylation-dependent restriction enzymes (MDRE, e.g. McrBC). The proportion of digested DNA compared to undigested DNA is obtained by quantitative PCR, thereby allowing for the analysis of CpG methylation patterns in a target DNA region.

Reagents:

- Aqua ad iniectabilia
- HhaI
- McrBC

- New England Biolabs NEB2 Digestion buffer (100 µg/ml BSA, 10mM GTP in 1x NEB2-buffer)
- Glycerine solution (50% in Aqua ad iniectabilia)

Procedure:

1. Each of four 1.5ml reaction tubes was filled with 1µg DNA and digestion buffer (1x) up to a total volume of 97µl
2. The restriction enzymes or glycerine, respectively, were added as follows:
 - A. + 3µl glycerine (50 %) (mock)
 - B. + 3µl HhaI (60U)
 - C. + 3µl McrBC (30U)
 - D. + 3µl HhaI + 3µl McrBC
3. The DNA was digested over-night at 37°C in a thermomixer
4. Stopping of the enzymatic reaction was achieved by heating to 65°C for 20 min followed by cooling on ice for 5 min
5. The samples were stored at -20°C
6. For further analysis by real-time PCR, 3µl DNA was diluted in 2µl Aqua ad iniectabilia and PCR was performed as described in 3.2.30
7. DNA methylation occupancy calculation was calculated using following formula:

$$Z = \left| 100 - \left(\frac{\text{quantity (enzyme)}}{\text{quantity (mock)}} \cdot 100 \right) \right| \%$$

3.2.30 Quantitative Real time Polymerase Chain Reaction (Q-PCR)

Background:

Q-PCR is an effective molecular-biological technique developed for the amplification and simultaneously quantification of DNA. Primers complementary to the target region anneal to a template DNA. A key role in the process of amplification plays the DNA polymerase, which enzymatically assembles a new DNA strand by elongating the primers at their 3'end. In the course of PCR progression the newly-synthesized DNA serves in turn as template leading to exponential amplification of initial DNA templates.

The PCR can be divided into two different forms. In the conventional PCR agarose gel electrophoresis is used for size-separation and visualizing of the PCR products. In contrast, real-time PCR measures the amount of DNA product after each round of amplification by detection of double-strand DNA-intercalating reporter dyes such as SYBR Green. The emitted light of the dye (emission maximum 529nm) increases relative to the amount of PCR product. Measurement of the DNA-intercalated fluorescent signals after every cycle enables the detection of the exponential phase. The number of cycles needed to exceed a certain threshold for fluorescence detection is called the cycle threshold (C_t). For gene expression quantification, the $\Delta\Delta C_t$ method is

applied. Herein, the C_t for the RNA/DNA of a gene of interest is normalized to the C_t of RNA/DNA of a housekeeping gene (porphobilinogen deaminase) of the same sample (ΔC_t). Subsequently, the expression disparity among reference sample (e.g. untreated control) and sample is obtained by subtraction of their C_t values ($\Delta\Delta C_t$). The relative expression difference between sample and reference sample normalized to a housekeeping gene is calculated as follows (Livak and Schmittgen 2001):

$$\text{ratio} = 2^{-\Delta\Delta C_t}$$

In this thesis, QPCR was applied for mRNA expression analysis and the Methyl screen assay. The Methyl screen assay did not involve the $\Delta\Delta C_t$ method but was evaluated as demonstrated in 3.2.29.

Reagents:

- Aqua ad iniectabilia
- Brilliant SYBR Green QPCR Master Mix
- Primer dissolved in Aqua ad iniectabilia
- cDNA

Procedure:

1. Separate mastermixes were prepared for each, the gene of interest and the housekeeping gene, in a sterile 1.5ml reaction tube on ice as summarized in table 7

Table 7. Reagents per cDNA/DNA sample for QPCR (25µl)

Reagent	Volume [µl]
Aqua ad iniectabilia	10
SYBR Green QPCR mastermix	12.5
Primer sense (2 µM)	1.25
Primer antisense (2 µM)	1.25

2. 2 µl cDNA was added to 23µl mastermix and pipetted into a PCR reaction tube
3. Amplification was performed as shown in table 8
4. The Primers used in QPCR are listed in table 9 and 10

Table 8. PCR program

Temperature	Duration	Cycles
50°C	20 s	1x
95°C	15 min	1x
95°C	30 s	45x
56°C or 58°C (see table 9)	30 s	
20°C	∞	

Table 9. Primer for mRNA analysis

hCTLA-4 58°C	sense 5'-3' TCTGCAAAGCAATGCACGTG	159 bp
	antisense 5'-3' CCGCACAGACTTCAGTCAC	
hPPAR γ 58°C	sense 5'-3' GGGATGTCTCATAATGCCATCA	66 bp
	antisense 5'-3' CGCCAACAGCTTCTCCTTCT	
hZIP8 58°C	sense 5'-3' CCTCGGATTGATTTTGACTCCACT	258 bp
	antisense 5'-3' AGCAGGATTGTCATAGCATGTCAC	
hIFN γ 58°C	sense 5'-3' AGAATTGGAAAGAGGAGAGTGACAG	128 bp
	antisense 5'-3' GTCTTCCTTGATGGTCTCCACAC	
hIL-4 58°C	sense 5'-3' TTGAACAGCCTCACAGAGCAGA	80 bp
	antisense 5'-3' GTTGTGTTCTTGGAGGCAGCA	
hPBGD (porphobilinogen deaminase) 58°C	sense 5'-3' ACGATCCCGAGACTCTGCTTC	87 bp
	antisense 5'-3' GCACGGCTACTGGCACACT	

Table 10. Primer for Methyl Screen Assay

hFoxp3 "Intron" 56°C	sense 5'-3' CATCCACCAGCACCCATGT	250 bp
	antisense 5'-3' GGGATGTTTCTGGGACACAGA	12 CpGs

5. Data analysis was performed with the program Abi Prism 7000

3.2.31 [³H] Thymidine Proliferation Assay

Background:

Proliferation of cells can be measured by determining their incorporation of [³H]-thymidine into cellular nucleic acids. For this purpose cell cultures are pulsed with [³H]-thymidine during the last 16 h before harvesting. Quantification of the incorporated [³H]-thymidine is accomplished by cell lysis, accumulation and drying of released DNA on filter papers, and, finally, dissolving of filter papers in a liquid scintillation cocktail. The scintillation cocktail contains liquid chemical medium capable of converting the kinetic energy of nuclear emissions into light energy, which can then be measured by a scintillation counter. Thus, the β -emission originating by [³H] decay serves as a parameter for the amount of incorporated [³H]-thymidine and, therefore, for DNA synthesis. The degree of proliferation is indicated as counts per minute (CPM) and is expressed as proliferation index.

Reagents:

- RPMI medium containing 10% heat-inactivated FCS, 1% L-glutamine and 1% penicillin/streptomycin
- [³H]-thymidine solution
- Scintillation cocktail Lipoluma
- Aqua dest.
- Ethanol 70% (v/v)

The [³H]-thymidine was diluted 1:20 in RPMI-medium to a concentration of 1850 kBq/ml. Every sample of a 96 well plate received 10 μ l of this solution (18.5 kBq/well).

Procedure:

1. 200 μ l/well of PBMCs (2×10^6 /ml) were stimulated according to the experiment and incubated at 37°C and 5% CO₂ in a 96 well plate
2. 10 μ l [³H]-thymidine solution was added to every well
3. Incubation for 16 h at 37°C and 5% CO₂
4. The incubation was stopped (plate can be frozen -20°C for later analysis)
5. The cells were lysed with a cell harvester machine and DNA was accumulated on a filter paper
6. The filter papers were washed 5 times with Aqua dest. and one time with ethanol (70%)
7. The filter paper were transferred into scintillation tubes and dried for 5 min at 70°C in an incubator
8. Every filter paper was dissolved in 3ml Lipoluma and the scintillation tubes were sealed
9. The CPM was detected by a liquid scintillation β counter
10. The proliferation index was calculated by dividing the CPM measured in stimulated cells by the CPM detected in unstimulated cells

3.2.32 Sirtuin 1 (Sirt-1) Assay

Background:

For measuring Sirtuin 1 (Sirt-1) enzyme activity, the fluorogenic Sirt-1 Assay Kit was used. In this assay the fluorometric substrate containing an acetylated lysine side chain is incubated with the purified Sirt-1 enzyme. Sirt-1-induced deacetylation sensitizes the substrate so that subsequent treatment with the Lysine Developer produces a fluorophore, which can then be measured by a fluorescence reader. The Sirt-1-inhibitor nicotinamide serves as a control.

Reagents:

- ZnSO₄ (10μM; 1μM, 100nM)
- Fluorogenic Sirt-1 Assay Kit

Procedure:

1. The Sirt-1 activity assay was performed as suggested in the instructions manual.

3.2.33 Detection of Labile Zinc

Background:

Labile zinc levels can be detected by specific fluorescent zinc-sensors. Two zinc-probes, FluoZin-3 and ZinPyr-1, were used in this thesis.

The lipophilic Zinpyr-1 (C₄₆H₃₆C₁₂N₆O₅) is a membrane-permeant fluorescent sensor with high specificity and affinity for zinc (K_d = 0.7 nM). The excitation and emission wavelength are 490 nm and 530nm, respectively. Binding of zinc ions induces altered ZinPyr-1 fluorescence properties, which can then be detected by a fluorescence reader or by flow-cytometry. In T cells ZinPyr-1 is used to detect intracellular free zinc levels.

In addition, the chelator FluoZin3-AM (K_d = 8.9nM) is a specific zinc-selective sensor. Following zinc binding, FluoZin3-AM exhibits a single excitation peak at 494nm and an emission peak at 516nm. Two forms of FluoZin-3 are available; FluoZin3-AM and FluoZin-3A. FluoZin3-AM is present as an acetoxymethyl (AM)-ester, which is able to permeate cell membranes and therefore detect intracellular zinc. FluoZin-3A, on the other hand, is the free acid of FluoZin-3 and is used to detect free zinc levels in buffer, medium, or cell lysates. In contrast to ZinPyr-1, FluoZin-3 is used in T cells for the detection of vesicular zinc levels.

For the calculation of the free zinc concentration, 50μM of the zinc chelator TPEN (N,N,N',N'-tetrakis(-)[2-pyridylmethyl]-ethylenediamine) and 100μM ZnSO₄ are added, in order to determine minimal and maximal zinc concentrations, respectively. For the detection of labile intracellular zinc, maximal zinc levels are induced by incubation with 100μM ZnSO₄ plus the ionophore pyrithione (50μM). The labile zinc concentration is then calculated by the formula:

$$[Zn]=Kd*((F-F_{min})/(F_{max}-F))$$

published by Grynkiewicz et al. (Grynkiewicz et al. 1985)

3.2.33.1 FluoZin-3A Detection

Reagents:

- FluoZin-3A (1mM in DMSO)
- ZnSO₄ (10μM; 1μM, 100nM)
- TPEN (1mM)

Procedure (all measurements were conducted as triplicates):

1. The investigated buffer was dispersed in a 96 well plate (90 μl/well)
2. 5μl of diluted (1:50) FluoZin-3A was added (=1μM)
3. TPEN was added (50μM) and zinc concentrations were generated (0.1; 1; 2; 2.5; 3; 4; 5 μM)
4. The plate was incubated (shaking) for 10 min in the dark
5. The detection was performed with the fluorescence plate reader at 485nm excitation- and 535nm emission-wavelength
6. The zinc concentration was calculated as described in 3.2.33

3.2.33.2 Intracellular Zinc Detection

Reagents:

- FluoZin3-AM (1mM in DMSO) or ZinPyr-1 (2.5 mM in DMSO)
- ZnSO₄ (10μM; 1μM, 100nM)
- TPEN (1mM)
- Pyriothione (5mM)
- RPMI medium containing 1% L-glutamine and 1% penicillin/streptomycin
- PBS 1x

Procedure:

1. 1x10⁶ PBMCs were distributed in 1 ml in RPMI medium without FCS
2. FluoZin3-AM or ZinPyr-1 was added at a final concentration of 1μM or 10μM, respectively
3. The cells were incubated at 37°C for 30 min while shaking
4. The cells were centrifuged at 300g for 5 min and the supernatant was discarded
5. The pellets were resuspended in 100μl PBS (1x10⁶ cells/ml)
6. 10μl of mouse anti-human CD3-PE was added and the cells were incubated for 10 min at RmT in the dark
7. The cells were centrifuged at 300g for 5 min and the supernatant was discarded and the pellets were resuspended in 1ml PBS

8. 330µl of this cell suspension was added in each FACS tube:
 - a. TPEN (8.25µl) → minimal zinc concentration
 - b. ZnSO₄ (3.3µl) + pyrithione (3.3µl) → maximal zinc concentration
 - c. Cells only → detection of intracellular zinc level
9. The cells were incubated at 37°C for 30 min
10. Single cell fluorescence intensity was detected by FACS analysis (FL-1 for the zinc probe and FL-2 for CD3-PE) and zinc concentration was calculated as described in 3.2.33

3.2.34 Statistical Significance and Program Analysis

The results derive from series of experiments (number of experiments is shown as n = x) and are expressed as mean values; the standard error of the mean (SEM) is presented. The statistical significance was calculated using GraphPad Prism (GraphPad software, La Jolla, CA, USA). Statistical significances calculated by Student t-test and Mann-Whitney test are represented as follows: *p< 0.05, **p< 0.01 and ***p<0.001. Multiple comparisons involved ANOVA calculation with Tukey's post-hoc-test. Mean values with significant differences are indicated by diverse letters, which indicate a significance level of p<0.05.

IV. Results

4.1 Zinc Attenuates the Allogeneic Immune Reaction

In MLCs, PBMCs derived from genetically diverse and immune-competent donors get mixed and cultured. Expression of divergent HLA haplotypes triggers the allogeneic immune reaction characterized by strong lymphocyte proliferation, the formation of T cell blasts, and pronounced IFN- γ production. The trace-element zinc has been discovered to inhibit IFN- γ production in MLCs (Campo et al. 2001). Exploration of the immunomodulating zinc-effect in MLCs was the aim of the following study.

4.1.1 Modulated Cytokine Production by Zinc

Cytokine production is a crucial feature in the MLC. Especially IFN- γ production was reported as a key parameter for allogeneic activity (Danzer et al. 1994). For this reason, MLC-production of the Th1 cytokine IFN- γ was detected by ELISA in the present study to confirm inhibition by zinc. Moreover, levels of the Th2 cytokine IL-10 were assessed in MLCs. The ratio of IFN- γ /IL-10 provides insight into the Th1/Th2 cytokine balance.

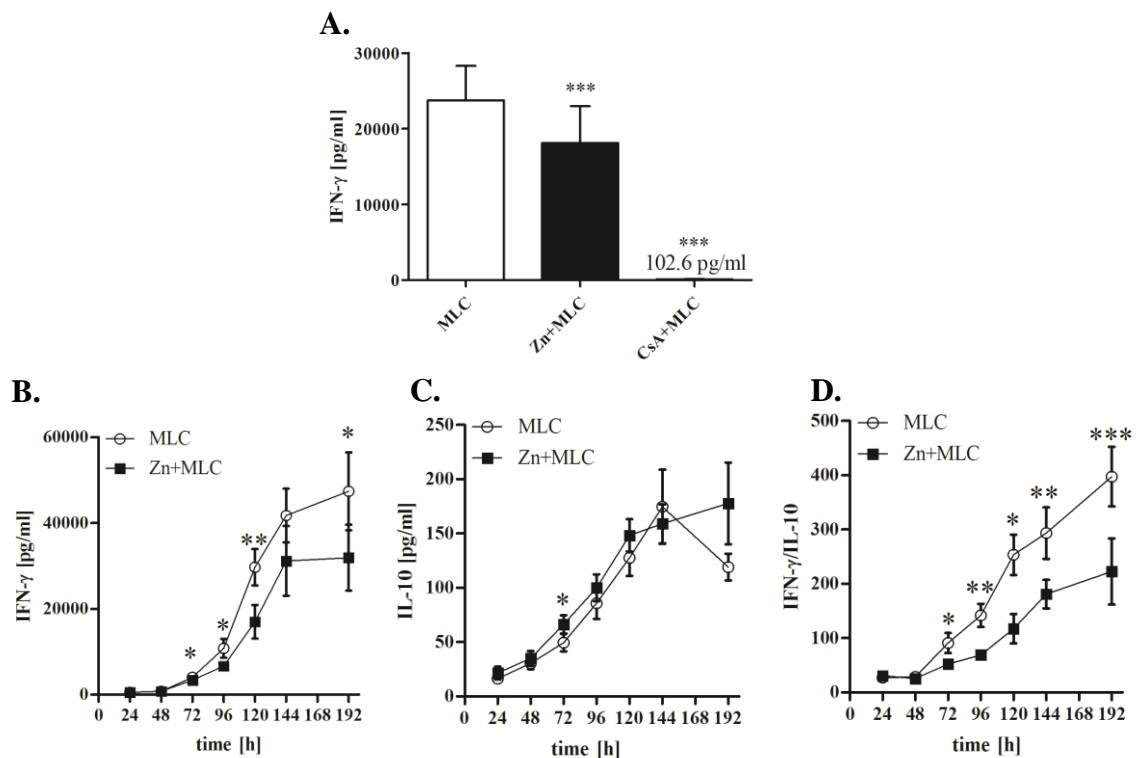


Fig. 2. Zinc modulates IFN- γ and IL-10 cytokine levels in the MLC. 2×10^6 /ml PBMCs were preincubated either with or without $50 \mu\text{M}$ zinc, respectively, or with $1 \mu\text{g/ml}$ CsA (A) for 15 min before mixing of MLCs. Supernatants were collected after 8 days of incubation (A) and at indicated time points (B, C, D) and cytokine levels were measured by ELISA (A $n=13$; B, C, D $n=11$). * indicates a significance of $p < 0.05$, ** indicates a significance of $p < 0.01$, *** indicates a significance of $p < 0.001$ (student's t-test), mean values + SEM mean (A.) or mean values \pm SEM (B., C., D.) are shown.

As presented in Fig. 2 A., IFN- γ production in MLCs was significantly inhibited after 8 days of MLC culture in cells pretreated with 50 μ M zinc for 15 min prior to PBMC mixing. Hence, the results of Campo et al., were successfully reproduced. Fig. 2 B shows that IFN- γ levels in MLC supernatants of cells supplemented with zinc were decreased compared with the control as early as 3 days (72 h) following MLC initiation. At day 8 (192 h) the zinc-dependent inhibition of IFN- γ production was most prominent. Usage of the immunosuppressive drug cyclosporine A (CsA) demonstrated that IFN- γ production can be completely abrogated in MLCs. Thus, IFN- γ production was not entirely suppressed by zinc proposing different strategies of immune-modulation.

In contrast to IFN- γ , IL-10 levels were significantly increased in zinc-supplemented MLCs after 3 days of MLC incubation (Fig. 2 C). Notably, IL-10 production rose continuously in MLCs until day 6 regardless of treatment, revealing that Th2 cells contribute to the allogeneic reaction. Hence, a significantly reduced Th1/Th2 ratio in zinc-supplemented MLCs compared to control MLCs at each stated time point was observed starting from day 3 (Fig. 12 D). Accordingly, a shift from a mainly Th1-driven response in the direction of a Th2 response underlines the immunomodulating zinc effect.

Th1-cytokine production also comprises IL-2. In contrast to IFN- γ , IL-2 production of allogeneic activated lymphocytes was not inhibited by zinc supplementation (Fig. 3 A). Remarkably, IL-2 levels in the supernatant of MLCs were significantly elevated after 48 h of MLC incubation.

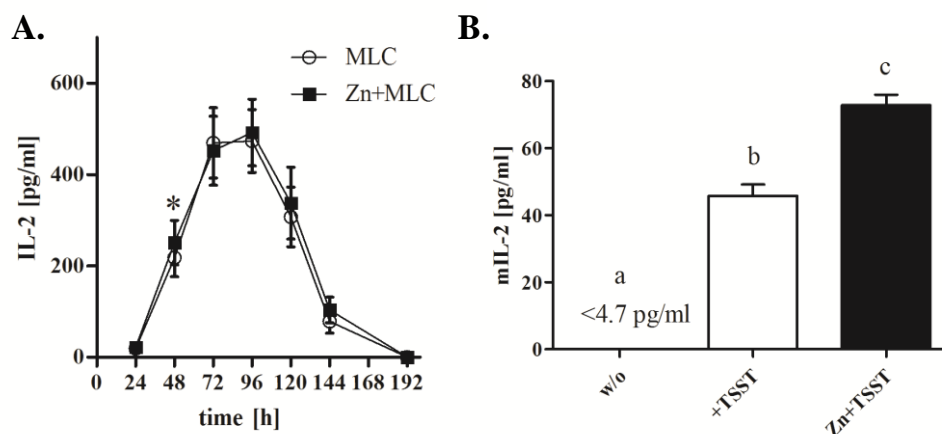


Fig. 3. **Impact of zinc on IL-2 cytokine levels.** 2×10^6 /ml PBMCs were preincubated with or without 50 μ M zinc for 15 min before mixing of MLCs. Supernatants were collected at indicated time points of incubation and cytokine levels were measured by ELISA (A n=14). Murine V β ₂ T cells were preincubated with or without 50 μ M zinc for 15 min before stimulation with or without 250 ng/ml TSST in the presence of MHC II expressing cells. Supernatants were collected after 48 h of incubation and mIL-2 levels were detected by ELISA (B n=3). * indicates a significance of $p < 0.05$ (student's t-test) between with and without zinc treatment, different letters indicate significant differences of $p < 0.05$ (ANOVA, post test: Tukey), mean values \pm SEM (A) or mean values + SEM (B) are shown.

Since both cytokines belong to the group of Th1 cytokines, a similar regulation was expected. Therefore, the impact of zinc on activation-induced IL-2 expression was further validated by measuring IL-2 expression in response to zinc-supplementation in murine V β T cell clones overexpressing the TCR V β ₂ chain. Significantly enhanced IL-2 production, following zinc preincubation, was observed in V β cells stimulated with toxic shock syndrome toxin (TSST) superantigen for 48 h in the presence of APCs (Fig. 3 B).

4.1.2 Attenuated Proliferation in Zinc-Supplemented MLCs

Lymphocyte proliferation reflects the severity of alloresponsiveness and is therefore one of the key parameter characterizing the MLC. In the following experimental series the cell proliferation rate was measured as an indicator of the impact of zinc on MLC severity. Cell proliferation was assessed by addition of ³H-thymidine for the last 16 h of the 8 days lasting MLC incubation, since after 8 days IFN- γ production was prominently reduced. As a control proliferation of untreated and zinc-supplemented PBMCs was assessed, and MLC proliferation values were normalized to the proliferation of control PBMCs to gain normalized results. Furthermore, 1 μ g/ml of CsA was used as an internal control as well as for a direct comparison between the zinc-impact and the well-known CsA-impact regarding MLC proliferation.

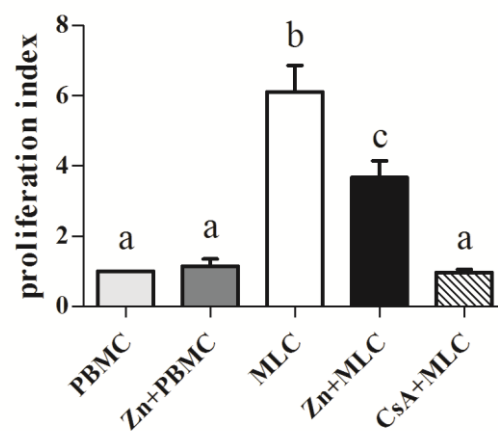


Fig. 4. **Zinc inhibits MLC proliferation.** 2×10^6 /ml PBMCs were preincubated with or without 50 μ M zinc for 15 min or 1 μ g/ml CsA before mixing of MLCs. After 7 days of incubation cells were pulsed for the last 16 hrs with ³H-thymidine prior to washing and measuring of ³H-thymidine incorporation by detection of radioactivity in the β -counter as counts per minute (cpm). Results are presented as proliferation index (cpm/cpm untreated control PBMC) (n=10). Diverse letters indicate significant differences of $p < 0.05$ (ANOVA, post test: Tukey); mean values + SEM are shown.

As displayed in Fig. 4, the proliferation rate of unstimulated PBMCs was not affected by zinc supplementation. As expected, mixing of PBMCs into MLCs resulted in profound proliferation due to allogeneic stimulation. Concomitantly to IFN- γ production, zinc-supplementation significantly reduced MLC proliferation rates, albeit not to the level of unactivated PBMCs. CsA-

treated MLCs, on the other hand, showed completely abrogated proliferation levels, comparable to those of the untreated PBMCs. Incubation of MLCs with zinc consequently demonstrates an immunomodulatory capacity which is indicated in reduced, yet not completely suppressed proliferation. Zinc-induced Tregs were suggested to play a role in the modulation of MLCs by inhibiting the immune response, since IL-2 and IL-10 levels, in contrast to IFN- γ levels, were not reduced by zinc despite reduced cell proliferation. Notably, IL-2 serves as Treg survival factor and IL-10 is reported to be produced by Tregs (Barrat et al. 2002). Therefore, the amount of Tregs in MLCs was investigated.

4.2 Zinc-Induced Treg Upregulation in the MLC

4.2.1 Zinc Upregulates Expression of the Treg-Associated Molecules Foxp3 and CTLA-4

Detection of Foxp3 protein levels in MLCs by western blot analysis at different time points (72h, 120h, 192h) revealed the capacity of zinc to induce Tregs. β -actin protein levels served as a loading control. MLCs were generated from allogeneic PBMCs preincubated with or without 50 μ M zinc, respectively, prior to mixing. Foxp3 protein levels intensified significantly at day 3 (72 h) and day 8 (192 h) in zinc-supplemented MLCs compared to controls (Fig. 5 A, B).

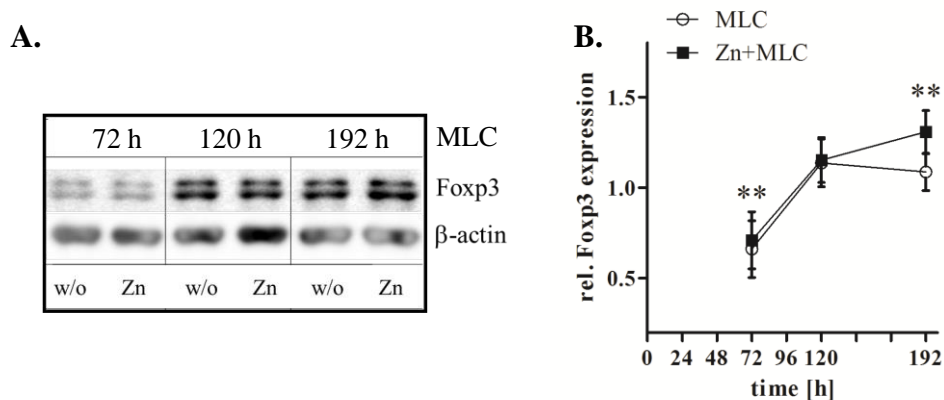


Fig. 5. **Zinc-enhanced Foxp3 expression in the MLC.** 2×10^6 /ml PBMCs were preincubated with or without 50 μ M zinc for 15 min before mixing of MLCs. Cells were harvested after 72, 120, and 192 h of MLC culture and cell lysates were generated. Foxp3 and β -actin protein levels were detected by western-blot analysis, one representative blot out of $n=6$ is presented in A. Quantification by optical density determination was performed and Foxp3 values were normalized to β -actin values (B.) ($n=6$). ** indicates a significance of $p < 0.01$ (student's t-test), mean values \pm SEM are shown.

Surprisingly, after 5 days (120 h) no significant difference was found in expressed Foxp3 protein levels between control and zinc-treated cells. Additionally, Fig. 5 B. reveals increasing Foxp3 levels after 5 days compared to 3 days of incubation in both control and zinc-supplemented cells,

followed by a decline in the control cells, but stabilization in zinc supplemented cells at day 8. Thus, zinc may play a role in prolonging Foxp3 protein levels resulting in elevated iTreg levels.

A further Treg marker is the co-inhibitory molecule CTLA-4 (see Introduction), which is constitutively expressed by nTregs and upregulated along with Foxp3 in iTregs following T cell activation (Takahashi et al. 2000). CTLA-4 expression was detected at 3, 5, and 8 days of MLC incubation by measuring CTLA-4 mRNA levels (Fig. 6). Concomitantly, mRNA levels of the housekeeping-gene PBGD were assessed for relative quantification. Relative CTLA-4 expression levels were normalized to the relative expression levels of the untreated control after 72 h of MLC incubation in an effort to detect expression changes during the MLC course. Similar to the Foxp3 protein level CTLA-4 mRNA of zinc-supplemented MLCs was significantly enhanced compared to their controls at day 3 (Fig. 6). At day 5 the expression level increased in both control cells and zinc-treated cells, but Fig 6 reveals a significant higher CTLA-4 expression level in zinc-supplemented cells after 8 days of incubation compared to the control. Due to the correlation between Foxp3 protein levels and CTLA-4 expression there is evidence for zinc-induced upregulation of iTregs in MLCs.

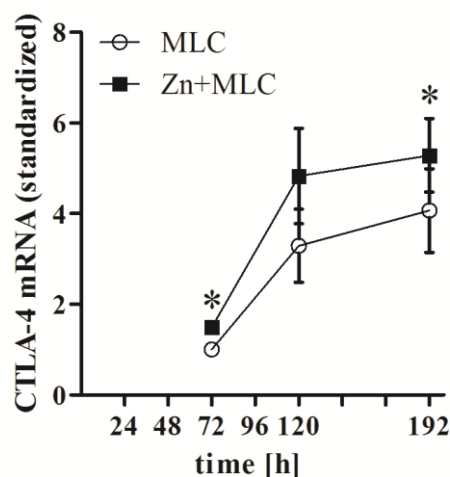


Fig. 6. **Zinc-enhanced CTLA-4 mRNA expression in the MLC.** 2×10^6 /ml PBMCs were preincubated with or without $50 \mu\text{M}$ zinc for 15 min before mixing of MLCs. mRNA was isolated after 72, 120, and 192 hrs of MLC culture. CTLA-4 expression levels were quantified by RT-PCR and were normalized to PBGD. Results were standardized to CTLA-4 expression levels of MLCs without zinc at 72 hrs ($n=7$). * indicates a significance of $p < 0.05$ (student's t-test), mean values \pm SEM are shown.

4.2.2 Zinc-Induced Upregulation of Tregs Occurs in Allogene-Activated Blasts

Western blot analysis and mRNA detection examine over-all Foxp3 and CTLA-4 expression of complete cell lysates. Therefore, the cellular source of Foxp3 and CTLA-4 in MLCs was not revealed. In order to confirm that zinc-upregulated Foxp3 and CTLA-4 expression derive from induced allogene-activated iTregs, 2-color and 3-color flow-cytometric analyses were performed. The amount of Tregs was assessed after 8 days of MLC incubation as this time point revealed

significantly enhanced CTLA-4 and Foxp3 levels (Fig. 5 and Fig. 6). Detection of CD4⁺Foxp3⁺ cells was used to measure the amount of Tregs in the MLC by flow cytometry. Alloactivated T cells occurred in the form of T cell blasts displaying greater side scatter (SSC) and forward scatter (FSC) values than naïve CD4⁺ T cells, which enables gating of alloreactive CD4 blasts to obtain the amount of Tregs among all T cells. This gating-strategy as presented in Fig. 7A comprises activated blasts, as confirmed by measuring the specific expression of the activation marker CD69 on those cells. Gating on CD4⁺SSC^{hi} blasts revealed a significant increase in the amount of Foxp3 expressing cells following zinc supplementation compared to the control (Fig. 7 B). Hence, elevated amounts of Foxp3-expressing cells among the alloactivated T cell blasts manifest an enhancing effect of zinc on the amount of iTregs.

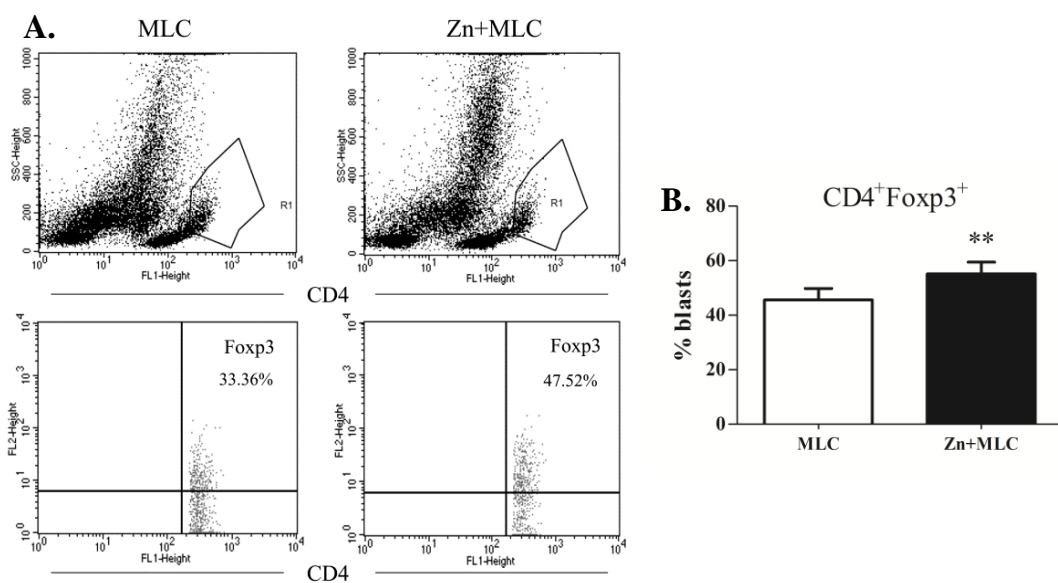


Fig. 7. **Elevated Foxp3 expression among CD4⁺ blasts.** 2×10^6 /ml PBMCs were preincubated with or without 50 μ M zinc for 15 min before mixing of MLCs. Cells were harvested after 8 days of incubation and analyzed for CD4⁺Foxp3⁺ expression by flow cytometry. Gating was performed on CD4⁺ blasts. A. displays one representative flow cytometric analysis out of n=16. B. The amount of Foxp3 expressing CD4 blasts was measured (n=16). ** indicates a significance of p<0.01 (student's t-test), mean values + SEM are shown.

4.2.3 Zinc Upregulates the Expression of Foxp3-Associated Molecules CD25 and CTLA-4

The transcription-factor Foxp3 induces the expression of its target genes including *cd25* and *ctla-4*, both contributing to the suppressive effects of Tregs (see Introduction). CD25, the IL-2 receptor alpha chain, is expressed on activated T cells and Tregs and associates with CD122 to form the heterodimeric IL-2 high-affinity receptor (Tsudo et al. 1987). Foxp3 drives Tregs to express strongly increased levels of CD25 (further referred to as CD25^{hi}), whereas activated T cells reveal medium CD25-expression levels (CD25^{mid}). Naïve T cells do not show CD25 expression. It was therefore of great interest to investigate whether the enhanced Foxp3 expression was reflected in an enhanced expression of CD25. Flow cytometric analysis of

CD4⁺CD25^{hi} expressing cells was performed 8 days after MLC incubation and by gating on CD4⁺ blasts (Fig. 8 A) the percentage and CD25 MFI (geometrical mean fluorescence intensity) of CD25^{hi} expressing activated blasts was determined. Fig. 8 demonstrates an increased amount of CD25^{hi} expressing cells among the alloactivated blasts in the MLC in zinc-treated versus control cells. This held true not only for the relative amount of CD25^{hi} expressing cells among the activated cells (Fig. 8 B), but also the CD25 expression level per cell was enhanced as observed in the significantly elevated MFI levels (Fig. 8 C). These findings support the idea that zinc-upregulated iTregs are the cellular source of increased Foxp3 protein levels and, more importantly, increased Foxp3 levels result in increased CD25 expression, which is involved in downregulation of T effector cell (Teff) activity due to outcompeting these cells for IL-2.

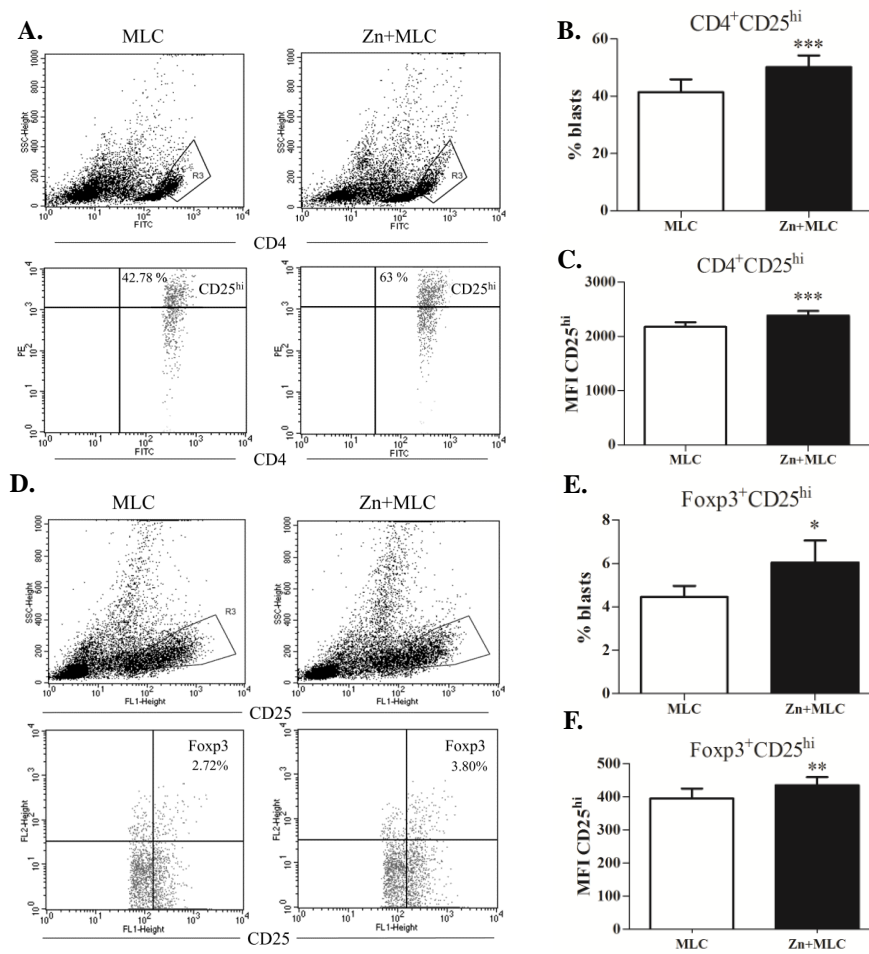


Fig. 8. Elevated CD25 expression among CD4⁺ and Foxp3⁺ blasts. 2x10⁶/ml PBMCs were preincubated with or without 50μM zinc, respectively, for 15 min before mixing of MLCs. Cells were harvested after 8 days of incubation and analyzed for CD4 and CD25 expression by flow cytometry. Gating was performed on CD4⁺ blasts (A. displays one representative flow cytometric analysis out of n=10) and the amount of CD25 expressing CD4 blasts (B.) and CD25 MFI (geo mean) (C.) among CD4 blasts (n=10) was measured. D. Cells were analyzed for Foxp3 and CD25 expression by flow cytometry. Gating was performed on CD25⁺ blasts (D. displays one representative flow cytometric analysis out of n=8) and the amount of Foxp3⁺CD25^{hi} expressing CD25⁺ blasts (E.) and CD25 MFI (geo mean) of CD25^{hi}Foxp3⁺ cells (F.) was measured (n=8). * indicates a significance of p<0.05, ** indicates a significance of p<0.01, *** indicates a significance of p<0.001 (student's t-test), mean values + SEM are shown.

In order to confirm that the zinc-upregulated CD25 expression is related to the enhanced Foxp3 expression the amount of simultaneously Foxp3 and CD25^{hi} expressing cells was assessed by flow cytometry. Zinc-treated and control cells were analyzed after 8 days of MLC incubation. Gating was performed on CD25 expressing blasts as displayed in Fig. 8 D, comprising alloactivated Teffs and Tregs (CD25^{mid} and CD25^{hi} expressing blasts). Among the CD25⁺ blasts, the amount of CD25^{hi} Foxp3⁺ expressing cells was measured. Additionally, CD25-MFI of CD25^{hi}Foxp3⁺ cells was determined to reveal an association between Foxp3 and CD25 expression on the single cell level.

Among CD25 expressing blasts, the amount of CD25^{hi}Foxp3⁺ expressing cells was significantly elevated in the zinc-supplemented group compared to the control (Fig. 8 E). In addition, the CD25 MFI among the CD25^{hi} Foxp3 expressing cells showed significantly higher CD25 levels per Foxp3⁺ cell in zinc-treated MLCs (Fig. 8 F). This result uncovers a link between Foxp3⁺ and CD25^{hi} expressing cells, underlining the evidence for zinc-upregulated iTregs in the MLC. In particular, enhanced CD25 expression per cell in the zinc-treated MLCs suggests elevated Foxp3-induced gene expression.

CTLA-4, a negative regulator of TCR signaling, also underlies the regulation of the transcription factor Foxp3. Therefore, to confirm the idea of zinc-upregulated iTregs the amount of CD4⁺CTLA-4⁺ expressing cells was assessed. Tregs were recently associated with enhanced intracellular CTLA-4 expression and increased capacity to traffic CTLA-4 to the cell surface following stimulation (Wang et al. 2011). In order to gain a better understanding of zinc-induced modulation of Tregs surface (sCTLA-4) and intracellular (icCTLA-4) CTLA-4 the expression of both was analyzed in CD4⁺ blasts after eight days of MLC. Both, their percentage and CTLA-4 MFI in CD4⁺CTLA-4⁺ blasts were determined (Fig. 9 A and D). Fig. 9 B reveals an increased amount of sCTLA-4 expressing cells among the CD4 expressing blasts in the zinc-treated cells compared to the control. Additionally, sCTLA-4 MFI was increased considerably (Fig. 9 C). The amount of icCTLA-4 expressing CD4⁺ blasts was slightly enhanced by zinc supplementation (Fig. 9 E), but this increase was not statistically significant. The same was true for the icCTLA-4 MFI in alloreactive CD4⁺blasts (Fig. 9 F).

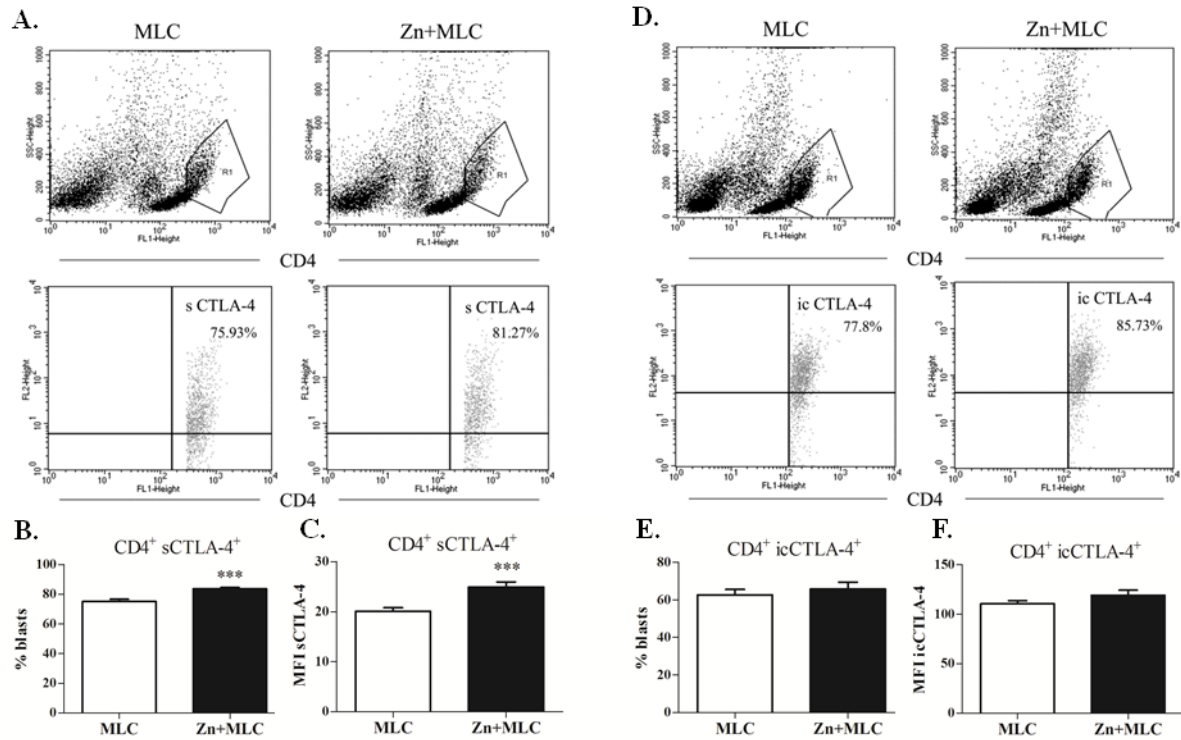


Fig. 9. Elevated CTLA-4 expression among CD4⁺ blasts. 2×10^6 /ml PBMCs were preincubated with or without 50 μ M zinc, respectively, for 15 min before mixing of MLCs. Cells were harvested after 8 days of incubation and analyzed for CD4 and surface CTLA-4 (sCTLA-4) expression (A.-C.) or CD4 and intracellular CTLA-4 (icCTLA-4) expression (D.-F.) by flow cytometry. Gating was performed on CD4⁺ blasts (A. and D. displays one representative flow cytometric analysis out of n=12) and the amount of surface CTLA-4 and intracellular CTLA-4 expressing CD4 blasts was measured (B., E.; n=12) and surface and intracellular CTLA-4 MFI (geo mean) (C., F.; n=12) among CD4 blasts was measured. *** indicates a significance of $p < 0.001$ (student's t-test), mean values + SEM are shown.

Similar to CD25 expression, sCTLA-4 expression was enhanced with regard to the amount of sCTLA-4 expressing cells as well as the sCTLA-4 MFI per CD4 blast in zinc supplemented MLCs. These results support the finding that zinc supplementation increases Foxp3 expressing iTregs. Notably, increased amounts of sCTLA-4 molecules exert elevated suppressive function on Teffs. The results presented in Fig. 9 are in accordance with the observed increased CTLA-4 mRNA levels in zinc-treated MLCs (Fig. 6). Changes in icCTLA-4 levels, which might also have been explained by increased CTLA-4 mRNA expression, were not as prominent as the increase in sCTLA-4 expression. This may be explained with immediate trafficking of newly expressed CTLA-4 molecules to the cell membrane leading to increasing sCTLA-4 expression with no detectable alteration in the icCTLA-4 level.

Not only do Tregs express CTLA-4, but also activated Teffs upregulate sCTLA-4 expression following TCR stimulation to regulate the strength of current immune responses. Resultantly, the enhanced CTLA-4 expression reported in Fig. 9 needs further analysis to confirm simultaneous CTLA-4 and Foxp3 expression in CD4⁺ blasts and hence to identify Tregs. For this purpose,

MLCs were incubated with or without 50 μ M zinc, respectively, for 8 days and analyzed for their CD4 and simultaneous sCTLA-4 and Foxp3 expression by flow cytometry. Gating of CD4⁺ cells is shown in Fig. 10 A. As displayed in Fig. 10 B, the amount of sCTLA-4⁺Foxp3⁺ expressing CD4⁺ blasts was significantly elevated in zinc-supplemented MLCs compared to the control, confirming that the increased CTLA-4 levels were allocated to enhanced Foxp3⁺ Tregs.

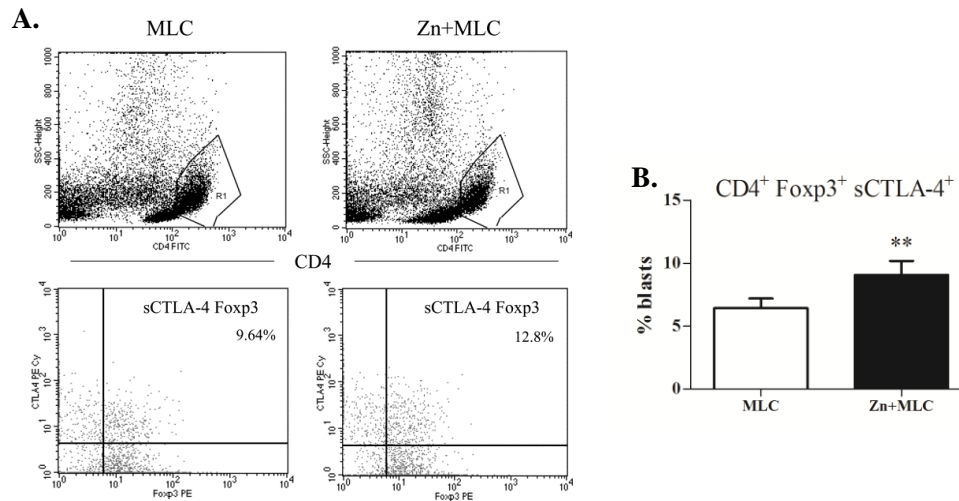


Fig. 10. Elevated amounts of sCTLA-4⁺Foxp3⁺ cells among CD4⁺ blasts. 2x10⁶/ml PBMCs were preincubated with or without 50 μ M zinc, respectively, for 15 min before mixing of MLCs. Cells were harvested after 8 days of incubation and analyzed for CD4, surface CTLA-4 (sCTLA-4) and Foxp3 expression by flow cytometry. Gating was performed on CD4⁺ blasts (A. displays one representative flow cytometric analysis out of n=10) and the amount of sCTLA-4⁺Foxp3⁺ (B.) among CD4⁺ blasts (n=10) was measured. ** indicates a significance of p<0.01 (student's t-test), mean values + SEM are shown.

Last of all, it was important to confirm co-occurrence of both enhanced CD25 expression and increased CTLA-4 levels in zinc-supplemented MLCs, both associated with increased amounts of Foxp3-expressing cells. For this reason, MLCs were incubated with or without 50 μ M zinc, respectively, for 8 days. Subsequently, cells were stained for CD25 and sCTLA-4 or CD25 and icCTLA-4, respectively, and analyzed by flow cytometry. Gating was performed on CD25⁺ (Fig. 11 A, D) cells to allow for analysis of the entire amount of alloreactive blasts (compare to Fig. 8 D.).

In zinc-supplemented MLCs the amount of CD25^{hi}sCTLA-4⁺ blasts increased significantly, as displayed in Fig. 11 B. In addition, with regard to the surface CTLA-4 MFI in CD25^{hi}CTLA-4⁺ blasts, a significant enhancement of sCTLA-4 expression per cell was observed. Similar to the results of CD4⁺icCTLA-4⁺ cells shown in Fig. 6 E. and F., the amount of CD25^{hi}icCTLA-4 expressing cells was not significantly altered by zinc supplementation. The icCTLA-4 MFI, on the other hand, was significantly increased in CD25^{hi}CTLA-4⁺ blasts (Fig. 11 F.).

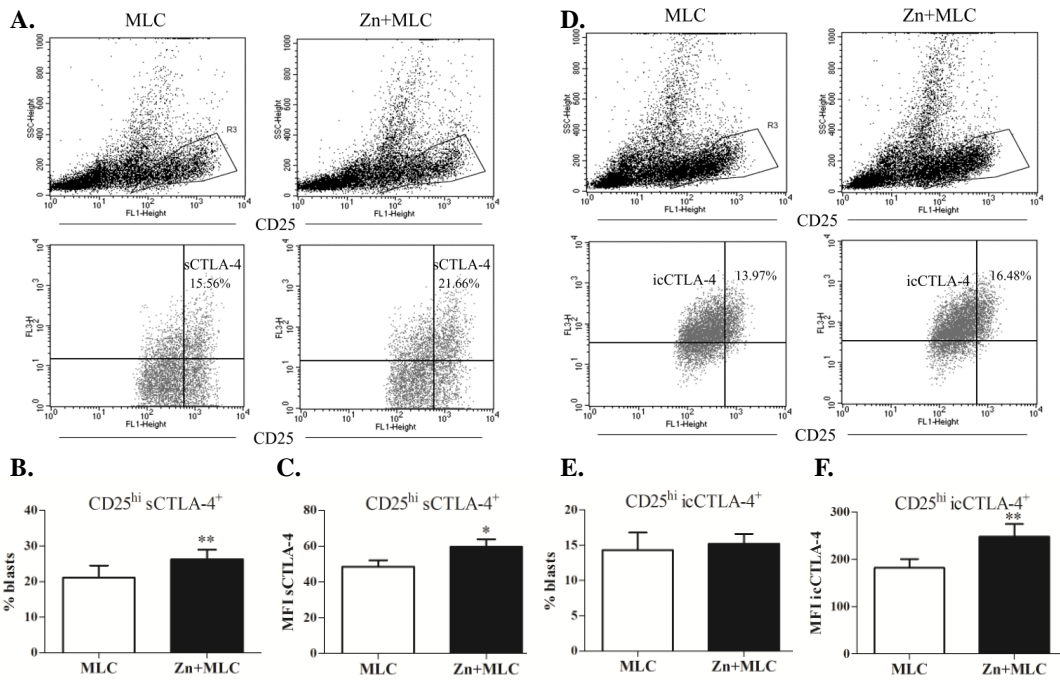


Fig. 11. **Elevated CD25^{hi}CTLA-4 expression among C25⁺ blasts by zinc.** 2×10^6 /ml PBMCs were preincubated with or without 50 μ M zinc, respectively, for 15 min before mixing of MLCs. Cells were harvested after 8 days of incubation and analyzed for CD25 and sCTLA-4 expression (A.-C.) or CD25 and icCTLA-4 expression (D.-F.) by flow cytometry. Gating was performed on C25⁺ blasts (A. and D. A. display one representative flow cytometric analysis out of n=5) and the amount of sCTLA-4 and icCTLA-4 expressing CD25 blasts (B., E.; n=5) and surface and intracellular CTLA-4 MFI (geo mean) (C., F.; n=5) of CD25^{hi}CTLA-4⁺ blasts was measured. * indicates a significance of $p < 0.05$, ** indicates a significance of $p < 0.01$, *** indicates a significance of $p < 0.001$ (student's t-test), mean values + SEM are shown.

These results confirm that the amount of concomitantly CD25^{hi} and sCTLA-4⁺ expressing cells grew in zinc supplemented blasts, supporting the finding that iTregs become upregulated in MLCs by zinc supplementation. Increasing Foxp3-levels, which upregulate *cd25* and *ctla-4* gene-expression, presumably were the reason for elevated CD25 and sCTLA-4 expression. sCTLA-4 as well as CD25 expression are important for the downregulation of immune responses and belong to the group of Treg markers.

4.2.4 Zinc Upregulates Expression of Activation-Marker CD69 in T Cells

The C-type lectin receptor CD69, a member of the type II C-lectin natural killer membrane receptor family, is highly upregulated following T cell activation and is postulated to be an early activation marker (Testi et al. 1989). For a more in-depth investigation of the immunomodulating effect of zinc in the MLC the amount of CD69 expressing alloactivated blasts was analyzed.

In CD4⁺ blasts, gated as displayed in Fig. 9 A., the amount of CD69 expressing cells was significantly elevated in zinc-incubated MLCs after 8 days of MLC culture. In addition, gating on CD25⁺ blasts, shown in Fig. 9 B., revealed increasing CD69 levels in CD25^{hi} expressing cells in zinc-treated MLCs. These results support the idea that zinc upregulates activation-induced Tregs,

since the greater amount of CD25^{hi} expressing cells in the zinc supplemented MLCs are CD69 positive, characterizing them as recently activated cells.

Lately, mounting evidence linked CD69 to the Treg subset, as mice lacking CD69 developed allergies and autoimmune diseases (Martin and Sanchez-Madrid 2011). Taking these findings into account, upregulation of CD4⁺CD69⁺ blasts and CD25^{hi}CD69⁺ blasts seems to contribute to the idea of zinc as a modulator of the allogeneic immune response and an inducer of allogeneic-specific iTregs.

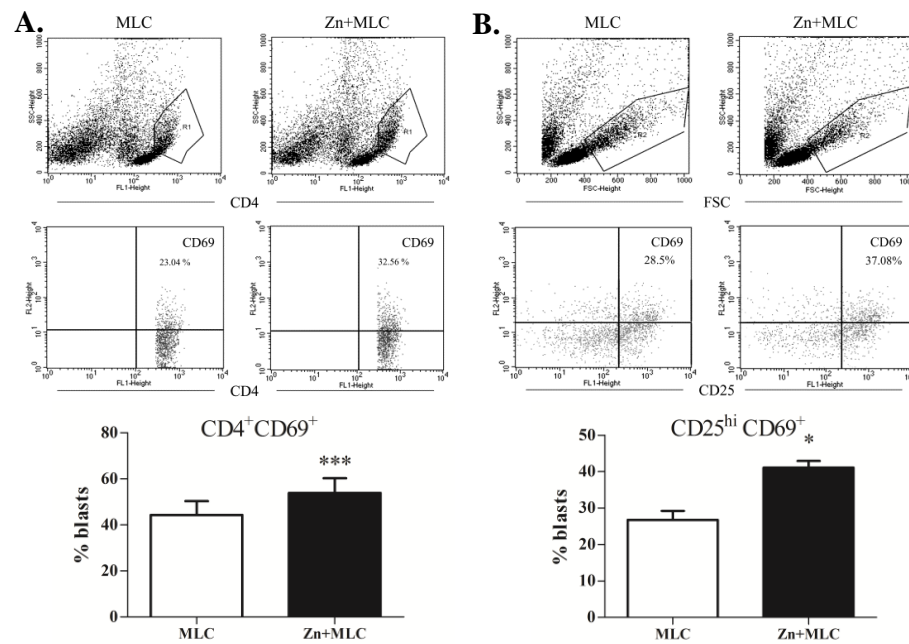


Fig. 12. Zinc elevates CD69 expression in alloactivated blasts. 2×10^6 /ml PBMCs were preincubated with or without $50 \mu\text{M}$ zinc for 15 min before mixing of MLCs. Cells were harvested after 8 days of incubation and analyzed for CD4⁺CD69⁺ (A) and CD25^{hi}CD69⁺ (B) expression by flow cytometry. Gating was performed on CD4⁺ blasts (A displays one representative flow cytometric analysis out of $n=6$) or CD25⁺ blasts (B. displays one representative flow cytometric analysis out of $n=4$) and the amount of CD4⁺CD69⁺ and CD25^{hi}CD69⁺ blasts was measured (A $n=6$, B $n=4$). * indicates a significance of $p < 0.05$, *** indicates a significance of $p < 0.001$ (student's t-test), mean values \pm SEM are shown.

4.2.5 Zinc Enhances PPAR- γ mRNA Expression

Recently, the peroxisome proliferator-activated receptor (PPAR)- γ was reported to have immunoregulatory function and has been proposed to prevent immunoinflammatory disorders (Hontecillas et al. 2011). In addition, PPAR γ is upregulated in activated T cells and therefore serves as an additional marker of T cell activation. Consequently, it was of interest to investigate whether PPAR γ is modulated by zinc in MLCs.

MLC mRNA was isolated from zinc-supplemented and control MLCs, respectively, after 72 h, 120 h, and 192 h. PPAR γ -expression was detected by real-time PCR. PBDG expression served as

housekeeping gene. The relative PPAR γ expression levels were normalized to the relative expression levels of the control at 72 h of MLC incubation to gain the changes in PPAR γ expression during the MLC course.

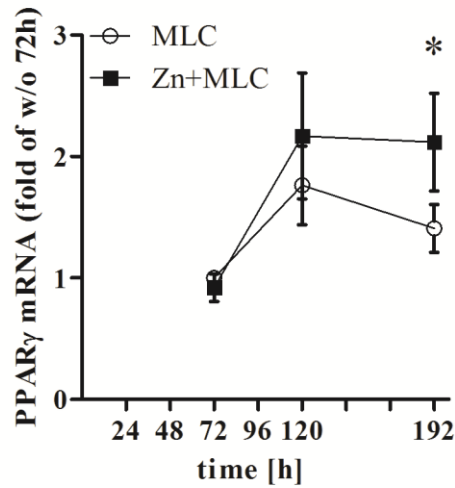


Fig. 13. **Zinc-enhanced PPAR γ mRNA expression in the MLC.** 2×10^6 /ml PBMCs were preincubated with or without $50 \mu\text{M}$ zinc for 15 min before mixing of MLCs. mRNA was isolated after 72, 120, and 192 hrs of MLC culture. PPAR- γ expression levels were quantified by RT-PCR and were normalized to PBGD. Results are compared to PPAR- γ expression levels of MLCs without zinc at 72 h ($n=7$). * indicates a significance of $p < 0.05$ (student's t-test), mean values \pm SEM are shown.

Fig. 13 displays higher increases of PPAR γ mRNA levels in the zinc supplemented MLCs compared to the untreated control after 8 days of incubation. This finding indicates a potential role for PPAR γ in zinc-induced allogeneic response modulation. Yet, the role of PPAR γ in Tregs has to be further elucidated. Zinc-induced upregulation of PPAR γ might also, similar to CD69 expression, suggest that the amount of activated T cells increases in the MLC, supporting the idea of iTreg induction.

Overall, the above presented data together with the finding that zinc enhances the amount of CD25^{hi} Foxp3⁺ and CTLA-4⁺Foxp3⁺ expressing cells among the alloactivated CD4 blasts, confirm the hypothesis that zinc is capable of upregulating CD4⁺ Foxp3⁺CTLA-4⁺ CD25^{hi} iTregs. Consecutively, molecular zinc targets responsible for elevated Tregs and immunomodulation of the MLC were investigated in a further experimental series described in the following.

4.3 Investigation of Molecular Zinc-targets in Tregs

4.3.1 Analysis of Foxp3 Promoter Methylation Pattern

Interestingly, zinc was shown to be associated with the modulation of epigenetic mechanisms (Wessels et al. 2013). Moreover, a role for DNA methylation patterns in the Foxp3 locus was identified, which discriminates Tregs from activated Foxp3-expressing effector T cells by affecting stability of Foxp3 expression (Lal et al. 2009). Increasing methylation of the *foxp3* locus is associated with decreasing stability of Foxp3 expression. Since zinc is capable of Foxp3-upregulation in activated T cells, as presented above, zinc may be capable of enhancing Foxp3-locus demethylation. This way, transient Foxp3 expression in activated T cells would be stabilized and Foxp3 protein expression would be prolonged. DNA methylation patterns were analyzed using the MethylScreen assay, which involves DNA ingestion by methylation-sensitive restriction enzymes (HhaI) and methylation-dependent restriction enzymes (McrBC) followed by quantitative real-time PCR of restriction-refractory template. Primers were designed to amplify a CpG rich template located within the human *foxp3* promoter region (first intron, containing 9 CpGs) to assess the Foxp3 methylation pattern. PBMCs derived from healthy male donors were used to measure methylation changes in the X-chromosomal directed *foxp3* locus. Zinc-supplemented PBMCs and MLCs were analyzed for the detection of Foxp3 CpG methylation pattern after 8 days of incubation.

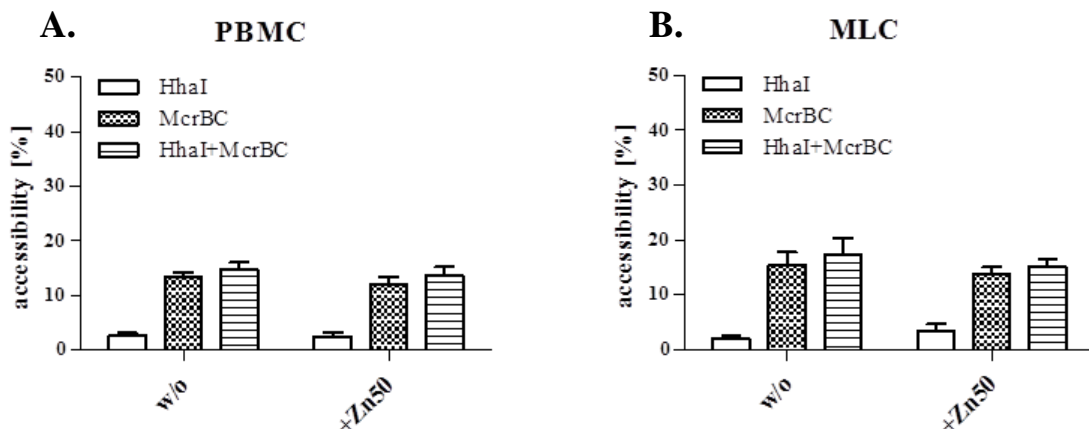


Fig. 14. **Zinc does not affect the Foxp3 methylation pattern.** 2×10^6 /ml PBMCs were incubated with or without 50 μM zinc for 8 days (A.). MLCs were generated comprising cells preincubated with or without 50 μM zinc for 15 min (B.). After eight days of incubation DNA was isolated and ingested by 60U HhaI, and 30U McrBC or both for 6 h at 37°C followed by quantitative real-time PCR of restriction-refractory template. Primers were used for a CpG-containing Foxp3 intron. Shown are the mean values+SEM of n=7 experiments.

In PBMCs no difference was detected in the accessibility of the DNA in both, methylation-sensitive and methylation-dependent restricted Foxp3 DNA between zinc-supplemented and

control cells (Fig. 16 A). In MLCs, a slight yet not significant increase in the amount of demethylated Foxp3 CpG islands in the promoter region by zinc supplementation was detected (Fig. 16 B). This effect underlined the above described upregulation of Foxp3 expression by zinc, but did not actually reveal the underlying mechanism. Therefore, further potential zinc targets were investigated.

4.3.2 Zinc-Associated Inhibition of the HDAC Sirt-1

Recent research demonstrated the capacity of zinc ions to inhibit the activity of various enzymes including the histone-deacetylase Sirt-1 (Chen et al. 2010). Chen et al. observed that exogenous zinc strongly inhibits Sirt-1 deacetylase activity (IC₅₀ of 0.82μM for Zn(Gly)). As Sirt-1 can deacetylate various histone and non-histone substrates, including Foxp3, a potential role for zinc-associated Sirt-1 inhibition in MLC modulation may exist, as decreased Sirt-1 activity was observed to stabilize Foxp3 protein levels (van Loosdregt et al. 2011).

In order to verify the ability of zinc to inhibit the HDAC Sirt-1, a Sirt-1 enzyme activity assay was performed. Purified Sirt-1 enzyme was incubated with various amounts of zinc, and the deacetylase-activity was obtained by detection of released fluorescence from deacetylated substrates. Furthermore, the general deacetylase inhibitor nicotinamide was used as control for assay functionality and for a comparison between the capacity of zinc and nicotinamide to inhibit Sirt-1. The IC₅₀ of nicotinamide for Sirt-1 inhibition is reported to be 88 μM (Lavu et al. 2008).

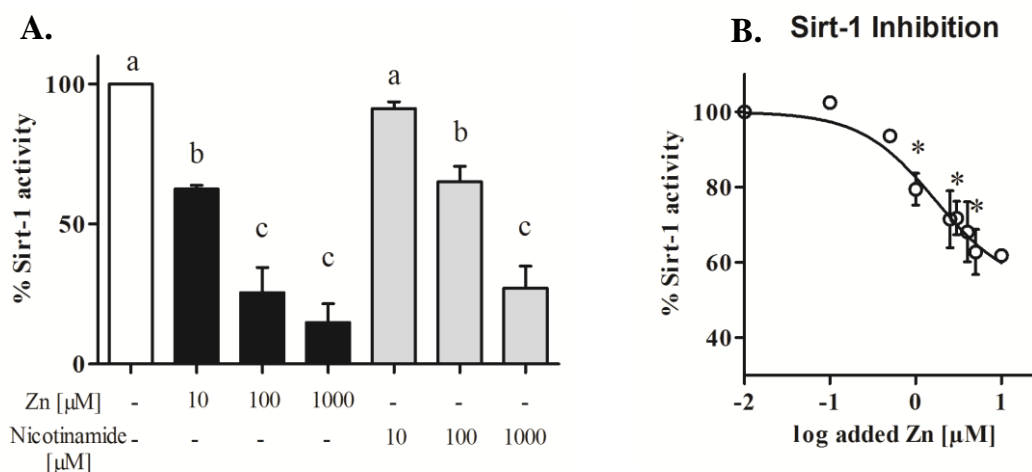


Fig. 15. **Zinc inhibits Sirt-1 activity.** Impact of zinc and nictotinamide on the activity of purified Sirt-1 enzyme was assessed using a Sirt-1 activity assay. A. 10, 100, and 1000 μM zinc or nicotinamide was added and Sirt-1 activity is shown as percentage of activity in the untreated control (n=3). B. Zinc was added ranging from 0.1 – 5 μM. Sirt-1 activity is shown as percentage of enzyme activity in the untreated control (n=3). * indicates a significance of p<0.05 (student’s t-test), different letters indicate significant differences (ANOVA, post test: Tukey); mean values + SEM (A) or mean values ± SEM (B) are shown.

Fig.15 A. shows that zinc was capable of inhibiting Sirt-1 activity significantly when added in concentrations of 10, 100, and 1000μM, suppressing Sirt-1 activity down to approximately 15%.

Since equal concentrations of nicotinamide reduced Sirt-1 activity to a much smaller amount, it was assumed that zinc inhibits Sirt-1 more effectively. Therefore, the IC₅₀ of zinc was further narrowed down by addition of zinc concentrations ranging from 0.1 – 5 μM zinc. Fig. 15 B. displays that Sirt-1 was significantly inhibited by applying zinc concentrations of 1 μM and more. Although zinc in these more physiological concentrations was not capable of inhibiting Sirt-1 completely, zinc reduced Sirt-1 activity to about 60%.

Due to the reaction-buffer composition used in the activity assay added zinc was buffered to a certain amount. Therefore, the actual amount of free zinc in the buffer was assessed to reveal the absolute amount of zinc required to obtain 50% Sirt-1 activity. Furthermore, 10 μM of the zinc-chelator TPEN was used to access Sirt-1 activity in very low zinc-levels. 50 μM TPEN and 50 μM zinc were added to reach minimal and maximal zinc levels needed for the quantification of free zinc, which was detected by usage of 1 μM of the zinc-specific probe FluoZin3-A. The obtained IC₅₀ value lies at 12.9 nM (with a confidence interval ranging between 5.36 and 31.31 nM), shown in Fig. 16.

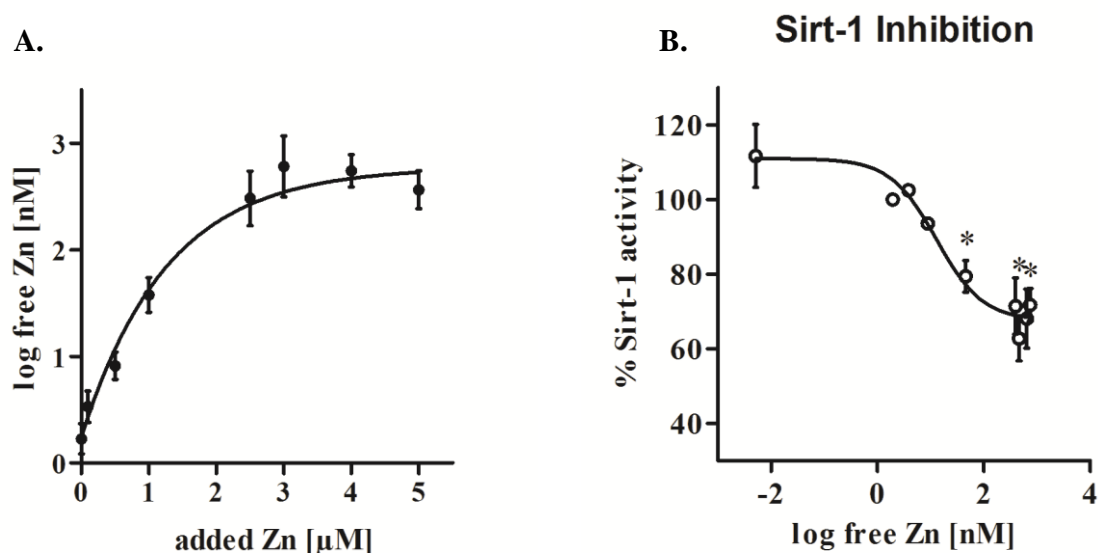


Fig. 16. **IC₅₀ determination of zinc-related Sirt-1 inhibition.** IC₅₀ was assessed by using a Sirt-1 activity assay (B). Zinc concentrations ranging from 0.1 to 5 μM zinc were added and Sirt-1 activity was measured. In addition, 10 μM TPEN was added and Sirt-1 activity was detected. Results are presented as percentage of the untreated control (n=3). The amount of definite free zinc in the assay was determined by 1 μM FluoZin-3 (A). Addition of 50 μM TPEN and 50 μM zinc were added to reach minimal and maximal zinc levels needed for quantification of free zinc (n=3). The IC₅₀ was calculated by searching the zinc concentration with inducing 50% Sirt-1 inhibition.* indicates a significance of p<0.05 (student's t-test); mean values ± SEM are shown.

Based on the above findings, it was of interest to measure the amount of free zinc in T cells treated with and without zinc in order to clarify if the intracellular zinc concentration reached a relevant level capable of intracellular Sirt-1 inhibition. In order to determine the free intracellular zinc levels of T cells, PBMCs were isolated and incubated with or without 50 μM zinc,

respectively, for 15 min prior to zinc-probe incubation and subsequent flow-cytometric analysis of intracellular zinc in CD3-labeled cells was performed. The time span of 15 min of zinc-incubation was chosen in accordance with the MLC experiments involving 15 min of zinc preincubation prior to MLC mixture.

The zinc probes ZinPyr-1 and FluoZin-3-AM were used for this purpose. Whereas FluoZin-3 measures the zinc content in T cell vesicles, Zinpyr-1 detects the amount of T cell cytosolic free zinc. Preincubation with zinc elevated cytosolic free zinc levels significantly up to around 0.1nM (Fig. 17 A). Vesicular zinc, on the other hand, did not increase following 15 min zinc preincubation. However, elevation of vesicular zinc was detected after 15 min of zinc preincubation with subsequent T cell activation via cells of the B cell-line Raji for 60 min compared to non-preincubated B cell-activated T cells, which were not preincubated with zinc. The increased vesicular zinc reached concentrations of around 0.9nM zinc (Fig. 17 B).

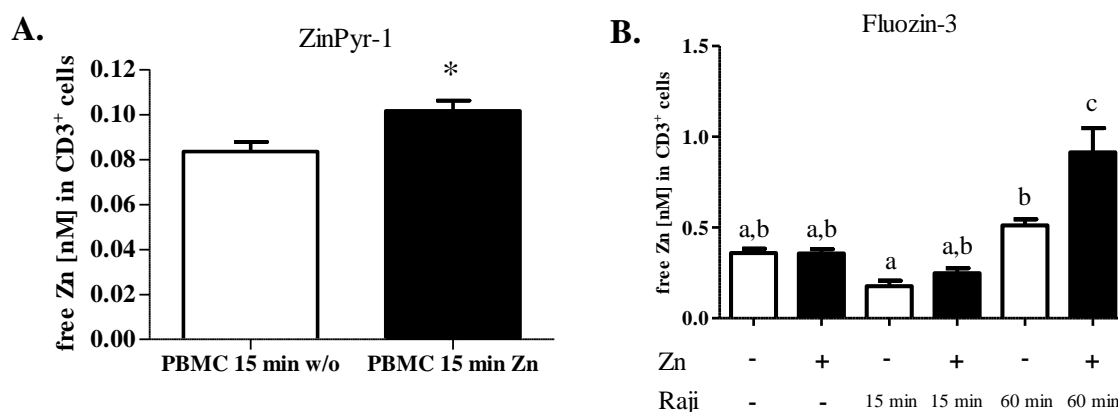


Fig. 17. **Zinc-supplementation increases intracellular zinc levels in T cells.** 2×10^6 /ml PBMCs were incubated with or without $50 \mu\text{M}$ zinc for 15 min. (A.) Intracellular free zinc was detected in 1×10^6 cells by using $10 \mu\text{M}$ of the zinc probe ZinPyr-1 ($n=6$). In addition, by gating on CD3^+ cells the zinc content of T cells was analyzed specifically. Minimum and maximum values were obtained by addition of $50 \mu\text{M}$ TPEN or $100 \mu\text{M}$ zinc and $50 \mu\text{M}$ pyrithione, respectively, to enable calculation of free zinc. B. The zinc probe FluoZin-3 ($1 \mu\text{M}$) was used to detect vesicular zinc in CD3^+ PBMCs. In addition, after preincubation with or without $50 \mu\text{M}$ zinc, cells were activated by the addition of 5×10^5 /ml Raji cells for 15 or 30 min prior to flow cytometry ($n=6$). * indicates a significance of $p < 0.05$ (student's t-test) and different letters indicate significant changes (ANOVA, post test: Tukey). Mean + SEM are shown.

4.3.3 Sirt-1 Inhibition Enhances Foxp3-Acetylation

Since the detected intracellular zinc levels in T cells comes below the determined Sirt-1 IC₅₀ of 13nM the relevance of the elevated zinc contents with regard to cellular Sirt-1 activity and its Foxp3 deacetylase capacity was assessed by immunoprecipitation/westernblot. It has been described earlier that Sirt-1 can function as protein deacetylase using Foxp3 as substrate (Kwon et al. 2012). The level of acetylated Foxp3 was assessed by immunoprecipitation of Foxp3 prior to western blotting using antibodies against Foxp3 and K31-acetylated Foxp3.

Although the results of the zinc-related IC₅₀ for Sirt-1 inhibition and the intracellular zinc concentration obtained in zinc supplemented T cells were somewhat inconsistent, Fig. 18 demonstrates an increasing effect on Foxp3-acetylation by zinc. Even if this effect was not statistically significant, it hints at zinc-inhibition of Sirt-1 and subsequent Foxp3-acetylation, leading to reduced Foxp3 protein degradation, as shown in Fig. 5.

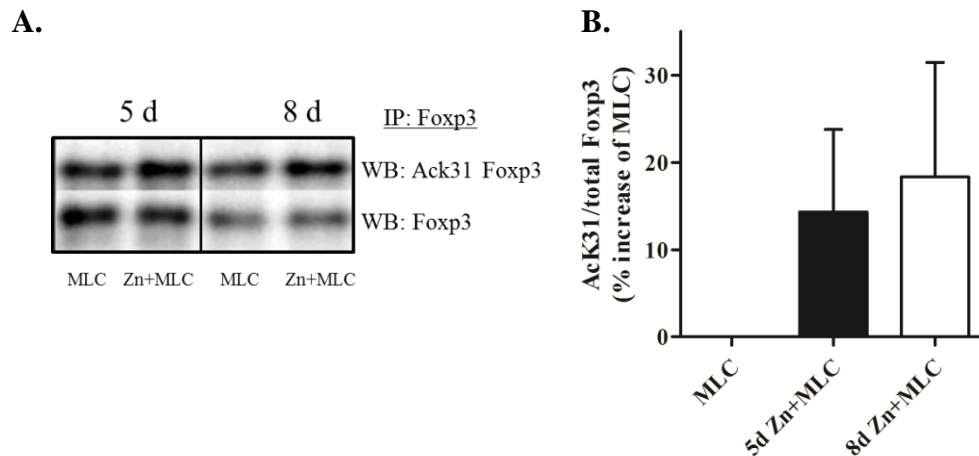


Fig. 18. **Zinc-supplementation increases Foxp3 acetylation.** 2×10^6 /ml PBMCs were incubated with or without $50 \mu\text{M}$ zinc for 15 min prior to mixing of MLCs. After 5 days and 8 days of incubation cell lysates were generated and Foxp3 protein was enriched by immunoprecipitation followed by western blotting. Protein levels of Ack31-acetylated and total Foxp3 were obtained. A. Representative blot out of $n=10$ is shown. B. Quantification by optical density determination was performed and AcK31-Foxp3 values were normalized to total Foxp3 values and presented as fold of untreated MLC. Mean values + SEM are shown.

4.3.4 Sirt-1 Inhibitor Ex-527 Mirrors Zinc Effects in MLCs

To validate the capacity of zinc to enhance Tregs by Sirt-1 inhibition, Ex-527 was used to investigate whether a Sirt-1-specific inhibitor was able to mimic the demonstrated zinc-effect. MLCs were generated and $\text{CD4}^+\text{Foxp3}^+$ expression was analyzed by flow cytometry. Gating of CD4^+ blasts was performed as described before (Fig. 4 A).

Indeed, the addition of $50 \mu\text{M}$ Ex-527 enhanced the amount of $\text{CD4}^+\text{Foxp3}^+$ expressing blasts significantly compared to the control (Fig. 19 B.), leading to abrogated IFN- γ expression in the MLC (Fig. 19 C). Concomitantly, addition of $5 \mu\text{M}$ Ex-527 caused the same effect to some extent, yet not significantly. Moreover, the effect of Ex-527 on cell viability was measured, revealing an increasing effect of Ex-527 on cell viability in the MLC (Fig. 19 D). These findings support the idea that Ex-527 attenuates the allogeneic immune reaction. In fact, the Sirt-1 inhibitor Ex-527 was capable of imitating the zinc effects observed in the allogeneic reaction, supporting the idea of zinc-inhibition of Sirt-1 being the molecular mechanism involved in Treg upregulation.

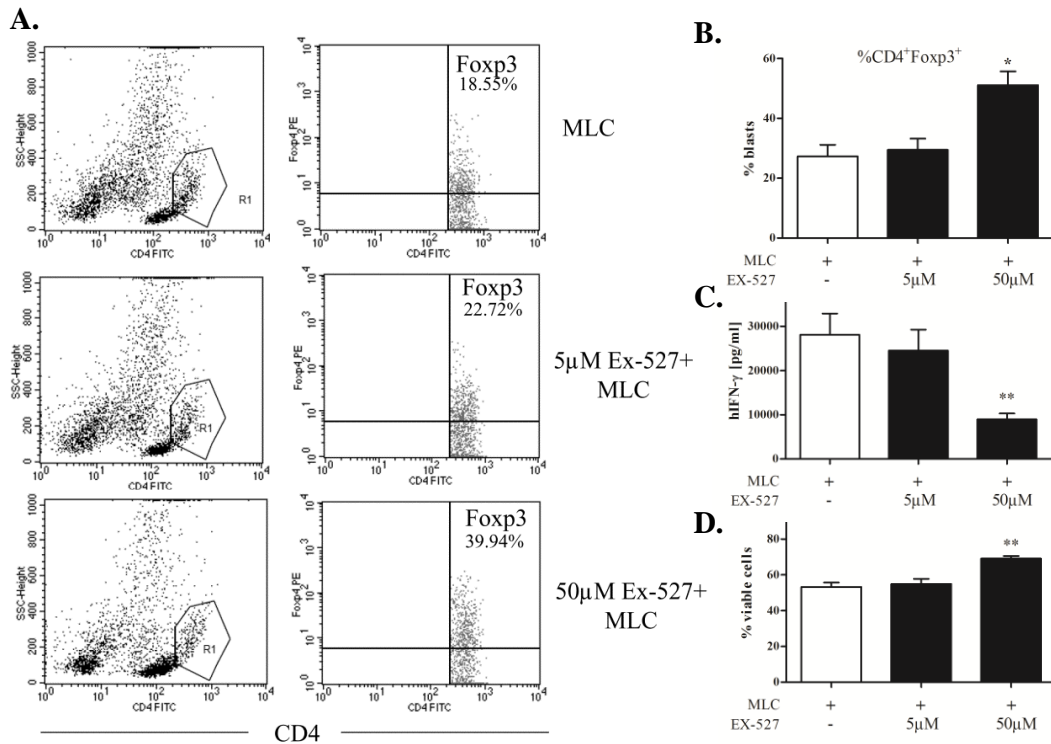


Fig. 19. Sirt-1 inhibitor Ex-527 imitates zinc-induced MLC modulation. 2×10^6 /ml PBMCs were incubated with or without 5µM or 50µM Ex-527 zinc for 15 min prior to MLC generation. After 8 days the cells were analyzed for CD4⁺Fxp3⁺ and supernatant was collected for IFN-γ ELISA. A. One representative flow-cytometric analysis out of n=6 is shown. B. The percentage of CD4⁺Fxp3⁺ cells is revealed. C. IFN-γ cytokine levels are presented. D. Cell viability was detected by PI staining of cells and results are displayed. * indicates a significance of p<0.05, ** indicates a significance of p<0.01 (student's t-test), and mean + SEM is shown.

Regarding the potential use of zinc or Ex-527 as therapeutic agents, the toxicity of both reagents in PBMCs was compared. Concentrations of 50µM zinc, which were applied in MLC experiments did not affect PBMC viability after 3 days of incubation (Fig. 20). Even increasing zinc concentrations did not prove to be toxic. In contrast, increasing concentrations of Ex-527 decreased the PBMC viability significantly. Therefore, while showing similar effects as Ex-527, zinc displays less toxicity and is hence more beneficial than Ex-527. Notably, Ex-527 treatment of MLCs increased total cell viability due to decreased allogeneic reaction, which overlays the toxic effect of Ex-527 on PBMCs (Fig.19). Yet, incubation of non-activated PBMC with Ex-527 reveals its potential harm, which was not achieved by zinc-incubation.

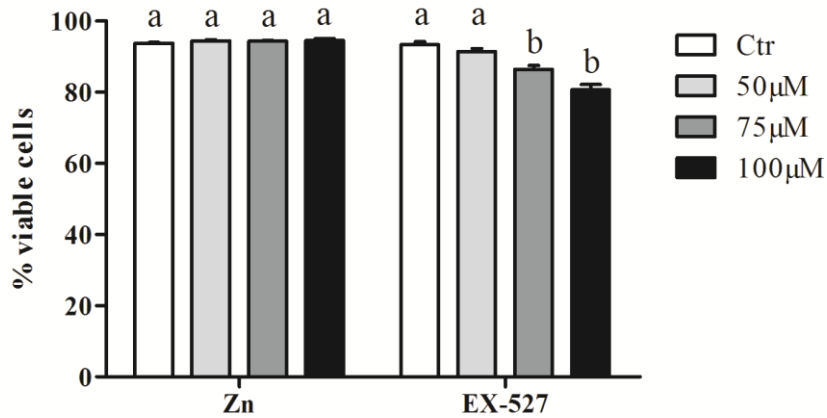


Fig. 20. **Effects of zinc and Ex-527 on viability of PBMCs.** 2×10^6 /ml PBMCs were incubated for 3 days with or without 50, 75, and 100 μ M zinc or Ex-527. Cell toxicity was obtained by PI staining (1 μ g/ml) prior to flow-cytometric analysis and is displayed as percentage of viable cells. Shown are the mean values + SEM of n=3 experiments. Different letters indicate significant differences (ANOVA, post test: Tukey).

4.4 *In Vivo* Zinc-Supplementation Upregulates Tregs in *In Vitro* Generated MLCs

In the previous section, MLC supplementation with zinc was shown to upregulate Tregs *in vitro*, leading to diminished allogeneic immune reaction. The relevance of these findings for a potential therapeutic application of zinc to modulate the allogeneic response *in vivo* was investigated in this study by measuring the effect of physiological relevant zinc doses supplemented to immune-competent subjects. For this purpose healthy male subjects were administered either 10 mg zinc/day supplemented as Zn-Aspartate (n=9) or placebo (n=7) over a time period of 10 days. Blood samples were taken before administration (t=0d) and again after 10 days of intake (t=10d). Serum zinc levels were also measured at these time points to assess the subject's zinc status. Furthermore, PBMCs were isolated and MLCs were generated at day 0 and 10. The combination of different donor PBMCs in the MLC resulted in n=9 MLCs in the placebo group and n=16 MLCs in the zinc group. Uneven amounts of MLCs in the placebo and zinc group was due to a drop out of volunteers. After 8 days of *in vitro* MLC incubation, the amount of CD4⁺Foxp3⁺ expressing cells within the CD4⁺ blasts was analyzed by flow cytometry (Fig. 21 A, B).

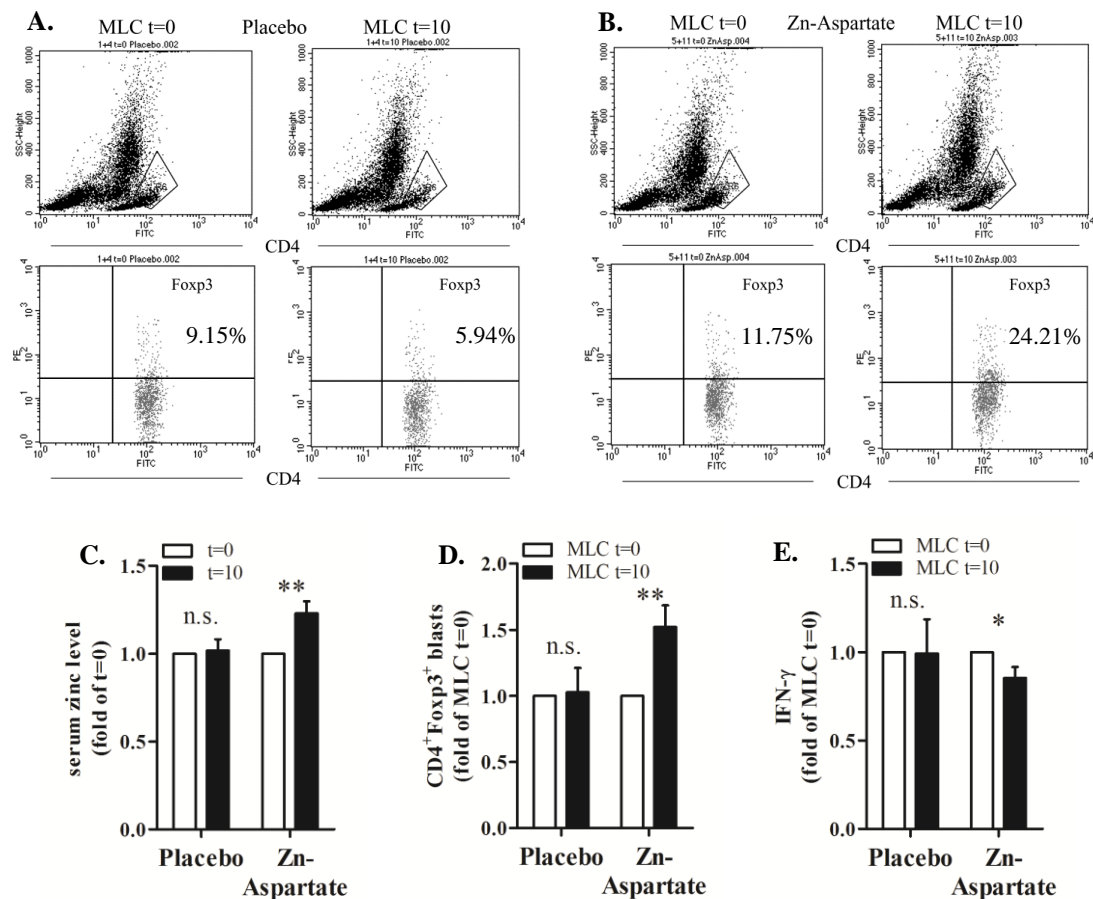


Fig. 21. **Impact of in vivo zinc supplementation on ex vivo generated MLCs.** 7 healthy, male subjects were supplemented with placebo (10 mg/day) for 10 days; 9 healthy, male subjects were supplemented with 10mg/day zinc supplied as Zn-Aspartate for 10 days. Blood was collected at day 0 and day 10 and serum zinc levels were detected by atomic absorption (C. placebo n=7, Zn-Aspartate n=9.). At time points t=0 and t=10 MLCs were generated. After 8 days supernatants were collected and IFN- γ levels were measured (E. placebo n=9, Zn-Aspartate n=16) and CD4⁺Foxp3⁺ expression was analyzed by flow cytometry (D. placebo n=9, Zn-Aspartate n=16). Gating on CD4⁺ blasts was performed as presented in A. and B. (A. and D. display one representative flow cytometric analysis of n=9 or n=16, respectively). Values of MLC generated at t=10 were normalized to values of MLC generated at t=0. * indicates a significance of p<0.05, ** indicates a significance of p<0.01 (student's t-test), mean values + SEM are shown.

Other than *in vivo* placebo supplementation, *in vivo* supplementation with Zn-Aspartate significantly increased the amount of CD4⁺Foxp3⁺ blasts in *ex vivo* generated MLCs (Fig.21 D). Concomitantly, MLC supernatants were collected after 8 days of MLC incubation and analyzed for IFN- γ expression in MLCs generated at t=0 and t=10. IFN- γ levels were significantly reduced in the MLCs generated at t=10 compared to MLCs generated at t=0 in the zinc-group compared to the placebo group (Fig.21 E). Verification of serum-zinc levels revealed increased zinc levels after 10 days of zinc administration in the zinc-supplemented volunteers, which were not detected after 10 days of placebo administration (Fig. 14 C).

These findings indicate an increased amount of Tregs in MLCs generated of PBMCs derived from *in vivo* zinc-supplemented individuals, mirroring the results observed in *in vitro* zinc

supplementation experiments and thus emphasizing the relevance of zinc supplementation in pharmacological doses for modulation of the allogeneic immune reaction.

4.5 Zinc-Induced Tregs Attenuate the Allergen-Induced Immune Response

Besides the Graft-versus-Host disease, allergic diseases belong to the group of adverse immune overreactions. Allergies are an abundant health problem, affecting a copious number of people worldwide. As such, the development of therapeutic agents to ameliorate allergic immune reactions remains thus a primary research goal. Notably, allergies are frequently accompanied by zinc-deficiency (Di Toro et al. 1987). Subsequently, another important aim of this study was to verify zinc capabilities, if any, of upregulating Tregs in the allergic immune reaction, to lead to an improvement of the disease.

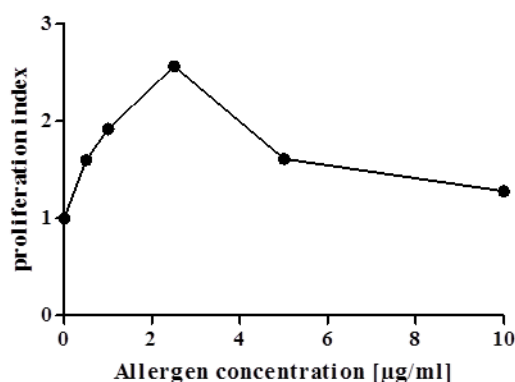


Fig. 22. **Timothy grass allergen extract induces PBMC proliferation.** Different allergen concentrations ranging from 1-10 µg/ml were used to detect the most potent allergen concentration for PBMC proliferation in further experiments. Shown are data from one experiment using PBMC of an allergic individual. Proliferation was measured by ³H-thymidine assay.

The allergic immune reaction was investigated using extracted timothy grass pollen, known to trigger hay fever in allergic individuals. With the aim of establishing the most effective *in vitro* allergen concentration, PBMCs were isolated from one individual suffering from seasonal hay fever. The cells were subsequently stimulated with various concentrations of the timothy grass allergen extract. After five days of stimulation, proliferation of the cells was assessed, revealing the most potent allergen concentration to activate allergenic immune reactions *in vitro*. Based on this result, further experiments were performed using 2.5 µg/ml (Fig. 22).

Subsequently, the capacity of zinc to attenuate the allergic immune reaction was investigated by measuring various immune parameters, including proliferation and cytokine production. The allergen-induced proliferation of responder derived PBMCs was compared to non-responder PBMCs, with the aim of confirming that the allergen-extract activates PBMCs of allergic

individuals specifically. Furthermore, the effect of zinc on the allergen-induced proliferation was assessed. Proliferation was measured by the ^3H -thymidine assay. The results were normalized to the respective control (PBMC without zinc and without allergen treatment) for a sound comparison.

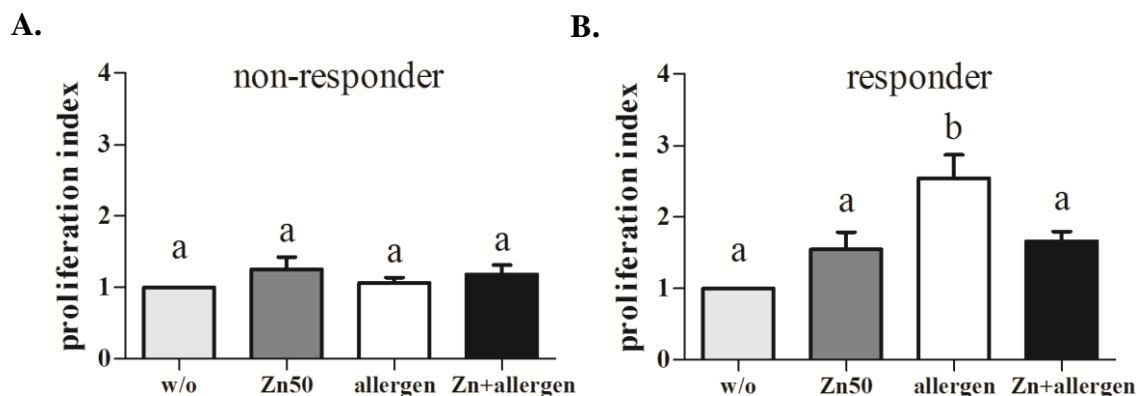


Fig. 23. **Impact of zinc on proliferation levels in timothy-grass treated cells.** PBMCs from non-allergic (A) and allergic (B) subjects were preincubated with or without 50 μM zinc before stimulation with or without 2.5 $\mu\text{g}/\text{ml}$ timothy-grass allergen for 5 days. Proliferation was assessed by ^3H -thymidine assay (A: n=8; B: n=12). Non-identical letters indicate a significance of $p < 0.05$ (ANOVA, post test: Tukey), mean values \pm SEM are shown.

As shown in Fig. 23, five days of allergen-incubation significantly enhanced proliferation in PBMCs derived from allergic individuals (B), in contrast to PBMCs of control individuals (A). Pre-incubation with zinc abolished the allergen-induced proliferation of allergic PBMCs, reaching a proliferation level comparable to those obtained by treatment with zinc only. These results confirm a beneficial impact of zinc in the allergic immune reaction.

As the measurement of PBMC proliferation serves as a potent parameter for the detection of proceeding immune reactions, whilst lacking detailed information about the immune response, additional immune parameters were investigated. These involved the detection of cytokine levels in the supernatant of PBMCs incubated with allergen extract following pretreatment with or without zinc. The cytokine production of the Th1 cytokines IFN- γ and TNF- α , as well as levels of the Th2 cytokine IL-10 were verified by ELISA. Following 24 h of incubation with 2.5 $\mu\text{g}/\text{ml}$ allergen of PBMCs pretreated with or without zinc revealed that PBMC did express TNF- α only when stimulated with allergen (Fig. 24 A), confirming the results provided by the proliferation assay (Fig. 24 B). Pre-incubation with zinc further increased the amount of released TNF- α significantly. After 5 days of allergen exposure the expression of the determining Th1 cytokine IFN- γ was slightly elevated following zinc preincubation (Fig. 24 B). In contrast, the Th2 cytokine IL-10 showed decreased levels after 5 days of allergen exposure when pre-treated with zinc (Fig. 24 C).

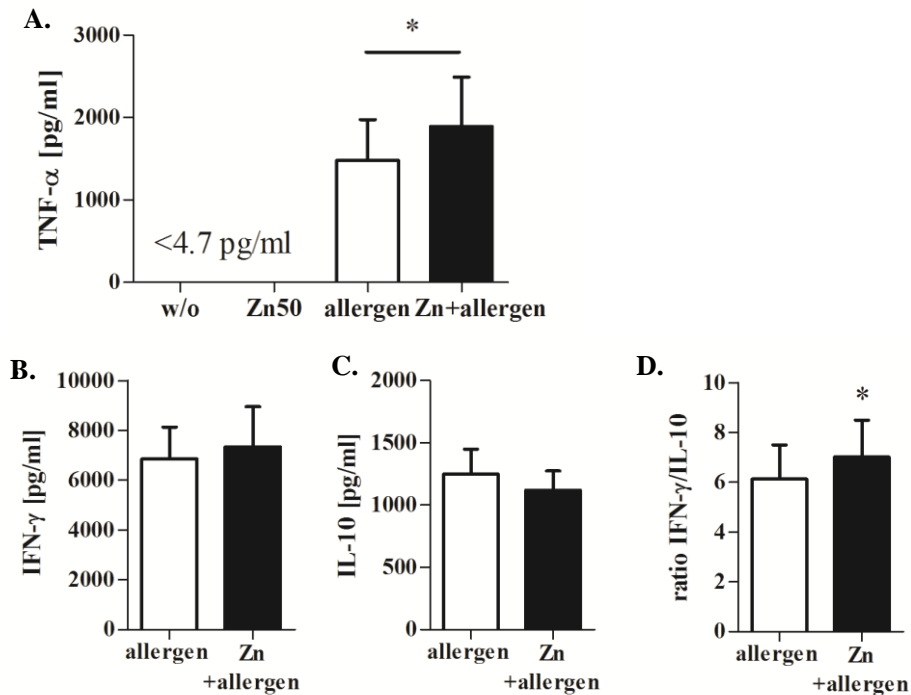


Fig. 24. **Altered Th1 and Th2 cytokine levels in allergen-activated zinc-supplemented PBMCs.** 2×10^6 /ml PBMCs of allergic subjects were pre-incubated with or without $50 \mu\text{M}$ zinc for 15 min prior to activation with $2.5 \mu\text{g/ml}$ timothy-grass allergen. Supernatants were collected after 24hrs for TNF- α (A.; $n=6$), and 5 days for IFN- γ (B; $n=6$) and IL-10 (C; $n=6$) and cytokine levels were analyzed by ELISA. D. ratio of IFN- γ to IL-10 is shown. * indicates a significant difference with $p < 0.05$ (student's t-test), and mean values + SEM are shown.

Information on the ratio of Th1 to Th2 cytokines was obtained by calculating the ratio of IFN- γ / IL-10 levels. This ratio revealed a significant zinc-induced shift towards Th1 cytokines, which was further underlined by the finding that the Th1 cytokine TNF- α showed enhanced levels in zinc-preincubated cells after 24 h of allergen exposure compared to allergen-activated cells without zinc (Fig. 24 A). Considering the type-I allergic reaction as a Th2 driven immune response, a shift towards Th1 cytokines by zinc promotes allergy attenuation.

Moreover, the levels of Th1 and Th2 cytokines were obtained by measuring IFN- γ and IL-4 mRNA expression by real-time PCR since IL-4 detection by ELISA is not feasible in human PBMC. The cytokine's mRNA levels were detected of zinc-pretreated and control PBMCs derived from allergic volunteers activated with $2.5 \mu\text{g/ml}$ allergen after 4 h and 3 days. The cytokine expression levels were normalized to the expression levels of the housekeeping gene PBGD and standardized to the values of 4 h allergen-treated PBMCs. Fig. 25 A displays increasing IFN- γ production by cells preincubated with zinc in response to allergen compared with the control. The increase was only marginal after 4h of incubation and increased slightly, yet not significantly, after 3 days of incubation. In contrast, the Th2 cytokine IL-4 mRNA levels

decreased after 4 h of allergen-incubation in the zinc-treated samples, which was not statistically significant (Fig. 25 B). After 3 days of incubation IL-4 levels were almost abolished.

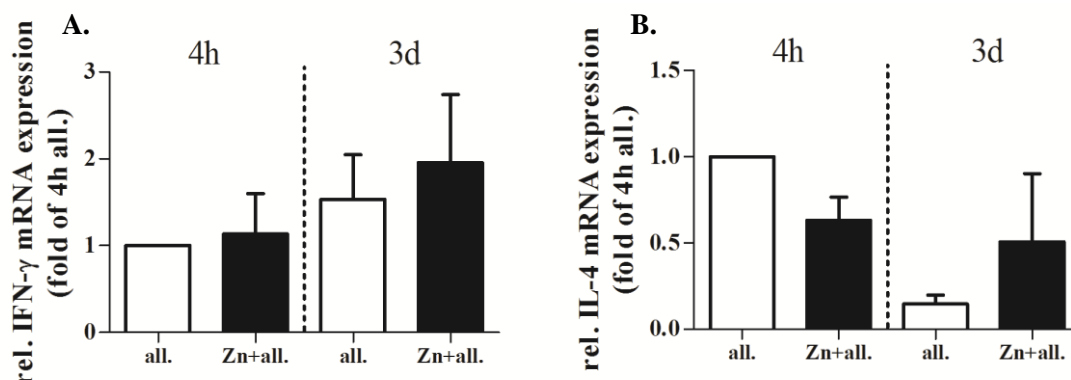


Fig. 25. Zinc-induced shift of Th1/Th2 ratio towards Th1 cytokines in allergen-activated PBMCs. 2×10^6 /ml responder-derived PBMCs were preincubated with or without $50 \mu\text{M}$ zinc and activated with $2.5 \mu\text{g/ml}$ allergen extract. RNA was isolated after 4h and 3 days of incubation and IFN- γ (A; $n=6$) and IL-4 (B; $n=6$) mRNA expression levels were quantified by RT-PCR and normalized to PBGD. Results were standardized to expression levels without zinc at 4 hrs of allergen incubation. Mean values + SEM are shown.

The reason for non-significant differences between the control and zinc-treated cells may be due to the fact that only a considerably small amount of T cells are activated by allergen-exposure. However, these results are in accordance with the cytokine levels detected by ELISA and support the idea that zinc modulates the allergic immune reaction as mirrored in decreased proliferation and modified cytokine expression. As zinc was shown to upregulate Tregs in the MLC the capacity of zinc to upregulate Tregs among the allergen-activated cells was assessed. PBMCs from individuals suffering from seasonal hay fever were isolated and preincubated with or without $50 \mu\text{M}$ zinc for 15 min followed by incubation with $2.5 \mu\text{g/ml}$ of timothy grass allergen extract. After 5 days of incubation $\text{CD4}^+\text{Foxp}^+$ allergen-activated blasts were analyzed by flow-cytometry. Gating was performed on CD4^+ blasts as displayed in Fig. 26 A, analogous to flow cytometric analyses in MLCs (Fig. 4 A). Indeed, zinc supplemented cells revealed a significant increase in $\text{CD4}^+\text{Foxp}^+$ blasts compared to control cells (Fig. 26 B).

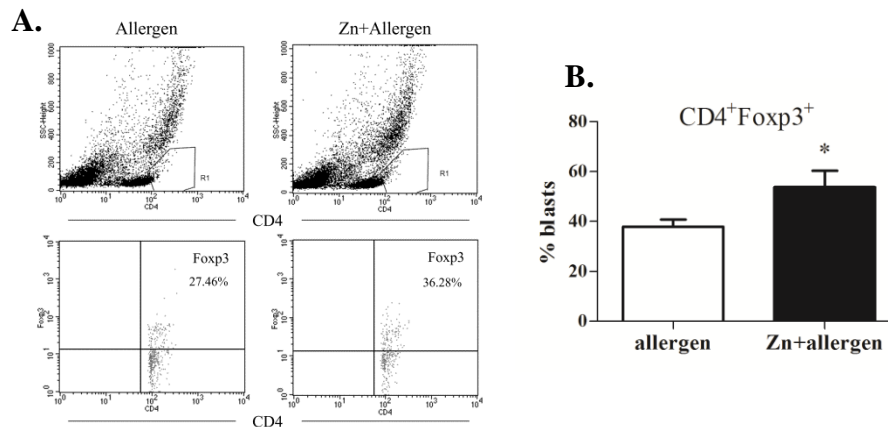


Fig. 26. **Zinc induces the upregulation of Foxp3 expression in allergen-activated CD4⁺ blasts.** 2×10^6 /ml PBMCs derived from allergic individuals were preincubated with or without $50 \mu\text{M}$ zinc for 15 min followed by stimulation with $2.5 \mu\text{g}/\text{ml}$ timothy-grass allergen for 5 days. The amount of Foxp3⁺ allergen-activated CD4⁺ blasts within $50 \mu\text{M}$ zinc-pretreated PBMCs was analyzed by flow-cytometry (n=5). Fig. A displays one representative flow cytometric analysis out of n=5. * indicates a significance of $p < 0.05$ (student's t-test), and mean values + SEM are shown.

Additionally, PBMCs derived from hay-fever affected individuals (responder) and control PBMCs derived from donors lacking immune sensitivity towards this allergen (non-responder) were preincubated either with or without $50 \mu\text{M}$ zinc for 15 min prior to stimulation either with or without timothy grass allergen extract. After 5 days of incubation, the cells underwent flow-cytometric analysis for the detection of CD4⁺CD25^{hi} expressing cells among CD4⁺ activated blasts. CD4⁺ blasts were gated as described above (Fig. 26). Within the non-responder group, zinc supplementation enhanced the amount of CD4⁺CD25^{hi} expressing blasts significantly compared to the control (Fig. 27 C). Stimulation with the allergen alone did not affect Treg levels; yet, slightly increasing Treg amounts were observed in zinc-preincubated PBMCs stimulated with allergen (Fig. 27 C). This result confirmed the insensitivity of non-responders to the allergen and approves the induction of iTregs in otherwise activated CD4⁺ cells by zinc. Within the responder group zinc alone also increased the Treg level, though not significantly (Fig. 27 D). This may be related to the declined Treg response found in allergic patients. Incubation with the allergen only, caused an insignificant increase in Tregs as well, due to allergen-induced Tregs, whereas preincubation with zinc prior to allergen exposure showed a significant upregulation of CD4⁺CD25^{hi} Tregs (Fig. 27 D). These results confirm the idea that zinc is capable of upregulating Tregs in activated T cell populations, including allergen-activated T cells. Again, upregulation of the transcription factor Foxp3 is likely to be associated with the increased CD25 expression.

For further verification an additional Treg marker, CTLA-4, was measured in the CD4⁺ blasts of cultured responder PBMCs. The flow cytometric analysis of the CD4⁺ blasts was performed as described before (Fig. 4 A). Since the non-responder cells did not exhibit elevated Treg levels after allergen treatment, thereby excluding the detection of unspecific allergen effects, further

analysis was conducted with PBMCs from allergic subjects only. Moreover, as a declared aim of this experiment was the investigation of zinc-related modulation of Tregs in an allergy model, the effect of zinc pretreatment was assessed only in allergen-exposed PBMC, omitting the effect of zinc in allergen-untreated PBMC.

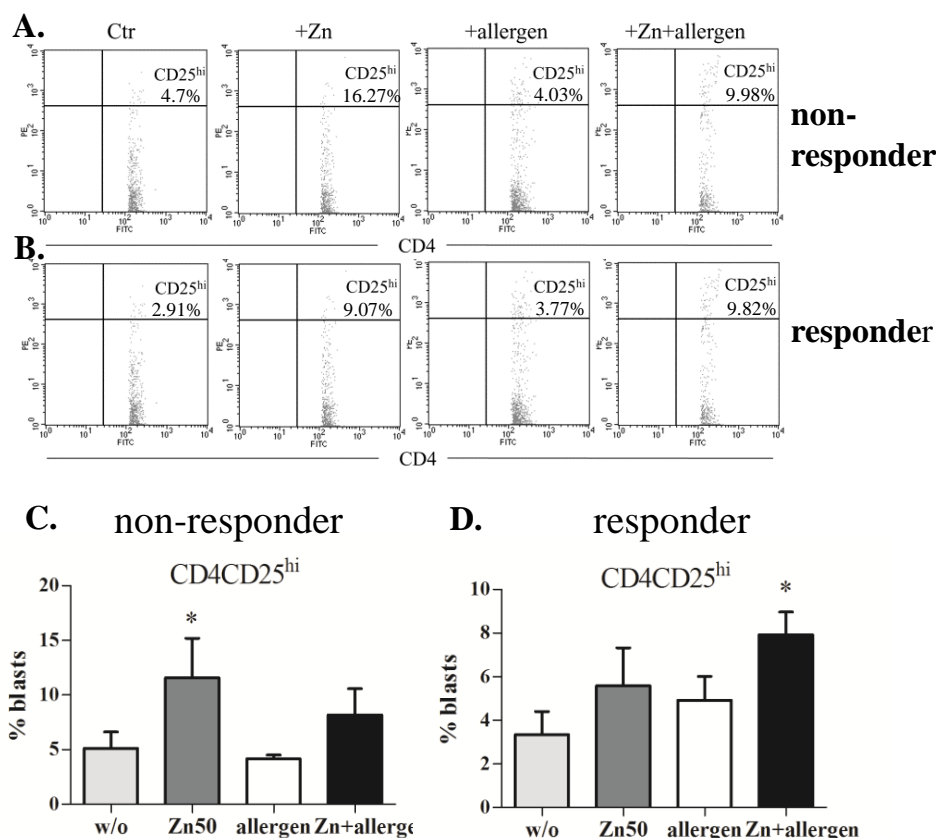


Fig. 27. Zinc upregulates the amount of CD25^{hi} expressing Tregs in allergen-activated blasts. 2×10^6 /ml PBMCs were preincubated with or without $50 \mu\text{M}$ zinc and subsequently stimulated with or without $2.5 \mu\text{g}/\text{ml}$ allergen for 5 days. A. and B. show one representative flow cytometric analysis out of $n=6$ for non-responder or one out of $n=6$ for responder respectively. In Fig. C the amount of CD25^{hi} expressing CD4⁺ blasts is shown including PBMCs of non-timothy grass allergic subjects ($n=6$). Fig. D displays results for responder-derived PBMCs ($n=6$). * indicates a significance of $p < 0.05$ (student's t-test), and mean values \pm SEM are shown.

In this experiment the expression of surface CTLA-4 was detected only, because no significant impact of zinc on the intracellular expression was observed in MLCs (Fig. 9 E, F). The percentage of CD4⁺sCTLA-4⁺ expressing cells and the MFI of sCTLA-4 among CD4⁺sCTLA-4⁺ cells was analyzed. In addition, CTLA-4 mRNA expression was measured to gain information about zinc-induced changes in the amount of total CTLA-4 expression. CTLA-4 mRNA expression was normalized to PBGD mRNA levels and standardized to respective values of the control. Zinc-supplemented responder PBMCs showed an increased amount of CTLA-4⁺ cells among the CD4⁺ blasts compared to the control, as provided in Fig. 28 A, which was nearly statistically significant ($p=0.06$). Whereas CTLA-4 MFI did not show a zinc-related association

(Fig. 28 B), CTLA-4 mRNA expression was significantly increased in the zinc-preincubated samples compared to the control (Fig. 28 C). Hence, these experiments confirmed an upregulation of iTregs, although not as sound as in the MLC. Still, enhanced CTLA-4 mRNA expression points to the fact that zinc influences the expression of this Treg marker.

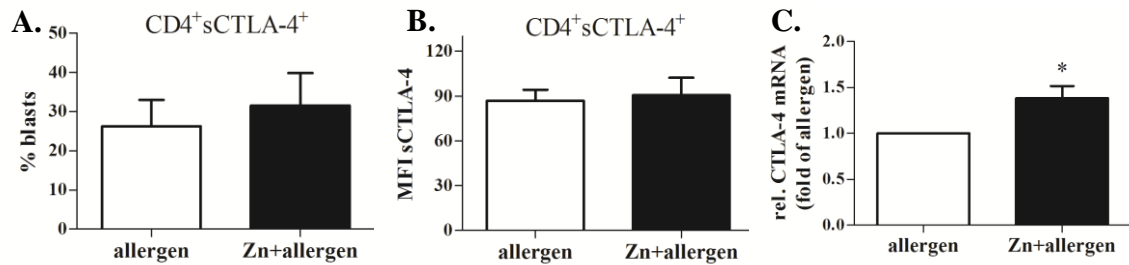


Fig. 28. Zinc affects CTLA-4 expression in allergen-activated PBMC. 2×10^6 /ml PBMCs of allergen-responder were preincubated with or without $50 \mu\text{M}$ zinc and subsequently stimulated with $2.5 \mu\text{g}/\text{ml}$ allergen for 5 days. In Fig. A the amount of CTLA-4⁺ expressing CD4⁺ blasts is shown (n=5). In Fig. B CTLA-4 MFI of CTLA-4⁺CD4⁺ blasts is displayed (n=5). (C.) CTLA-4 expression levels were quantified by RT-PCR and were normalized to PBGD. Results were standardized to CTLA-4 expression levels of PBMCs stimulated with allergen (n=6). * indicates a significance of $p < 0.05$ (student's t-test), and mean values \pm SEM are shown.

In conclusion, the results sustain the finding that zinc has the capacity to enhance immunomodulating Tregs upon T cell activation, inducing the attenuation of the allergic reaction. That way, a potent therapeutic role for zinc supplementation for the alleviation allergic diseases could be assumed.

4.6 Zinc Ameliorates Murine EAE Disease Course

4.6.1 Zinc Upregulates Tregs in Murine MLCs

A prerequisite for the usage of zinc in murine disease models for further investigations of the immunomodulating role of zinc is its verification in murine MLCs *in vitro*. Murine splenocytes were isolated from C57BL/6 mice and cultured in MLCs with cells of the murine macrophage cell line RAW264.7 (BALB/c-derived). The disparate H-2 haplotypes (H-2^b in C57BL/6 and H-2^d in BALB/c) triggered the allogeneic response. After 5 and 8 days of incubation either with or without $50 \mu\text{M}$ zinc, cell lysates were generated and Foxp3 expression was analyzed by western blot. Additionally, expression of the housekeeping gene β -actin was assessed and Foxp3 levels were normalized to β -actin (Fig. 29 A). Quantification of western blot results displayed elevated, albeit statistically insignificantly, enhanced Foxp3 protein levels in zinc-supplemented cells (Fig. 29 B). Moreover, cells were used for the measurement of CD4⁺Foxp3⁺ expressing blasts by flow-cytometry after 5 and 8 days. Gating of CD4⁺ blasts was performed as described for human

MLCs above (Fig. 4 A). Notably, flow cytometric analysis of CD4⁺ blasts revealed significantly increased amounts of CD4⁺Foxp3⁺ cells after 5 and 8 days of MLC incubation (Fig 29 C).

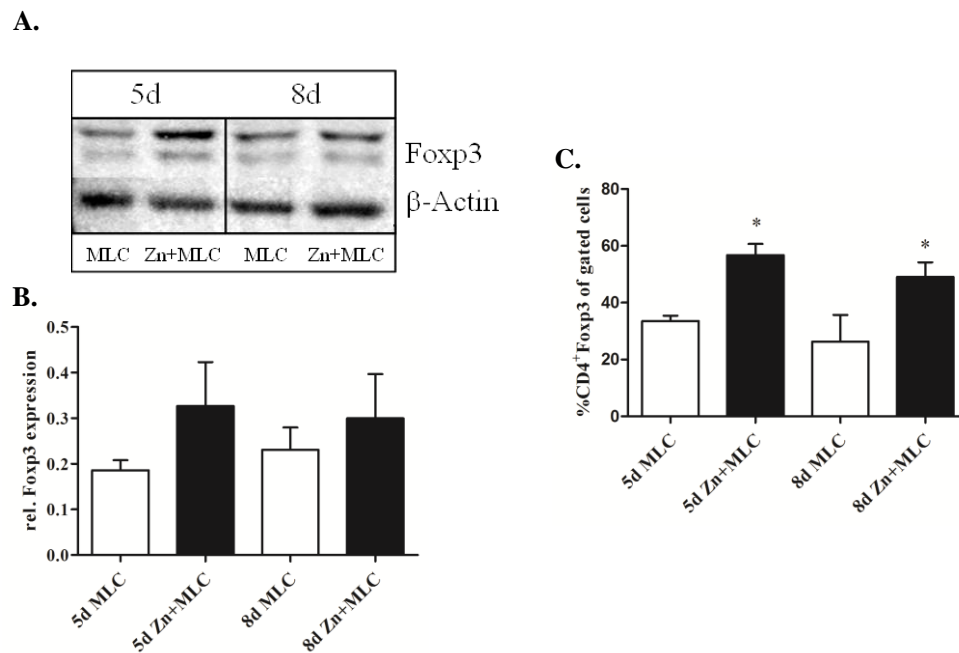


Fig. 29. Zinc upregulates Tregs in murine MLCs. 2×10^6 /ml splenocytes derived from C57BL/6 mice were cultured with 1×10^6 /ml RAW264.7 cells after preincubation with or without $50 \mu\text{M}$ zinc. Cell lysates were generated after 8 days of incubation and Foxp3 and β -actin protein levels were detected by western blotting, one representative blot out of $n=3$ is displayed in A. Western blot results were quantified by optical density determination and Foxp3 values were normalized to β -actin values (B.). Flow cytometric analysis was performed to detect Foxp3 expression in gated CD4⁺ blasts (C.). $n=3$, * indicates a significance of $p < 0.05$ (student's t-test), mean values + SEM are shown.

This data suggests that zinc is capable of inducing Tregs not only in human alloactivated cells but also in murine MLCs, which gives way for further analysis of zinc on the modulation of immune responses in *in vivo* animal studies. This study used the murine experimental autoimmune encephalomyelitis (EAE) model to gain insight into the potential impact of zinc in autoimmune diseases.

4.6.2 Zinc-Supplementation Affects Treg-Levels *In Vivo*

Before performing the EAE experiment it was of interest to verify if zinc affects the amount of Tregs in mice *in vivo*. Therefore, 2 groups each consisting of 4 animals were injected daily with either $30 \mu\text{g}$ zinc/day supplied as Zn-Aspartate, or the same volume of NaCl, respectively. After 21 days, the animals were sacrificed and blood cells as well as splenocytes were analyzed for their amount of Foxp3-expressing Tregs and ROR γ t-expressing Th17 cells. Flow-cytometric analysis of CD4⁺ blasts (Fig. 30 A) revealed increased Foxp3 expression in splenocytes derived from zinc-treated animals compared to the placebo group (Fig. 30 B). Due to the low case number of 4 animals per group this result was not statistically significant. In contrast to Foxp3⁺ cells, the

amount of the Th17 lineage-specific transcription factor ROR γ t expressing cells showed a slight decrease among splenocytes, which may be associated with increased Foxp3⁺ cells. These results were more obvious when presented as the ratio of Th17 cells/Tregs as zinc decreases this ratio in splenocytes. Additionally, blood cells of the control animals did not differ in their amount of Foxp3 expressing CD4⁺ blasts, as well as in their amount of ROR γ t⁺ cells, between placebo-treated and zinc-treated animals (Fig. 30 B).

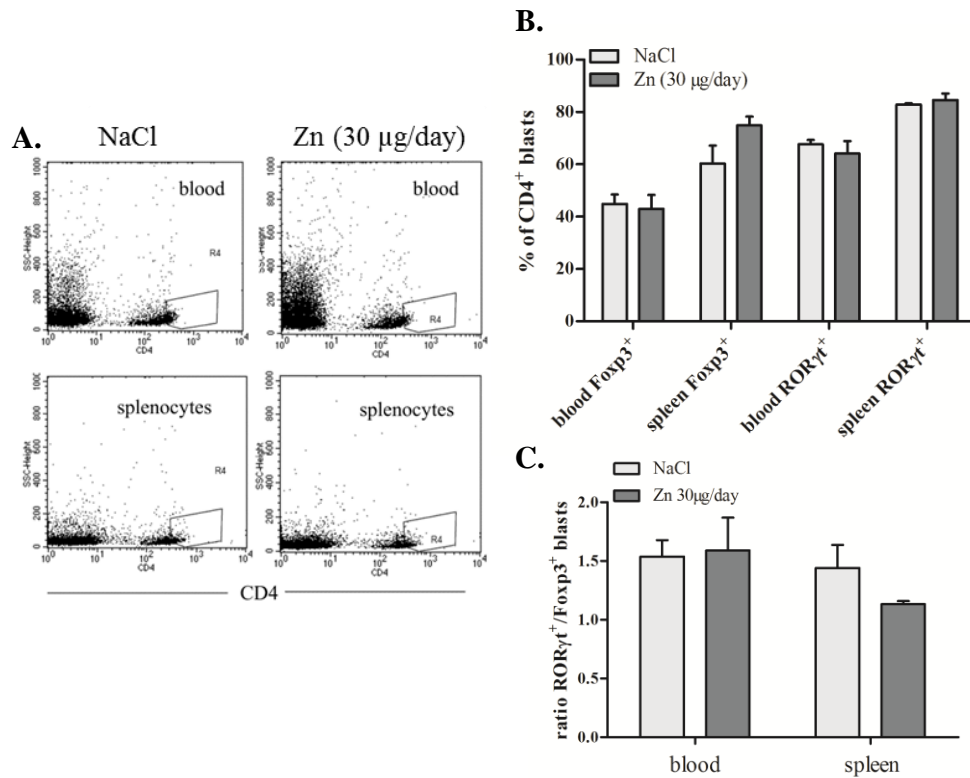


Fig. 30. **Impact of zinc treatment on the amount of peripheral Tregs and Th17 cells in control animals.** Mice were injected daily with NaCl (n=4) or 30 µg/day (n=4) zinc supplied as Zn-Aspartate. After 21 days, animals were sacrificed and blood and splenocytes were obtained for flow cytometric analysis. Gating was performed on CD4⁺ blasts (A. shows one representative flow cytometric analysis for blood and splenocytes) and the percentages of CD4⁺Foxp3⁺ and CD4⁺ROR γ t⁺ blasts were assessed (B). The ratio of CD4⁺ROR γ t⁺/CD4⁺Foxp3⁺ blasts was determined (C). Mean values + SEM are shown.

CD4⁺ blasts in control animals were most likely to originate from marginal inflammatory processes due to daily i.p. zinc injections. Since these animals were not further antigen-challenged and revealed only slight immune T cell activation, a substantial increase in iTregs by zinc was not expected. Nonetheless, the increasing Treg percentage in zinc-treated animals supports the idea of zinc to affect Treg upregulating agent *in vivo*. The fact that splenocytes constitute a larger amount of T cells compared to peripheral blood may contribute to the different results in splenocytes and blood. The impact of zinc seen on the induction of Tregs in the spleen

is promising for an ameliorating effect of zinc on EAE and encourages the investigation of zinc on EAE-induced mice.

4.6.3 Zinc-Induced Tregs Attenuate EAE Disease

Similar to allergic diseases, autoimmune disorders arise from inappropriate immune responses and affects multitude patients worldwide. Since a general immune suppression increases the susceptibility towards perilous pathogens, strategies to control specifically autoimmune responses without serious adverse effects need to be developed. Regarding the immunomodulating effects of zinc on allergic- and alloimmune responses (see above), application of zinc in autoimmune diseases is a promising approach.

The investigation of zinc-immunomodulatory effects on autoimmune diseases was performed using the induction of experimental autoimmune encephalomyelitis (EAE). EAE serves as a murine model of multiple sclerosis and is characterized by CNS-inflammation, demyelination, and paralysis, mediated by myelin-specific CD4⁺ T cells. In our experimental setting the animals were injected daily with either low-dose (6 µg/day; 0.3 mg/kg body weight) or high-dose (30 µg/day; 1.5 mg/kg body weight) zinc supplied as Zn-Aspartate starting 2 days prior to EAE immunization (Fig. 31). A placebo group received the same volume of NaCl instead. EAE progression was monitored on a daily basis by disease-staging, conducted under blinded conditions.

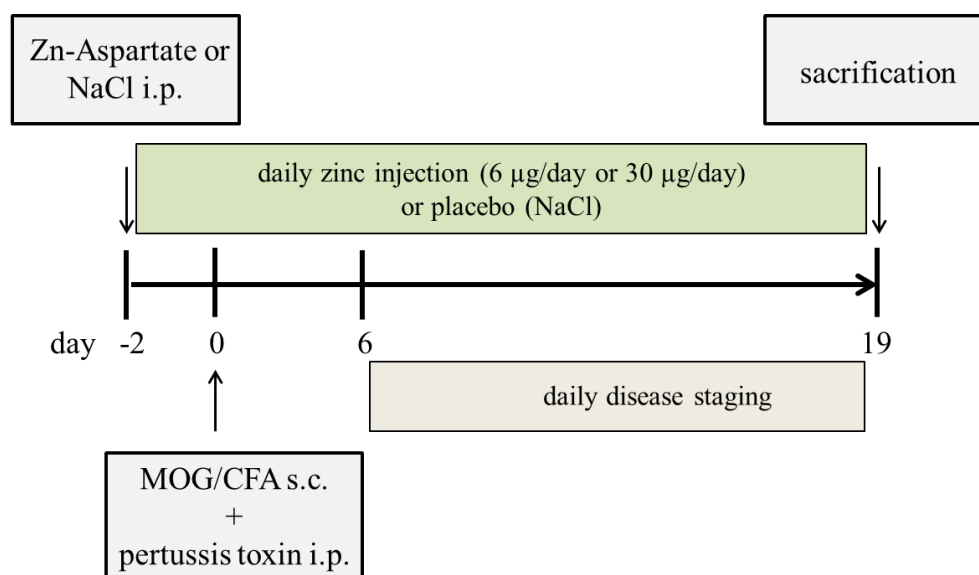


Fig. 31. **Schematic of the experimental setting.** Mice were injected i.p. with NaCl or high (30 µg/ml) or low (6 µg/ml) doses of zinc supplied as Zn-Aspartate daily for 21 days, starting 2 days prior to EAE induction. Disease progression was obtained daily beginning 6 days after MOG injection, when disease symptoms start to emerge. 19 days following EAE induction all mice were sacrificed.

This experimental setting inquired the effect of prophylactic zinc administration on the EAE disease course. Furthermore, this experiment dealt with the question of whether Treg upregulation

owes to a potential beneficial zinc effect. Remarkably, zinc was capable of modulating the amount of Foxp3 expressing Tregs among activated murine MLCs *in vitro* (Fig. 29) and *in vivo*, which suggests its contribution to EAE attenuation.

Fig. 32 displays the attenuating effect of prophylactic zinc on the EAE disease incidence. Indeed, both low dose and high dose zinc applications, decreased the EAE disease incidence in a zinc concentration-dependant way. About 70% of the high-zinc treated animals and about 82% of the low zinc treated animals developed EAE, whereas in the placebo group the disease incidence reached about 91%. Therefore, injection of zinc exerted a protective impact regarding the development of EAE. Furthermore, this figure validates the effectiveness of the EAE-induction procedure as nearly 100% of the placebo animals developed EAE symptoms.

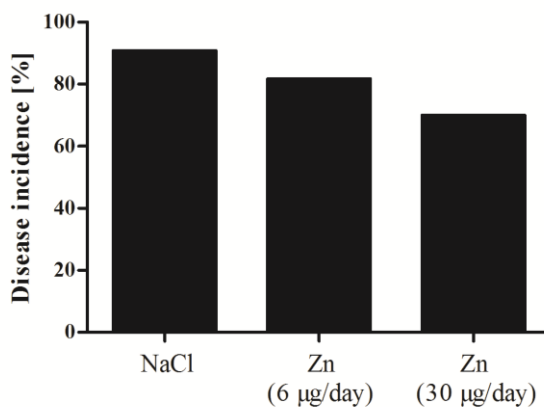


Fig. 32. **EAE-disease incidence in differently-treated groups.** Mice were injected daily with placebo (n=11), 6 µg/day (n=11) or 30 µg/day (n=10) zinc supplied as Zn-Aspartate, starting 2 days prior to EAE induction. The disease incidents among the different groups are shown.

Not only was the disease incidence affected by zinc treatment, but also disease intensity and disease course as presented in Fig. 32. The placebo animals severely suffered from EAE, reaching a mean scoring of 3 out of 5, with 5 corresponding to death (see chapter 3.2.12), whereas animals receiving zinc injections showed a decelerated EAE onset, which reached a mean score of 2 in the low-zinc group (Fig. 33 A), or even 1.5 in the high zinc group (Fig. 33 B), respectively. The changes in disease severity were statistically significant on days 16 and 17 following EAE induction in low-zinc treated mice and at days 16, 17, and 18 in the high-zinc treated animals. Thus, prophylactic zinc effect was demonstrated to attenuate the disease course in addition to disease incidences in a dose-dependent manner.

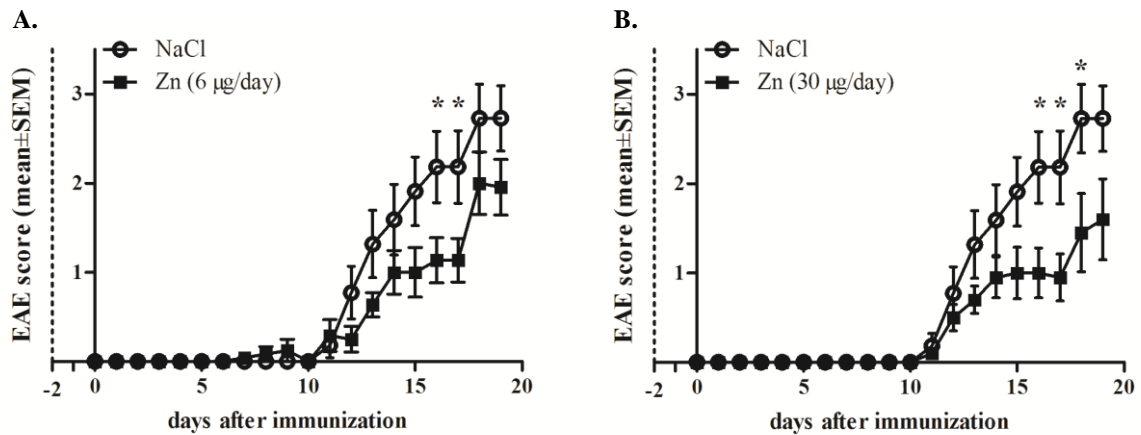


Fig. 33. **EAE-disease course in differently-treated groups.** Mice were injected daily with placebo (n=11), 6 µg/day (n=11) or 30 µg/day (n=10) zinc supplied as Zn-Aspartate, starting 2 days prior to EAE induction. The disease course was obtained by daily staging of the animals starting from day 6 following EAE induction. * indicates a significant difference with $p < 0.05$ (student's t-test), and mean values \pm SEM are shown.

In addition, the animals' body weight is a crucial indicator of their well-being and was thus measured daily or at least every two days. The results are presented in Fig. 34. The animals' body weight slightly decreased in the first five days after EAE induction in all groups due to the antigen challenge, and increased as soon as the first disease symptoms occurred. With disease progression the body weights in all groups sharply decreased, but to distinct extents comparing placebo and zinc-treated animals.

The high zinc group revealed a significantly higher mean body weight compared to the placebo group coincidentally with lower EAE symptom scores (Fig. 34 A). The difference in body weight between both groups started as early as 9 days after EAE induction. Interestingly, significant differences in disease severity were not detected before day 16 (Fig. 33 B). The low-zinc group's mean body weight was significantly lower at day -2 compared to the control group (Fig. 34 B). Hence, the mean body weights were normalized to the mean body weight at day -2 in order to display differences between placebo and low-zinc groups' changes in body weight during the disease course (Fig. 34 C, D). Using this analysis a difference was also obtained between the placebo and low zinc group depicting a better well-being in the low zinc-treated mice. Standardization of body weights to the body weights at the starting day revealed for the high zinc treated group a reduction in body weight before disease onset compared to the placebo group. Yet, with increasing disease progression the body weight increases to levels similar to those the beginning whereas the placebo-treated animals' body weight decreases correspondingly to disease severity. In conclusion, zinc attenuated the autoimmune disease EAE, which is reflected in disease incidence, disease symptoms, and body weight.

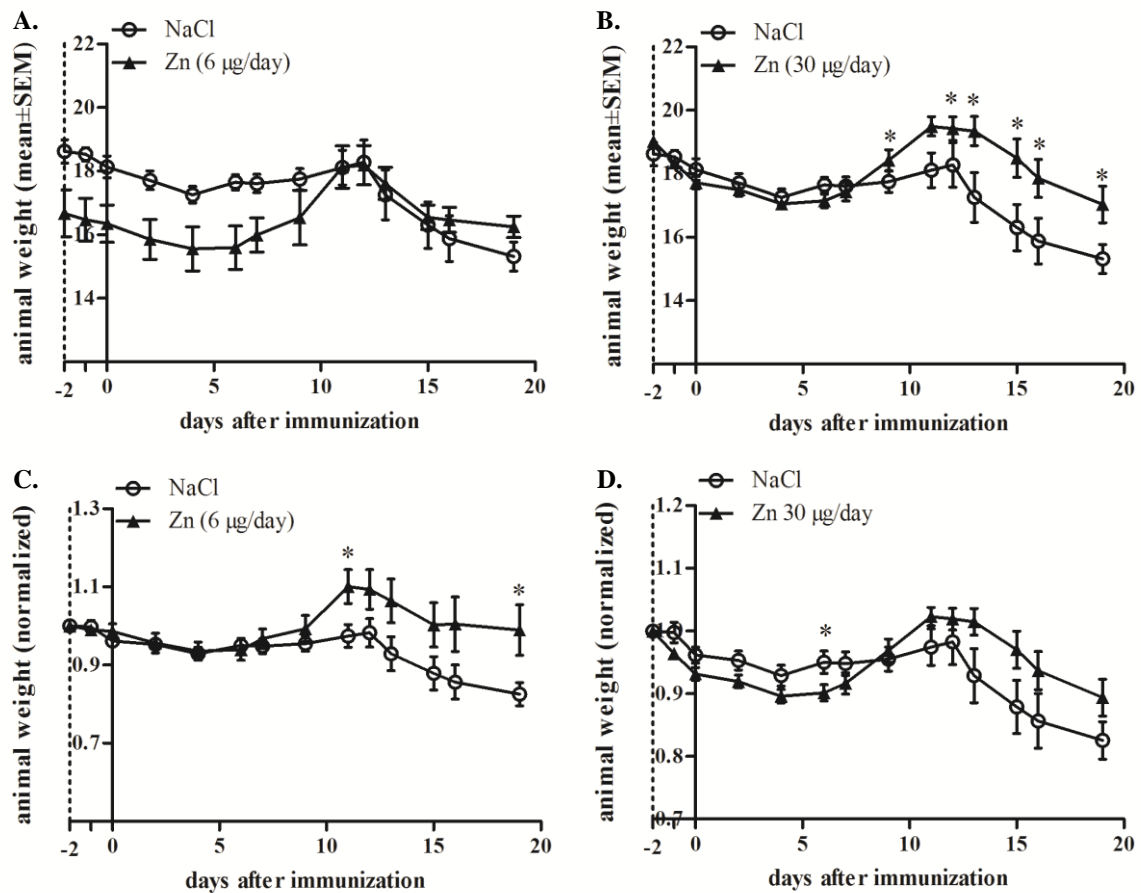


Fig. 34. **Weight-course in differently-treated animal groups.** Mice were injected daily with placebo (n=11), 6 µg/day (n=11) or 30 µg/day (n=10) zinc supplied as Zn-Aspartate, starting 2 days prior to EAE induction. The weight was obtained daily or at least every second day. A. shows weight of placebo and low-zinc animals, B. displays weight course of placebo and high-zinc animals. In C and D weight normalized to weight obtained at day -2 is shown (n=4). * indicates a significance difference with $p < 0.05$ (student's t-test) comparing placebo and zinc-treated groups, and mean values \pm SEM are shown.

As soon as the EAE disease course reached a plateau phase within the placebo group all mice were sacrificed and prepared for further investigations. Splenocytes together with peripheral blood cells were isolated and analyzed for ROR γ t and Foxp3 expression among CD4⁺ blasts to assess the amount of peripheral Th17 cells and the amount of counteracting Tregs to investigate if increasing Treg counts owe to the attenuating zinc effect. For flow cytometric analysis, the same gating strategy was applied as demonstrated before (Fig. 4 A) comprising SSC versus CD4 dotblots to obtain CD4⁺ blasts (Fig. 35 A). The measurements revealed no significant alterations in Treg levels in the periphery, including splenocytes as well as blood cells (Fig. 35 B, D). Nevertheless, the amount of ROR γ t expressing Th17 cells among the peripheral blood cells was significantly reduced in the high zinc group compared to the placebo treated animals (Fig. 35 C). Alongside, a slightly diminished amount of CD4⁺ROR γ t blasts among splenocytes was detected (Fig. 35 D) supporting the finding that zinc attenuates the basically Th17 driven EAE disease.

The divergent Treg and Th17 levels in EAE-derived cells from results observed in EAE-free animals (Fig. 30) arise from the vigorous inflammation in EAE-induced animals.

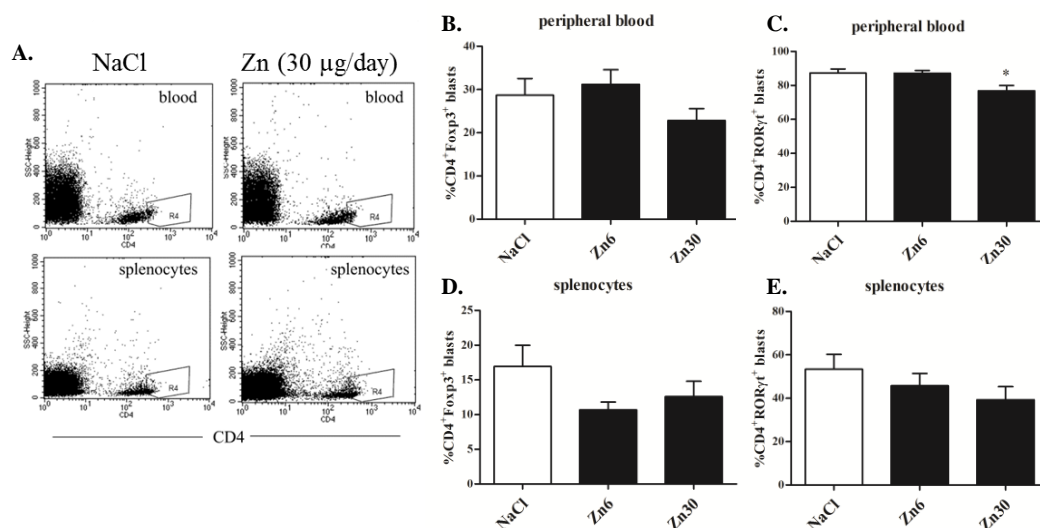


Fig. 35. Impact of zinc treatment on the amount of peripheral Tregs and Th17 cells in EAE-induced animals. Mice were injected daily with placebo (n=11), 6 µg/day (n=11) or 30 µg/day (n=10) zinc supplied as Zn-Aspartate, starting 2 days prior to EAE induction. At day 19, animals were sacrificed and blood and splenocytes were obtained for flow cytometric analysis. Gating was performed on CD4⁺ blasts (A. shows one representative flow cytometric analysis for blood and splenocytes) and the percentages of CD4⁺Foxp3⁺ (B., D.) and CD4⁺RORγt⁺ (C., E.) cells were measured. * indicates a significance difference with p<0.05 (student's t-test), and mean values + SEM are shown.

All in all, flow cytometric analysis did not convincingly affirm that zinc-induced Tregs are responsible for EAE attenuation. Therefore, immunohistochemical staining of spinal cord sections for Foxp3 and CD3 was performed to measure the amount of infiltrated Tregs. As EAE provokes inflammatory immune reactions at the spinal cord, infiltration of activated Tregs at the site of inflammation is feasible. This might also explain the decreasing Treg levels in the periphery (Fig. 35). CD3 and Foxp3 staining was not doable on the same slide but was done on consecutive slides derived from the same lumbar spinal cord region. Furthermore, counting of stained cells was performed by 3 blinded individuals to rule out biased values. As the zinc effect was most prominent in the high zinc treated group compared to the control group histological analysis was conducted in these groups only. In addition, this analysis solely included animals which developed EAE since healthy animals did not exhibit perivascular infiltration due to intact blood-brain barriers and restricted immune cell entry.

Concomitantly to CD3 or Foxp3 staining, cells were counterstained with haematoxylin to visualize cell nuclei. Thus, CD3⁺ and Foxp3⁺ cells appeared as brown events; cell nuclei emerged as blue events. Whereas the amount of CD3⁺ cells mirrors the degree of the infiltration of

immunoreactive T-cells, Foxp3⁺ cells represent the amount of Tregs. The percentage of Foxp3⁺ cells of CD3⁺ cells was calculated to reveal the relative amount of Tregs compared to CD3⁺ cells.

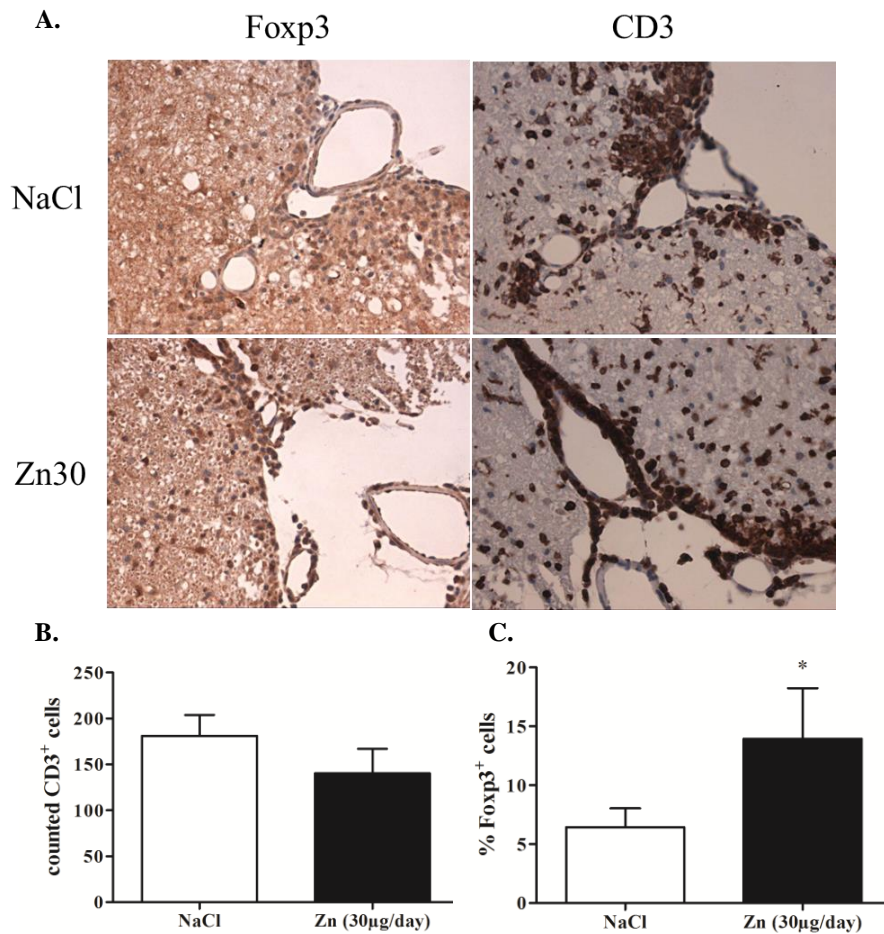


Fig. 36. Impact of zinc treatment on the amount of infiltrated Tregs in EAE-induced animals. Mice were injected daily with placebo (n=11) or 30 µg/day (n=10) zinc supplied as Zn-Aspartate, starting 2 days prior to EAE induction. At day 19, animals were sacrificed, perfused, and spinal cords were isolated. Spinal cord slides were stained for CD3 or Foxp3 and concomitantly with haematoxylin for cell nuclei visualization (A). CD3⁺ stained cells were counted independently by 3 different individuals (B) and the percentage of Foxp3⁺ cells of CD3⁺ cells (C) was calculated. Mean values + SEM are shown for n=9 EAE-developing placebo animals and n=7 EAE-developing Zn-treated animals (B). * indicates a significance difference with p<0.05 (Mann-Whitney test).

Notably, the percentage of Foxp3⁺ cells relative to CD3⁺ cell infiltration was significantly higher in the high zinc treated animals compared to the placebo group (Fig. 36 B). This result indicates that the amount of Foxp3-expressing Tregs increases on the basis of zinc-treatment, which is associated with amelioration of EAE severity. Since in the periphery no considerable alterations of Treg amounts were found zinc seemed to mainly affect Foxp3-stabilization in activated infiltrating T cells. These results support the idea of zinc-induced activated Tregs as presented above.

To conclude, the results of this thesis indicate that zinc has modulating effect on immune responses by enhancing Treg levels within activated T cells due to deceleration of Foxp3 degradation. Zinc-based modulation of immune responses was shown in MLCs (Th1-reactive), the allergic immune reaction (Th2-reactive), and the autoimmune reaction (Th17-reactive). Moreover, the impact of zinc was evaluated *in vitro*, *ex vivo*, and *in vivo*, emphasizing the relevance of the presented results for a future treatment of adverse immune reactions with zinc.

V. Discussion

The aim of this thesis was to investigate the immunomodulating capacity of zinc in diverse T cell-dominated immune reactions. The study has expanded on previous work that revealed the capability of zinc to inhibit IFN- γ production in the allogeneic mixed lymphocyte culture. In fact, Faber et al. observed that zinc in pharmacological doses of 50 μ M suppresses IFN- γ production in the MLC without affecting immune responses triggered by superantigens (Faber et al. 2004). Importantly, levels of the Th1 cell-derived cytokine IFN- γ are an important indicator for the allogeneic immune reaction in MLCs, since the MLC comprises prominent T cell activation (Danzer et al. 1994). In accordance, IFN- γ levels in MLCs between organ donors and recipients correlate with the severity of the acute GVHD (van der Meer et al. 1999). Reduced IFN- γ production by zinc hence mirrors attenuated T cell responses and the inhibition of the allogeneic immune reaction. Potential relevance for a therapeutic use of zinc in acute GVHD is therefore anticipated.

This thesis confirms that IFN- γ production in MLCs supplemented with zinc is significantly reduced after eight days compared to untreated control MLCs (Fig. 2). Indeed, IFN- γ production was slightly, yet significantly, inhibited from as early as 3 days after MLC incubation, showing the most prominent effect after 8 days. Moreover, not only was an ameliorating effect of zinc on the allogeneic immune reaction confirmed, but even fortified by finding decreased lymphocyte proliferation in zinc-treated MLCs after 8 days of incubation (Fig.4). Similar to IFN- γ production, cell proliferation indicates lymphocyte activation mediated by foreign histocompatibility antigens (mostly MHC class II molecules) expressed on the allogeneic cells (Kruisbeek et al. 2004).

In contrast to the complete abrogation of IFN- γ production and proliferation achieved by 1 μ g/ml Cyclosporine A (CsA), inhibition triggered by pharmacological zinc doses of 50 μ M was incomplete. Hence, this finding suggests that pharmacological doses of zinc induce immune tolerance by modulating allogeneic immune cells rather than by eliciting complete immunosuppression. Nevertheless, a direct comparison between the presented effects mediated by zinc and CsA on the MLC is not feasible, as the herein used high CsA concentration functioned as a control to demonstrate that the MLC reaction can be completely abrogated *in vitro*. Therapeutic doses of CsA lie in the range of 40 ng/ml (Miroux et al. 2009). Surprisingly, Faber et al., found that 50 μ M zinc inhibited the IFN- γ production in MLCs as effectively as 20 μ g/ml CsA when measured after 5 days of incubation (Faber et al. 2004). Moreover, 20 μ g/ml CsA did not abrogate IFN- γ production completely in their study, which stands in contrast to the result found in this thesis, which described complete IFN- γ suppression by 1 μ g/ml CsA. It is likely that a dose-dependent effect of CsA on the MLC exists, which reveals a most potent

inhibition at a concentration of 1 µg/ml. The impact of increasing CsA dosages was not within the scope of this thesis and as such, further investigation was not undertaken.

Modulation of the allogeneic immune reaction by zinc was further characterized by determining the ratio of Th1 to Th2 cytokines. Th2-derived IL-10 levels steadily increased in both, zinc-treated and control, MLCs until day 6 of incubation, reaching levels of ~150 pg/ml (Fig. 2). This result implies that both Th1 and Th2 cells are involved in the allogeneic immune reaction, which is consistent with previously published observations in patients with GVHD (Yeh et al. 2012). Notably, IL-10 levels were not as prominently elevated as IFN- γ levels (~40 ng/ml in the untreated control MLC), which verifies that the MLC is a mainly Th1-driven response. Three days following MLC incubation IL-10 levels were significantly, yet moderately, elevated in the zinc-treated MLC compared to the untreated control. This trend, prolonged by zinc supply, seemed to extend to after 8 days in contrast to the control MLCs. In accordance, the IFN- γ /IL-10 ratio showed a significant shift of IFN- γ (Th1) towards IL-10 (Th2) cytokines starting at day 3 of incubation and increasing until day 8. Remarkably, the IFN- γ /IL-10 ratio has previously been reported as an important measure of immune reactivity in transplantations (van den Boogaardt et al. 2006).

However, it has to be taken into account that the reduced zinc-mediated proliferation rates and hence decreased amounts of cytokine-producing cells affect the cytokine levels. Therefore, reduced IFN- γ levels may be due to restricted proliferation of IFN- γ producing cells in addition to limited T cell activity. With regard to IL-10 levels, reduced cell proliferation of IL-10-producing cells may conceal elevated IL-10 release per cell. Interestingly, exogenous addition of the Th2 cytokines rhIL-4 and rhIL-10 was demonstrated to reduce IFN- γ production in MLCs (Danzer et al. 1994), stressing the ameliorating effect of zinc-altered Th2 cytokine levels. Consistent with this finding, Th2 cells have been demonstrated to improve treatment outcome in clinical allogeneic stem cell transplantation (SCT). Studies by Fowler and colleagues, demonstrated that donor Th2 cells did not initiate acute GVHD, and that they can regulate GVHD mediated by unmanipulated donor T cells without impairing alloengraftment (Fowler and Gress 2000).

Surprisingly, IL-2 levels were not reduced after zinc treatment of MLCs (Fig. 3). Since both IFN- γ and IL-2 belong to the Th1 cytokine family additional to promoting both the allogeneic immune response, this result was striking. In fact, IL-2 levels were even slightly but significantly increased after 48 h in zinc-treated MLCs. Increased IL-2 levels after 48 h were also confirmed in zinc-pretreated V β T cells stimulated with superantigens in the presence of APCs. Consistently, a recent publication demonstrated elevated IL-2 production after IL-1 β stimulation associated with increasing intracellular zinc levels in murine EL-4 T cells (Daaboul et al. 2012). Increased IL-2 production by activated T cells may also arise because extracellular zinc levels can control TCR-

signal strength and calibrate the TCR-activation threshold, thereby allowing T cell responses already with suboptimal stimuli (Yu et al. 2011). As a consequence, T cells get activated more rapidly by zinc, which results in higher IL-2 production. In contrast, decreased IFN- γ levels in zinc-treated MLCs imply a divergent effect of zinc on IFN- γ and IL-2 production in the MLC.

It has to be emphasized that IL-2 is a survival factor for Tregs and increasing IL-2 levels are capable of inducing proliferation of otherwise non-proliferative Tregs (Zheng et al. 2007). Increased Treg activity by zinc might explain reduced overall proliferation and IFN- γ production, because Treg-mediated suppression not only affects Th1 cells but also effector cells such as IFN- γ -producing CD8⁺ T cells and B cells (Lim et al. 2005; Mempel et al. 2006).

Accordingly, IL-10, in addition to being a Th2 cytokine, is secreted by Tregs in order to exert immunosuppressive function (Maynard et al. 2007). Remarkably, IL-10 was slightly enhanced by zinc after 3 days of MLC culture whereas IFN- γ was slightly decreased at this time point, possibly due to Treg-mediated inhibition. Moreover, Th2 cells were proposed to be less susceptible to the suppressive activity of Tregs than Th1 cells (Cosmi et al., 2004), which might account for the distinctive impact of zinc on Th1-derived IFN- γ production and Th2-derived IL-10 production.

In addition, Foxp3 levels were enhanced by zinc after 3 days and after 8 days of MLC incubation (Fig. 5), further substantiating the idea of increased Treg amounts, as Foxp3 is generally accepted as lineage-specific Treg marker (Fontenot et al. 2005). The fact that 5 days of MLC culture did not lead to altered Foxp3 levels in neither control nor zinc-treated cells suggests that zinc modulates Tregs in two different phases: Firstly, an early effect arising after 48-72 h of MLC incubation, indicated by slightly increased Foxp3, IL-2, and IL-10 levels, and a later effect starting after roughly 6 days of MLC incubation, characterized by increased iTregs leading to decreased IFN- γ expression and proliferation. Since the effect of zinc on the allogeneic immune reaction was more prominent after 8 days than after 3 days, the second phase is likely to play a stronger role in immune-tolerance induction. To test this hypothesis, Tregs induced upon zinc supply after 8 days of MLC were further analyzed. The analysis revealed increased amounts of CD4, CD25^{hi}, Foxp3, and CTLA-4 expressing cells after 8 days in zinc-treated MLCs, all belonging to the group of Treg marker molecules (Akimova et al. 2011).

The fact that CD25, Foxp3 and CTLA-4 are proteins that are also transiently expressed by activated T cells (Walker et al. 2003) indicates an accumulation of iTregs rather than nTregs after 8 days of MLC incubation. More precisely, the presented data suggest increased stability of iTregs, which developed from activated antigen-specific T cells upon zinc supply. Taken together, this clearly demonstrates for the first time that zinc inhibits the allogeneic immune response by inducing immune-tolerance mediated by increasing antigen-specific iTreg levels.

This phenomenon is important for transplantation medicine, for which inhibition of the allogeneic immune reaction is crucial to ensure graft functionality. Immunosuppressive strategies completely suppress the allogeneic immune reaction and thereby prevent graft rejection, but they are also hazardous for the patient because antigenic immune reactions are also suppressed (Dunn 1990). The apparent ability of zinc to induce tolerance in the allogeneic immune response without acting completely immunosuppressive is therefore a promising approach. The idea of enriching allogeneic-specific Tregs is one proposed strategy to treat GVHD, comprising methods to converse or expand Tregs *in vivo* or *ex vivo* (d'Hennezel and Piccirillo 2012). But this labor- and cost-intensive process of generating the product may preclude their wide application.

The results illustrating that zinc reduces the allogeneic immune reaction are consistent with conducted studies by Kown et al., which show that the systemic application of 1 and 5 mg/kg ZnCl₂ dose-dependently reduced acute allograft rejection in a rat model of transplantation (Kown et al. 2000; Kown et al. 2002). The authors explain the observed prolongation of graft survival by a zinc-induced inhibition of apoptosis during the acute allogeneic immune reaction via inhibition of the proapoptotic enzyme caspase-3. Reduced apoptosis of graft-tissue cells would thus contribute to allograft survival. However, reduced apoptosis in allografts may be a secondary effect related to the attenuating impact of zinc on the immune reaction. Inhibition of effector cells by Tregs, as presented in this thesis might account for reduced graft cell apoptosis. Therefore, measuring the amount of Foxp3-expressing Tregs within the allografts would have been of great interest. The finding that zinc inhibits caspase-3 might be advantageous for Treg survival, but this idea was not further pursued in this study. However, the observations of Kown et al. indicate that the impact of zinc seen in *in vitro* MLCs might also prove relevant *in vivo*. This idea is supported by findings of Okamoto and co-workers, who concluded that zinc supplementation maintains functional grafts in intraportal islet transplanted rat recipients (Okamoto et al. 2011).

To further elucidate the relevance of zinc administration for therapeutic purposes, this study verified the bioavailability of physiological amounts of orally administered zinc and its impact on *ex vivo*-generated MLCs. It is encouraging that a daily oral supplementation with physiological amounts of zinc-aspartate (10mg) for 10 days significantly increased the amount of Tregs in *ex vivo* generated MLCs when comparing before and after supplementation (Fig. 21). As this effect was only observed in MLCs generated with PBMCs derived from zinc-supplemented volunteers, in contrast to MLCs generated from PBMCs derived from placebo-supplemented volunteers, it can be concluded that supplementation of 10mg zinc per day over a time period of 10 days or less is sufficient to modulate immune cells towards attenuating MLCs by upregulating Tregs. Notably, a recent study revealed that 10mg elemental zinc/day has no adverse effects (Bobat et al. 2005). It has to be mentioned that IFN- γ levels were not much decreased comparing MLCs before and after zinc-supplementation, respectively. But this can be explained by the fact that MLCs were

generated at two different time points, which may result in a slightly diverging cell composition or other parameters influencing cytokine levels in the MLC. Importantly, Faber et al., who supplemented individuals with 80 mg zinc/day for 1 week, observed prominent IFN- γ suppression in *ex vivo* generated MLCs when comparing before and after supplementation time points (Faber et al. 2004). This finding verifies the herein presented inhibition of IFN- γ expression in *ex vivo* generated MLCs from zinc-supplemented volunteers. In addition, data from this thesis suggests that increased amounts of Tregs are responsible for this result. However, it has to be kept in mind that the volunteers' nutritional status was not assessed in either study so it may be that nutritional zinc and phytic acid intake varied among the individuals. However, serum zinc levels were significantly increased after 10 days of zinc intake proving that zinc supplementation was not only effective in attenuating the allogeneic immune reaction in *ex vivo* generated MLCs but also in raising the volunteers' zinc-status.

Chronic disorders including allergies are often accompanied by zinc deficiency (Richter et al. 2003; Rink 2011). Allergies, which belong to the Th2-driven diseases, may be caused by the shift of Th1 to Th2 cytokine occurring during zinc-deficiency (Prasad 2000). Therefore, allergies are likely to be susceptible to zinc-induced modulation of the allergic immune reaction. This suggestion was followed-up in this thesis in *in vitro* allergy experiments. Most importantly, zinc was able to enhance Tregs in allergen-activated PBMCs resulting in decreased PBMC proliferation (Fig. 26, 23). Tregs can indeed inhibit T cell activation following allergen exposure and this process may be deficient in atopic subjects (Ling et al. 2004). The suggestion that allergic subjects show decreased Treg-mediated suppression is interesting as it might correlate with decreased zinc levels in allergic subjects.

However, increased amounts of Tregs were less prominent compared to the MLC. This can be explained by the relatively small pool of activated T cells and resulting iTregs levels, which are subsequently stabilized by zinc. Changes in Treg levels in this small pool are not as obvious and may be masked by present naive cells and activated effector cells. Consistently, cytokine levels show rather marginal changes after zinc supplementation (Fig. 24). Still, the measured cytokine changes indicate a shift of Th2 to Th1 cytokines since IFN- γ increased relative to IL-10. Allergies are Th2-dominated immune responses as indicated by the fivefold diminished IFN- γ production compared to its levels in the MLC. IL-10 levels, in contrast, were nearly 5 times higher than in the MLC. Thus, the shift towards Th1 cytokine suggests that zinc ameliorates the allergic reaction. In accordance, it was reported that the IL-4 production in short-term, allergen-stimulated pollen-reactive cells of individuals with seasonal allergic rhinitis was higher increased than the IFN- γ production (Imada et al. 1995).

The relatively limited suppression of Th2 cytokine production, also confirmed for IL-4 mRNA expression, might be further explained by the fact that Th2 cells are less susceptible to Treg suppression. Moreover, potentially reduced IL-10 levels are likely to be hidden by increased Treg-derived IL-10 expression.

Taken together, the Th1-reactive allogeneic and the Th2-directed allergic reaction follow different courses and mechanisms, but are both modulated by zinc. In this study, experiments were performed using the timothy-grass allergen that causes hay fever. As 400 people worldwide suffer from this form of allergic rhinitis, with high prevalence recorded in industrialised nations, these results are of great interest (Bousquet et al. 2001). The zinc-effect remains to be confirmed *in vivo*. In addition to this, further research on the impact of zinc on immune responses induced by various other forms of allergies is required.

The effect of zinc on autoimmune diseases, especially a Th17-dominated autoimmune disease, was investigated in a mouse model for multiple sclerosis (MS). This EAE model enables research not only on the immunomodulating capacity of zinc in Th17 driven immune responses, but also on zinc-mediated effects in *in vivo* immune reactions. A daily injection of zinc, starting 2 days prior to EAE induction, diminished the incidence of EAE development in zinc-treated groups (Fig. 32). This supports the existence of an early moderate impact of zinc on immunomodulation as seen in the MLC. Most notably, EAE course was significantly milder in zinc-treated animals. This dose dependent effect was reflected in the animals' body weight (Fig. 34). In contrast to the placebo group, the zinc-treated animals did not suffer from weight loss following EAE onset, thoroughly indicating improved health status. However, no changes in peripheral Treg levels were found when analysing blood cells and splenocytes (Fig. 35). The EAE-induced immune reaction allows immune cells to cross the blood-brain-barrier and infiltrate the otherwise immune-privileged CNS (Bartholomaeus et al. 2009). The amount of perivascularly recruited autoreactive CD3⁺ T cells was slightly reduced in zinc-treated animals. In contrast, the percentage of iTregs among these CD3⁺ cells that infiltrate into the spinal cord was significantly increased in zinc-treated mice (Fig. 36). Significantly enhanced Treg levels in the infiltrates of zinc-treated animals support the proposed model of zinc-stabilized Tregs, which develop in the course of T cell activation. These induced Tregs can exert immunosuppressive function on other immune cells and inhibit disease progression. The relevance of Tregs in EAE amelioration and MS is well established (McGeachy et al. 2005; Liu et al. 2006; Zozulya and Wiendl 2008).

The presented results are consistent with the results of other groups who published reduced EAE severity in zinc-treated mice (Kitabayashi et al. 2010; Stoye et al. 2012). Stoye et al. reported an ameliorating zinc effect however not until after the first peak of disease. Contrastingly, in this study the ameliorating effect of zinc was already evident before the first peak of disease occurred. Although the same zinc concentrations were used, several differences between both studies must

be acknowledged. Stoye et al. performed preventive zinc application from day 1 to day 10, whereas in this study, zinc application started 2 days before EAE induction and was continued until day 19, the end of the study. Moreover, we chose to investigate MOG35-55/CFA-induced EAE in C57BL/6 mice, being the mouse model of EAE with the fastest disease progression and with predictive value for the efficacy of a chosen compound in MS. In contrast, Stoye et al., used the PLP139-151/CFA-induced, remitting-relapsing EAE in SJL mice, which is recommended for testing the effect of compounds on the development of EAE relapses (therapeutic treatment) (Zhang et al. 2004). Yet, the work of Stoye et al. bears the advantage of observing both the therapeutic and preventive value of zinc by additionally starting zinc application 11 days after EAE induction for 10 days resulting in decreased EAE severity in the relapsing phase. Based on the fact that the MLC and allergy experiments involved preincubation with zinc for 15 min prior to T cell activation in the present study, we chose pretreatment with zinc for the EAE experiment. Of course, based on the study by Stoye et al., investigation of the therapeutic value of zinc and its underlying mechanisms are of great interest for further studies.

Interestingly, the zinc-mediated ameliorating effect of EAE was also seen in mice, which consumed zinc-enriched drinking water starting 1 month before EAE induction (Kitabayashi et al. 2010). EAE severity was greatly reduced in zinc-treated animals compared to control animals proving the protective effect of zinc on EAE disease. Certainly, one has to bear in mind the divergent bioavailability of the zinc supplements and the different application protocols used. Especially the approach from Kitabayashi et al. has to be interpreted with caution as the used zinc dosage of 3000 ppm in the animals' drinking water (equivalent to 480-1200 mg zinc/kg) is within the range of the oral LD50 of zinc sulphate heptahydrate (500 mg zinc/kg). Consequently, the observed effects are most likely due to high dose zinc toxicology.

Still, the protective value of zinc for autoimmune diseases was also shown in a model of collagen-induced arthritis (CIA) in the aforementioned study. Consistent with our results, analysis of peripheral cells in that study revealed decreased Th17 but unaltered Treg levels. Unfortunately, levels of tissue-infiltrated Tregs were not assessed. Furthermore, Kitabayashi et al. showed that following Th17 cell injection, zinc-treated mice developed EAE severity comparable to control mice. This finding suggests that zinc attenuates EAE by inhibiting Th17 cell development. Tregs are known to counteract Th17 development (Chaudhry et al. 2009) and increased amounts of Tregs may well explain decreased Th17 levels in zinc-treated animals. Overall, this data indicates that zinc ameliorates autoimmune responses. This may be of considerable interest as each year about 150 per 100,000 individuals worldwide are affected by the chronic and disabling disease MS, for which no cure is yet available. MS is mainly treated with immunosuppressive drugs that often exhibit toxic side effects (Rosati 2001).

Interestingly, the zinc-mediated increased Treg levels assessed in *in vitro* experiments were confirmed *in vivo* in mice, demonstrating physiological relevance. In a follow-up, the molecular mechanism behind the increase in Tregs by zinc was further investigated. As mentioned earlier the modulation of IL-2 production in activated T cells might play an important role. This hypothesis is further supported by results of Rouse et al. stating that pretreatment with moderate IL-2 concentrations caused significant amelioration of EAE (Rouse et al. 2012). Expanded Tregs and concomitant inhibition of Th17 induction were hypothesized to be the reason for IL-2-mediated EAE suppression. Notably, post-treatment with IL-2 failed to inhibit EAE despite an induction of Tregs. This data shows that IL-2 can expand Tregs at disease onset, which suppresses the disease. But once the antigen-specific response is triggered, IL-2 induced Tregs only play a limited role in controlling the immune response. According to these results the timing of enhanced IL-2 levels is critical for its impact on immune suppression. IL-2 supplementation to an already started immune reaction presumably expands Tregs but also stimulates T_H17 proliferation thus preventing tolerance induction. Hence, the importance of IL-2-elevation timing exacerbates the investigation of the potential impact of zinc-mediated IL-2 production on immune reaction. Moreover, it was demonstrated that zinc can improve the IL-2 signaling in T cells. Kaltenberg et al., published that the addition of zinc increases IL-2-induced ERK signaling and proliferation of T cells (Kaltenberg et al. 2010). Follow-up studies showed that zinc also increases IL-2-induced Akt signaling, which is partly due to a decreased PTEN (phosphatase and tensin homolog) activity by zinc (Plum et al. submitted). As a result IL-2-activated PIP3/Akt signaling is increased and influences cellular downstream processes. Improved IL-2-signaling in T cells by zinc may therefore be another factor involved in Treg upregulation and immune regulation. Yet, this idea was not further investigated in this thesis.

Instead, a different mechanism was revealed. Interestingly, a role for HDAC Sirt-1 inhibition by zinc in modulating Tregs was found. Sirt-1 modifies Foxp3 stability by promoting proteasomal degradation of Foxp3 protein (van Loosdregt et al. 2010; van Loosdregt et al. 2011). Deacetylation of specific lysine residues favours Foxp3 ubiquitinylation at these sites, subsequently inducing protein degradation. Abolished Sirt-1 activity supports prolonged Foxp3 stability along with Foxp3 function resulting in the presented immune modulations. The *in vitro* IC₅₀ of zinc-inhibition of Sirt-1 deacetylase activity in this study was determined to be ~13 nM (Fig. 16). Inhibition of Sirt-1 by zinc has been demonstrated previously (Chen et al. 2010). Yet, Chen and colleagues postulated an IC value of 820 nM. Different approaches account for the diverging results. Whereas Chen et al. used Zn(Gly)₂ consisting of zinc chloride and glycine with a molar ratio of 1:2, this study used ZnSO₄ without any addition. In this thesis, actual free zinc levels of the added zinc concentrations in the assay buffer were determined. This approach allows for a specific analysis of the IC₅₀ value. Yet, it is interesting that Chen et al., characterized zinc

as a non-competitive inhibitor for NAD^+ and the acetyl peptide, suggesting that zinc binds at a different site compared to the activators NAD^+ and the acetyl peptide (Chen et al. 2010).

The ability of zinc to inhibit Sirt-1 activity was underlined by the fact that the HDAC inhibitor nicotinamide showed a weaker inhibition of Sirt-1 than zinc when added in equimolar concentrations (Fig. 15). The physiological intracellular concentration of nicotinamide ranges between 40 and $50\mu\text{M}$ for human cells, which is suggested to be just below the threshold for significant inhibition of intracellular Sirt-1 activity (Revollo et al. 2004).

In order to evaluate the physiological relevance of the measured IC_{50} in activated T cells intracellular zinc levels in T cells were determined with the zinc probes FluoZin-3 and Zinpyr-1 (Fig. 17). FluoZin-3 labels lysosomal zinc compartments in T cells whereas Zinpyr-1 detects cytosolic zinc. Zinc concentrations detected with either probe were below 1nM in activated T cells. This result stands in contrast to results from other publications, which consider concentrations of 17nM to be likely *in vivo* (Yu et al. 2011). Thus, although zinc concentrations in activated zinc-treated T cells were increased compared to the activated control intracellular zinc levels in activated T cells either with or without zinc supplementation fell below concentrations required for Sirt-1 inhibition in this work.

Nonetheless, a zinc-mediated inhibition of Sirt-1 function cannot completely be ruled out for several reasons: Intracellular zinc levels were obtained in CD3^+ cells comprising CD4^+ T effs and Tregs as well as CD8^+ cells. Further analysis of specific cell subtypes may indicate that CD4^+ T cells have higher intracellular zinc levels than CD8^+ T cells. On the other hand, zinc affects the acetylation status of Foxp3 in MLCs as detected by Foxp3 immunoprecipitation. Subsequent western blot analysis revealed increased Foxp3 K31 acetylation by zinc (Fig. 18), which as per a recent publication established is crucial for human Foxp3 stabilization (Kwon et al. 2012). This increase was not statistically significant, which may be due to high variances between the subjects' responses. Further, in this thesis Foxp3 levels were upregulated after 5 days in both untreated and zinc-treated MLCs (Fig. 5). After 8 days Foxp3 expression in zinc-treated MLCs was sustained, whereas in control MLCs Foxp3 levels receded. These findings definitely support the idea that zinc prevents Foxp3 degradation by reducing Sirt-1 activity and consequently that stabilized Foxp3 expression is responsible for the immunomodulating effect of zinc. Furthermore, the Sirt-1 inhibitor EX-527 (6-Chloro-2,3,4,9-tetrahydro-1H-carbazole-1-carboxamide, $\text{IC}_{50} = \sim 38\text{ nM}$) was capable of mimicking the results obtained in zinc-treated MLCs (Fig. 19). In a consistent manner, a study by Beier et al. indicates that Sirt-1 targeting promotes Foxp3⁺ Treg cell function and prolongs allograft survival (Beier et al. 2011). Although these results were found in Sirt-1-deleted mice this does not alleviate their importance as mice and human MLCs reacted in similar ways to the zinc-treatment in the present thesis (Fig. 29). In addition, wild-type allograft recipients treated with EX-527 exhibited similar reactions as Sirt-1 deleted mice.

Interestingly, Sirt-1 deletion promotes the expression of Treg-associated genes as Foxp3, CD25 and CTLA-4, consistent with what we observed with zinc. Furthermore, the reduction of Teff cell-associated genes including the gene coding for IFN- γ was downregulated, which is in accordance with decreased IFN- γ expression mediated by zinc.

In contrast, complete Sirt-1 deletion was shown to promote susceptibility to EAE (Zhang et al. 2009). However, the difference in Sirt-1-deleted mice between transplantation model and EAE model are likely to be a result of different disease courses involving diverse T cells, mainly Th1 cells in allografts and Th17 cells in EAE. Complete Sirt-1 inhibition, which is not likely to be achieved by the used zinc concentrations, thus seems to have an adverse effect on EAE attenuation. Indeed, application of high zinc levels (120 $\mu\text{g}/\text{day}$), which may inhibit Sirt-1 to a greater extent, consistently had no influence on EAE severity (Stoye et al. 2012). Therapeutic application of 120 μg zinc/day applied from day 11 to 19 even aggravate the clinical disease. Supplementation of zinc in high concentrations therefore has to be considered carefully in Th-17-driven diseases.

Effects of zinc on Sirt-1 action may also be explained by higher intracellular zinc levels in the range of 13nM due to local cellular zinc gradients following T cell activation as suggested by Yu et al. (Yu et al. 2011). Moreover, zinc might promote translocation of the predominantly nuclear-located protein to the cytoplasm losing spatial proximity to the nuclear-located Foxp3 protein. The Sirt-1 inhibitors Sirtinol and EX-527 were shown to block translocation of Sirt-1 to the nucleus in endothelial cells (Kozako et al. 2012). In fact, translocation of Sirt-1 to the nucleus is important for cell survival (Hou et al. 2010), and EX-527-mediated modulation of Sirt-1 location presumably accounts for decreased PBMC viability (Fig. 20). Furthermore, a zinc-mediated inhibition of Sirt-1 expression is possible and would result in decreased Sirt-1 levels and hence Sirt-1 action. Consistently, IL-2 signaling was proposed to inhibit Sirt-1 expression in T cells (Gao et al. 2012). Although this was suggested to lead to a breakdown of T-cell tolerance in the referenced publication, it might also account for inhibited Sirt-1 expression in MLCs due to increased IL-2 production and IL-2 signaling by zinc. Unfortunately, until now no adequate Sirt-1 antibody that enables the measurement of CD4⁺Foxp3⁺ Sirt-1⁺ cells by flow cytometry is available to investigate Sirt-1 levels specifically in Tregs.

Regarding the similar effects of zinc and the Sirt-1 inhibitor EX-527, zinc could be a reasonable substitute in Sirt-1 inhibitor-treated diseases. For example, the Sirt-1 inhibitor Sirtinol induces apoptosis in cells of ATM (adult T cell leukemia-lymphoma) patients (Kozako et al. 2012). However, increasing amounts of Tregs in cancer patients aggravates their condition as tumor-specific effector cells become inhibited. Careful consideration is therefore advisable before using zinc as treatment in cancer. The complex impact of zinc-induced Sirt-1 inhibition on various cell

types provides an interesting future research topic. Apart from being an important factor for Treg differentiation, Sirt-1 was demonstrated to affect several signal transduction molecules, as for example NF κ B (Salminen et al. 2008). Sirt-1 can negatively regulate the transcriptional activity of p65, which leads to reduced production of proinflammatory cytokines in macrophages (Yoshizaki et al. 2010; Zhang et al. 2010). Therefore, zinc treatment has to be considered cautiously in inflammatory diseases with vast macrophage involvement. The complexity of Sirt-1 modulation is also obvious in that its biological function involves the control of gene expression, metabolism, and senescence (Haigis and Guarente 2006; Michan and Sinclair 2007). However, consistent with the presented results, Sirt-1 is highly expressed in activated T cells (Gao et al. 2012), which also express Foxp3 and allow for its modulation by increasing zinc levels.

It is in this context interesting that Sirt-1 was shown to inhibit PPAR- γ (Picard et al. 2004). In fact, cells in which Sirt1 had been downregulated showed higher levels of PPAR- γ mRNA and PPAR- γ protein. Although these results were observed in adipocytes, they support the proposed model of zinc-mediated Sirt-1 inhibition since zinc upregulated PPAR- γ mRNA in MLCs (Fig. 13). Interestingly, PPAR- γ was proposed previously to play an important role in both immunoregulation (Hontecillas et al. 2011) and in Tregs (Wohlfert et al. 2007; Hamaguchi and Sakaguchi 2012), a finding consistent with our results.

Collectively, the research presented in this thesis shows that zinc upregulates Tregs in Th1, Th2, and Th17 driven immune responses. This may prove zinc to be a substantial therapeutic agent for a vast number of common T cell-related disorders such as transplanted grafts, allergies, and autoimmune diseases. The results support earlier postulates of a beneficial effect of zinc supplementation and for the first time show that the inhibition of Sirt-1 is involved in zinc-mediated Foxp3 stability. Increased Foxp3 stability induces enhanced levels of specific iTregs, which are capable of promoting tolerance in adverse immune reactions and consequential diseases. The presented findings are summarized in Fig. 37.

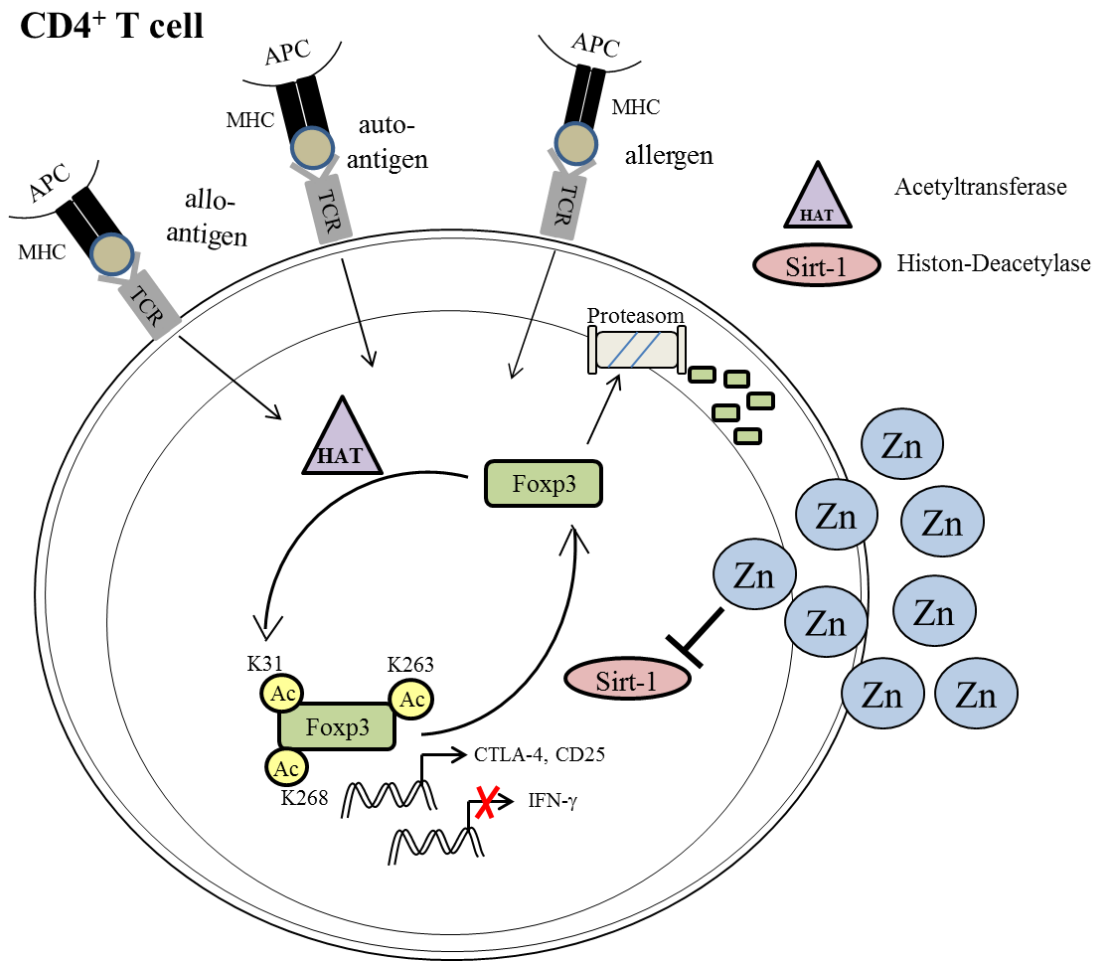


Fig. 37. A schematic overview of zinc-mediated induction of iTregs. CD4⁺ T cells activated by allergens, autoantigens, or alloantigens transiently express the transcription-factor Foxp3. Acetylation of Foxp3 protein by histone-acetyltransferases alleviates transcription of Foxp3-controlled genes including *cd25* and *ctla-4* and represses expression of *ifn-γ*. Foxp3-deacetylation of K263, K31, and K268 by the histone-deacetylase Sirt-1 allows for ubiquitination and subsequent proteosomal degradation. Zinc inhibits Sirt-1 activity thereby augmenting Foxp3 stability and function. Sustained CTLA-4, CD25 and Foxp3 expression characterize iTregs and contribute to effector immune cell inhibition and modulation of Th1, Th2, and Th17-controlled immune responses.

VI. Conclusion

The trace element zinc is essential for immune cell function as documented by impaired immune activity in zinc-deficient patients. But also supplementation of physiological zinc doses modulates immune responses. It was demonstrated before that zinc-treated MLCs are inhibited relative to control MLCs as indicated by decreased IFN- γ production. In addition, zinc was used successfully to ameliorate autoimmune diseases in mice. Therefore, an immunomodulatory effect of zinc was anticipated in this study, offering the opportunity to elaborate zinc application as a useful tool in controlling diseases, which involve excessive T cell activation.

This thesis confirms the ability of zinc to modulate Th1, Th2, and Th17 driven immune responses. More precisely, zinc was capable of inducing immune tolerance in *in vitro* MLCs, of inhibiting *in vitro* allergic immune responses towards timothy grass allergen, and of attenuating the *in vivo* EAE disease, an animal model of multiple sclerosis. Furthermore, this work expands on known zinc effects and reveals that the induction of Tregs by zinc is responsible for the presented immunomodulation. In fact, zinc prolonged levels of specific CD4⁺CD25^{hi}CTLA-4⁺ iTregs derived from activated T cells thereby accumulating antigen-specific Tregs with immunosuppressive capacity. This zinc-mediated effect was observed in alloantigen-, allergen-, and autoantigen-activated T cells. The molecular mechanism underlying zinc-mediated induction of Tregs involves increased K31-Foxp3 acetylation, which prevents Foxp3 degradation and stabilizes Foxp3 activity. In accordance, deacetylation of Foxp3 by the histone deacetylase Sirt-1 promotes ubiquitination of the vacant lysine residues leading to Foxp3 removal by the proteasome. One important finding of this work is that zinc inhibits Sirt-1 and thereby stabilizes Foxp3. The Sirt-1 inhibitor EX-527 mirrored the impact of zinc in the MLC, supporting the idea of zinc-mediated Sirt-1 inhibition. Experimental preincubation with zinc in the above mentioned scenarios reinforced the potential use of zinc as a preventive molecule. Further evidence for this powerful capacity is provided by the finding that orally administered zinc for 10 days enhanced Foxp3 expression in *ex vivo* generated MLCs.

Altogether, this work illustrates that zinc may modulate adverse T cell-driven immune responses by upregulating Tregs and Treg-mediated immune cell alleviation. Advancing our understanding of how zinc modulates immune responses can help to establish zinc as a new therapeutic tool for the fields of transplantation, allergy, and autoimmunity. The advantage of a zinc-based therapy as compared to immunosuppressive strategies becomes obvious in its lack of toxicity and its ability to induce immune tolerance without completely abrogating antigenic immune defence. This is an important aspect of the immune system's ability to fight infectious diseases, and hence a topic of broad interest which warrants further studies.

VII. References

- Akimova, T., U. H. Beier, et al. (2011). "Helios expression is a marker of T cell activation and proliferation." *PloS one* **6**(8): e24226.
- Andersen, K. G., T. Butcher, et al. (2008). "Specific immunosuppression with inducible Foxp3-transduced polyclonal T cells." *PLoS biology* **6**(11): e276.
- Andreini, C., L. Banci, et al. (2006). "Counting the zinc-proteins encoded in the human genome." *Journal of proteome research* **5**(1): 196-201.
- Andrews, G. K. (2001). "Cellular zinc sensors: MTF-1 regulation of gene expression." *Biomaterials : an international journal on the role of metal ions in biology, biochemistry, and medicine* **14**(3-4): 223-237.
- Aranami, T. and T. Yamamura (2008). "Th17 Cells and autoimmune encephalomyelitis (EAE/MS)." *Allergol Int* **57**(2): 115-120.
- Auld, D. S. (2001). "Zinc coordination sphere in biochemical zinc sites." *Biomaterials : an international journal on the role of metal ions in biology, biochemistry, and medicine* **14**(3-4): 271-313.
- Babbe, H., A. Roers, et al. (2000). "Clonal expansions of CD8(+) T cells dominate the T cell infiltrate in active multiple sclerosis lesions as shown by micromanipulation and single cell polymerase chain reaction." *The Journal of experimental medicine* **192**(3): 393-404.
- Bach, F. and K. Hirschhorn (1964). "Lymphocyte Interaction: A Potential Histocompatibility Test in Vitro." *Science* **143**(3608): 813-814.
- Baecher-Allan, C., V. Viglietta, et al. (2002). "Inhibition of human CD4(+)CD25(+high) regulatory T cell function." *Journal of immunology* **169**(11): 6210-6217.
- Bain, B., M. R. Vas, et al. (1964). "The Development of Large Immature Mononuclear Cells in Mixed Leukocyte Cultures." *Blood* **23**: 108-116.
- Barrat, F. J., D. J. Cua, et al. (2002). "In vitro generation of interleukin 10-producing regulatory CD4(+) T cells is induced by immunosuppressive drugs and inhibited by T helper type 1 (Th1)- and Th2-inducing cytokines." *The Journal of experimental medicine* **195**(5): 603-616.
- Barth, R., S. Counce, et al. (1956). "Strong and weak histocompatibility gene differences in mice and their role in the rejection of homografts of tumors and skin." *Ann Surg* **144**(2): 198-204.
- Bartholomaeus, I., N. Kawakami, et al. (2009). "Effector T cell interactions with meningeal vascular structures in nascent autoimmune CNS lesions." *Nature* **462**(7269): 94-98.
- Barton, A. L., R. A. Fisher, et al. (2011). "Zinc poisoning from excessive denture fixative use masquerading as myelopolyneuropathy and hypocupraemia." *Annals of clinical biochemistry* **48**(Pt 4): 383-385.

- Beier, U. H., L. Wang, et al. (2011). "Sirtuin-1 targeting promotes Foxp3+ T-regulatory cell function and prolongs allograft survival." Molecular and cellular biology **31**(5): 1022-1029.
- Bennett, C. L., J. Christie, et al. (2001). "The immune dysregulation, polyendocrinopathy, enteropathy, X-linked syndrome (IPEX) is caused by mutations of FOXP3." Nature genetics **27**(1): 20-21.
- Beyersmann, D. and H. Haase (2001). "Functions of zinc in signaling, proliferation and differentiation of mammalian cells." Biometals : an international journal on the role of metal ions in biology, biochemistry, and medicine **14**(3-4): 331-341.
- Bobat, R., H. Coovadia, et al. (2005). "Safety and efficacy of zinc supplementation for children with HIV-1 infection in South Africa: a randomised double-blind placebo-controlled trial." Lancet **366**(9500): 1862-1867.
- Bousquet, J., P. Van Cauwenberge, et al. (2001). "Allergic rhinitis and its impact on asthma." The Journal of allergy and clinical immunology **108**(5 Suppl): S147-334.
- Brieger, A. and L. Rink (2010). "Zink und Immunfunktion." Ernährung Medizin **25**: 156-160.
- Burbach, G. J., L. M. Heinzerling, et al. (2009). "GA(2)LEN skin test study II: clinical relevance of inhalant allergen sensitizations in Europe." Allergy **64**(10): 1507-1515.
- Campo, C. A., N. Wellinghausen, et al. (2001). "Zinc inhibits the mixed lymphocyte culture." Biological trace element research **79**(1): 15-22.
- Chaudhry, A., D. Rudra, et al. (2009). "CD4+ regulatory T cells control TH17 responses in a Stat3-dependent manner." Science **326**(5955): 986-991.
- Chen, L., Y. Feng, et al. (2010). "Dual role of Zn²⁺ in maintaining structural integrity and suppressing deacetylase activity of SIRT1." Journal of inorganic biochemistry **104**(2): 180-185.
- Chesters, J. K. and L. Petrie (1999). "A possible role for cyclins in the zinc requirements during G1 and G2 phases of the cell cycle." The Journal of nutritional biochemistry **10**(5): 279-290.
- Chu, C. Q., S. Wittmer, et al. (2000). "Failure to suppress the expansion of the activated CD4 T cell population in interferon gamma-deficient mice leads to exacerbation of experimental autoimmune encephalomyelitis." The Journal of experimental medicine **192**(1): 123-128.
- Cohen, J. L., A. Trenado, et al. (2002). "CD4(+)CD25(+) immunoregulatory T Cells: new therapeutics for graft-versus-host disease." J Exp Med **196**(3): 401-406.
- Curotto de Lafaille, M. A., N. Kutchukhidze, et al. (2008). "Adaptive Foxp3+ regulatory T cell-dependent and -independent control of allergic inflammation." Immunity **29**(1): 114-126.
- D'Amato, G., L. Cecchi, et al. (2007). "Allergenic pollen and pollen allergy in Europe." Allergy **62**(9): 976-990.

- d'Hennezel, E. and C. A. Piccirillo (2012). "Functional plasticity in human FOXP3(+) regulatory T cells: implications for cell-based immunotherapy." Human vaccines & immunotherapeutics **8**(7): 1001-1005.
- Daaboul, D., E. Rosenkranz, et al. (2012). "Repletion of zinc in zinc-deficient cells strongly up-regulates IL-1beta-induced IL-2 production in T-cells." Metallomics : integrated biometal science **4**(10): 1088-1097.
- Danzer, S. G., C. aCampo, et al. (1996). "Interferon-gamma plays a key role in the human mixed lymphocyte culture." Bone Marrow Transplant **18**(5): 991-996.
- Danzer, S. G., H. Kirchner, et al. (1994). "Cytokine interactions in human mixed lymphocyte culture." Transplantation **57**(11): 1638-1642.
- Dejaco, C., C. Duftner, et al. (2006). "Imbalance of regulatory T cells in human autoimmune diseases." Immunology **117**(3): 289-300.
- Dhodapkar, M. V., R. M. Steinman, et al. (2001). "Antigen-specific inhibition of effector T cell function in humans after injection of immature dendritic cells." The Journal of experimental medicine **193**(2): 233-238.
- Di Toro, R., G. Galdo Capotorti, et al. (1987). "Zinc and copper status of allergic children." Acta paediatrica Scandinavica **76**(4): 612-617.
- Dunn, D. L. (1990). "Problems related to immunosuppression. Infection and malignancy occurring after solid organ transplantation." Critical care clinics **6**(4): 955-977.
- Faber, C. (2004). Die Gemischte Lymphozytenkultur (MLC) als Testmodell für Immunsuppressiva und Histokompatibilitätstestung, Dissertation, Med. Fakultät, RWTH Aachen.
- Faber, C., P. Gabriel, et al. (2004). "Zinc in pharmacological doses suppresses allogeneic reaction without affecting the antigenic response." Bone marrow transplantation **33**(12): 1241-1246.
- Fagiolo, U., A. Cossarizza, et al. (1993). "Increased cytokine production in mononuclear cells of healthy elderly people." European journal of immunology **23**(9): 2375-2378.
- Fontenot, J. D., M. A. Gavin, et al. (2003). "Foxp3 programs the development and function of CD4+CD25+ regulatory T cells." Nature immunology **4**(4): 330-336.
- Fontenot, J. D., J. P. Rasmussen, et al. (2005). "Regulatory T cell lineage specification by the forkhead transcription factor foxp3." Immunity **22**(3): 329-341.
- Fosmire, G. J. (1990). "Zinc toxicity." The American journal of clinical nutrition **51**(2): 225-227.
- Fowler, D. H. and R. E. Gress (2000). "Th2 and Tc2 cells in the regulation of GVHD, GVL, and graft rejection: considerations for the allogeneic transplantation therapy of leukemia and lymphoma." Leukemia & lymphoma **38**(3-4): 221-234.

- Friedrich, D. (2008). Multiple Sklerose. Stuttgart, Trias Verlag.
- Frye, R. A. (1999). "Characterization of five human cDNAs with homology to the yeast SIR2 gene: Sir2-like proteins (sirtuins) metabolize NAD and may have protein ADP-ribosyltransferase activity." Biochemical and biophysical research communications **260**(1): 273-279.
- Gao, B., Q. Kong, et al. (2012). "Analysis of sirtuin 1 expression reveals a molecular explanation of IL-2-mediated reversal of T-cell tolerance." Proceedings of the National Academy of Sciences of the United States of America **109**(3): 899-904.
- Gross, U., A. K. Schroder, et al. (2006). "The superantigen staphylococcal enterotoxin A (SEA) and monoclonal antibody L243 share a common epitope but differ in their ability to induce apoptosis via MHC-II." Immunobiology **211**(10): 807-814.
- Group., S. C. T. C. (2005). "Allogeneic peripheral blood stem-cell compared with bone marrow transplantation in the management of hematologic malignancies: an individual patient data meta-analysis of nine randomized trials." J Clin Oncol **23**(22): 5074-5087.
- Grynkiewicz, G., M. Poenie, et al. (1985). "A new generation of Ca²⁺ indicators with greatly improved fluorescence properties." The Journal of biological chemistry **260**(6): 3440-3450.
- Haase, H., J. L. Ober-Blobaum, et al. (2008). "Zinc signals are essential for lipopolysaccharide-induced signal transduction in monocytes." Journal of immunology **181**(9): 6491-6502.
- Haase, H. and L. Rink (2009). "The immune system and the impact of zinc during aging." Immunity & ageing : I & A **6**: 9.
- Haase, H. and L. Rink (2010). "Das essentielle Spurenelement Zink." Biol. unserer Zeit **40**: 314-321.
- Haigis, M. C. and L. P. Guarente (2006). "Mammalian sirtuins--emerging roles in physiology, aging, and calorie restriction." Genes & development **20**(21): 2913-2921.
- Hamaguchi, M. and S. Sakaguchi (2012). "Regulatory T cells expressing PPAR-gamma control inflammation in obesity." Cell metabolism **16**(1): 4-6.
- Haribhai, D., J. B. Williams, et al. (2011). "A requisite role for induced regulatory T cells in tolerance based on expanding antigen receptor diversity." Immunity **35**(1): 109-122.
- Hoffmann, P., R. Eder, et al. (2004). "Large-scale in vitro expansion of polyclonal human CD4(+)CD25high regulatory T cells." Blood **104**(3): 895-903.
- Hofstetter, H., R. Gold, et al. (2009). "Th17 Cells in MS and Experimental Autoimmune Encephalomyelitis." International MS journal / MS Forum **16**(1): 12-18.
- Honscheid, A., L. Rink, et al. (2009). "T-lymphocytes: a target for stimulatory and inhibitory effects of zinc ions." Endocrine, metabolic & immune disorders drug targets **9**(2): 132-144.

- Hontecillas, R., W. T. Horne, et al. (2011). "Immunoregulatory mechanisms of macrophage PPAR-gamma in mice with experimental inflammatory bowel disease." Mucosal immunology **4**(3): 304-313.
- Hori, S., T. Nomura, et al. (2003). "Control of regulatory T cell development by the transcription factor Foxp3." Science **299**(5609): 1057-1061.
- Hou, J., Z. Z. Chong, et al. (2010). "Early apoptotic vascular signaling is determined by Sirt1 through nuclear shuttling, forkhead trafficking, bad, and mitochondrial caspase activation." Current neurovascular research **7**(2): 95-112.
- Hu, H., I. Djuretic, et al. (2007). "Transcriptional partners in regulatory T cells: Foxp3, Runx and NFAT." Trends in immunology **28**(8): 329-332.
- Imada, M., F. E. Simons, et al. (1995). "Allergen-stimulated interleukin-4 and interferon-gamma production in primary culture: responses of subjects with allergic rhinitis and normal controls." Immunology **85**(3): 373-380.
- Jacobsohn, D. A. and G. B. Vogelsang (2007). "Acute graft versus host disease." Orphanet journal of rare diseases **2**: 35.
- Janeway, C. A., Jr.; Murphy, Kenneth; Travers, Paul; Walport, Mark (2008). Janeway's immunobiology. New York, Garland Science, Taylor&Francis Group, LLC.
- Kahmann, L., P. Uciechowski, et al. (2008). "Zinc supplementation in the elderly reduces spontaneous inflammatory cytokine release and restores T cell functions." Rejuvenation research **11**(1): 227-237.
- Kaltenberg, J., L. M. Plum, et al. (2010). "Zinc signals promote IL-2-dependent proliferation of T cells." European journal of immunology **40**(5): 1496-1503.
- Katelaris, C. H. and L. Bielory (2008). "Evidence-based study design in ocular allergy trials." Curr Opin Allergy Clin Immunol **8**(5): 484-488.
- King, L. E., J. W. Frentzel, et al. (2005). "Chronic zinc deficiency in mice disrupted T cell lymphopoiesis and erythropoiesis while B cell lymphopoiesis and myelopoiesis were maintained." Journal of the American College of Nutrition **24**(6): 494-502.
- Kitabayashi, C., T. Fukada, et al. (2010). "Zinc suppresses Th17 development via inhibition of STAT3 activation." International immunology **22**(5): 375-386.
- Kong, X. X., R. Wang, et al. (2009). "Function of SIRT1 in physiology." Biochemistry. Biokhimiia **74**(7): 703-708.
- Kown, M. H., T. Van der Steenhoven, et al. (2000). "Zinc-mediated reduction of apoptosis in cardiac allografts." Circulation **102**(19 Suppl 3): III228-232.
- Kown, M. H., T. J. van der Steenhoven, et al. (2002). "Zinc chloride-mediated reduction of apoptosis as an adjunct immunosuppressive modality in cardiac transplantation." The Journal

of heart and lung transplantation : the official publication of the International Society for Heart Transplantation **21**(3): 360-365.

- Kozako, T., A. Aikawa, et al. (2012). "High expression of the longevity gene product SIRT1 and apoptosis induction by sirtinol in adult T-cell leukemia cells." International journal of cancer. Journal international du cancer **131**(9): 2044-2055.
- Kruisbeek, A. M., E. Shevach, et al. (2004). "Proliferative assays for T cell function." Current protocols in immunology / edited by John E. Coligan ... [et al.] **Chapter 3**: Unit 3 12.
- Kwon, H. S., H. W. Lim, et al. (2012). "Three novel acetylation sites in the Foxp3 transcription factor regulate the suppressive activity of regulatory T cells." Journal of immunology **188**(6): 2712-2721.
- Lal, G., N. Zhang, et al. (2009). "Epigenetic regulation of Foxp3 expression in regulatory T cells by DNA methylation." Journal of immunology **182**(1): 259-273.
- Landry, J., J. T. Slama, et al. (2000). "Role of NAD(+) in the deacetylase activity of the SIR2-like proteins." Biochemical and biophysical research communications **278**(3): 685-690.
- Lavu, S., O. Boss, et al. (2008). "Sirtuins--novel therapeutic targets to treat age-associated diseases." Nature reviews. Drug discovery **7**(10): 841-853.
- Lichten, L. A. and R. J. Cousins (2009). "Mammalian zinc transporters: nutritional and physiologic regulation." Annual review of nutrition **29**: 153-176.
- Lim, H. W., P. Hillsamer, et al. (2005). "Cutting edge: direct suppression of B cells by CD4+ CD25+ regulatory T cells." Journal of immunology **175**(7): 4180-4183.
- Ling, E. M., T. Smith, et al. (2004). "Relation of CD4+CD25+ regulatory T-cell suppression of allergen-driven T-cell activation to atopic status and expression of allergic disease." Lancet **363**(9409): 608-615.
- Litman, G. W., J. P. Cannon, et al. (2005). "Reconstructing immune phylogeny: new perspectives." Nature reviews. Immunology **5**(11): 866-879.
- Liu, Y., I. Teige, et al. (2006). "Neuron-mediated generation of regulatory T cells from encephalitogenic T cells suppresses EAE." Nature medicine **12**(5): 518-525.
- Liuzzi, J. P., J. A. Bobo, et al. (2004). "Responsive transporter genes within the murine intestinal-pancreatic axis form a basis of zinc homeostasis." Proceedings of the National Academy of Sciences of the United States of America **101**(40): 14355-14360.
- Livak, K. J. and T. D. Schmittgen (2001). "Analysis of relative gene expression data using real-time quantitative PCR and the 2⁻(Delta Delta C(T)) Method." Methods **25**(4): 402-408.
- Lonnerdal, B. (2000). "Dietary factors influencing zinc absorption." The Journal of nutrition **130**(5S Suppl): 1378S-1383S.

- MacDonald, R. S. (2000). "The role of zinc in growth and cell proliferation." The Journal of nutrition **130**(5S Suppl): 1500S-1508S.
- Maclaurin, B. P. (1965). "Homograft interaction in the test-tube." Lancet **2**(7417): 816-821.
- Mantel, P. Y., N. Ouaked, et al. (2006). "Molecular mechanisms underlying FOXP3 induction in human T cells." Journal of immunology **176**(6): 3593-3602.
- Maret, W. (2006). "Zinc coordination environments in proteins as redox sensors and signal transducers." Antioxidants & redox signaling **8**(9-10): 1419-1441.
- Maret, W. and H. H. Sandstead (2006). "Zinc requirements and the risks and benefits of zinc supplementation." Journal of trace elements in medicine and biology : organ of the Society for Minerals and Trace Elements **20**(1): 3-18.
- Marson, A., K. Kretschmer, et al. (2007). "Foxp3 occupancy and regulation of key target genes during T-cell stimulation." Nature **445**(7130): 931-935.
- Martin, P. and F. Sanchez-Madrid (2011). "CD69: an unexpected regulator of TH17 cell-driven inflammatory responses." Science signaling **4**(165): pe14.
- Maynard, C. L., L. E. Harrington, et al. (2007). "Regulatory T cells expressing interleukin 10 develop from Foxp3+ and Foxp3- precursor cells in the absence of interleukin 10." Nature immunology **8**(9): 931-941.
- McGeachy, M. J., L. A. Stephens, et al. (2005). "Natural recovery and protection from autoimmune encephalomyelitis: contribution of CD4+CD25+ regulatory cells within the central nervous system." Journal of immunology **175**(5): 3025-3032.
- Mellor, A. L., P. Chandler, et al. (2004). "Specific subsets of murine dendritic cells acquire potent T cell regulatory functions following CTLA4-mediated induction of indoleamine 2,3 dioxygenase." International immunology **16**(10): 1391-1401.
- Mempel, T. R., M. J. Pittet, et al. (2006). "Regulatory T cells reversibly suppress cytotoxic T cell function independent of effector differentiation." Immunity **25**(1): 129-141.
- Michan, S. and D. Sinclair (2007). "Sirtuins in mammals: insights into their biological function." The Biochemical journal **404**(1): 1-13.
- Mills, C. F. (1989). Physiology of Zinc: General Aspects. London, Springer Verlag.
- Miroux, C., O. Morales, et al. (2009). "Inhibitory effects of cyclosporine on human regulatory T cells in vitro." Transplantation proceedings **41**(8): 3371-3374.
- Miura, Y., C. J. Thoburn, et al. (2004). "Association of Foxp3 regulatory gene expression with graft-versus-host disease." Blood **104**(7): 2187-2193.
- Nelson, B. H. (2004). "IL-2, regulatory T cells, and tolerance." Journal of immunology **172**(7): 3983-3988.

- Neto, A. B., W. DeFaria, et al. (2000). "Mixed allogeneic chimerism by combined use of nonlethal radiation and antilymphocyte serum in a rat small bowel transplantation model." Transplantation proceedings **32**(6): 1311-1312.
- Nouri-Aria, K. T. (2009). "Foxp3 expressing regulatory T-cells in allergic disease." Advances in experimental medicine and biology **665**: 180-194.
- Okamoto, T., T. Kuroki, et al. (2011). "Effect of zinc on early graft failure following intraportal islet transplantation in rat recipients." Annals of transplantation : quarterly of the Polish Transplantation Society **16**(3): 114-120.
- Parkin, J. and B. Cohen (2001). "An overview of the immune system." Lancet **357**(9270): 1777-1789.
- Pawankar, R., S. Mori, et al. (2011). "Overview on the pathomechanisms of allergic rhinitis." Asia Pac Allergy **1**(3): 157-167.
- Picard, F., M. Kurtev, et al. (2004). "Sirt1 promotes fat mobilization in white adipocytes by repressing PPAR-gamma." Nature **429**(6993): 771-776.
- Pidala, J. (2011). "Graft-vs-host disease following allogeneic hematopoietic cell transplantation." Cancer control : journal of the Moffitt Cancer Center **18**(4): 268-276.
- Pilat, N., U. Baranyi, et al. (2010). "Treg-therapy allows mixed chimerism and transplantation tolerance without cytoreductive conditioning." American journal of transplantation : official journal of the American Society of Transplantation and the American Society of Transplant Surgeons **10**(4): 751-762.
- Plum, L. M., A. Brieger, et al. (submitted). "Zinc signals regulate IL-2-mediated Akt activation by inhibiting PTEN " Science signaling.
- Polansky, J. K., K. Kretschmer, et al. (2008). "DNA methylation controls Foxp3 gene expression." European journal of immunology **38**(6): 1654-1663.
- Prasad, A. S. (2000). "Effects of zinc deficiency on Th1 and Th2 cytokine shifts." The Journal of infectious diseases **182** Suppl 1: S62-68.
- Prasad, A. S. (2002). "Zinc deficiency in patients with sickle cell disease." The American journal of clinical nutrition **75**(2): 181-182.
- Prasad, A. S. (2008). "Clinical, immunological, anti-inflammatory and antioxidant roles of zinc." Experimental gerontology **43**(5): 370-377.
- Prasad, A. S. (2008). "Zinc in human health: effect of zinc on immune cells." Molecular medicine **14**(5-6): 353-357.
- Prasad, A. S. (2009). "Impact of the discovery of human zinc deficiency on health." Journal of the American College of Nutrition **28**(3): 257-265.

- Provoost, S., T. Maes, et al. (2009). "Decreased FOXP3 protein expression in patients with asthma." Allergy **64**(10): 1539-1546.
- Qureshi, O. S., Y. Zheng, et al. (2011). "Trans-endocytosis of CD80 and CD86: a molecular basis for the cell-extrinsic function of CTLA-4." Science **332**(6029): 600-603.
- Ramsdell, F. and B. J. Fowlkes (1990). "Clonal deletion versus clonal anergy: the role of the thymus in inducing self tolerance." Science **248**(4961): 1342-1348.
- Revollo, J. R., A. A. Grimm, et al. (2004). "The NAD biosynthesis pathway mediated by nicotinamide phosphoribosyltransferase regulates Sir2 activity in mammalian cells." The Journal of biological chemistry **279**(49): 50754-50763.
- Richter, M., R. Bonneau, et al. (2003). "Zinc status modulates bronchopulmonary eosinophil infiltration in a murine model of allergic inflammation." Chest **123**(3 Suppl): 446S.
- Rink, L. (2011). Zinc in Human Health. Amsterdam, IOS Press BV.
- Rink, L. and P. Gabriel (2000). "Zinc and the immune system." The Proceedings of the Nutrition Society **59**(4): 541-552.
- Robinson, D. S. (2004). "Regulation: the art of control? Regulatory T cells and asthma and allergy." Thorax **59**(8): 640-643.
- Rosati, G. (2001). "The prevalence of multiple sclerosis in the world: an update." Neurological sciences : official journal of the Italian Neurological Society and of the Italian Society of Clinical Neurophysiology **22**(2): 117-139.
- Rouse, M., M. Nagarkatti, et al. (2012). "The role of IL-2 in the activation and expansion of regulatory T-cells and the development of experimental autoimmune encephalomyelitis." Immunobiology.
- Sakaguchi, S. (2005). "Naturally arising Foxp3-expressing CD25+CD4+ regulatory T cells in immunological tolerance to self and non-self." Nature immunology **6**(4): 345-352.
- Sakaguchi, S., N. Sakaguchi, et al. (1995). "Immunologic self-tolerance maintained by activated T cells expressing IL-2 receptor alpha-chains (CD25). Breakdown of a single mechanism of self-tolerance causes various autoimmune diseases." Journal of immunology **155**(3): 1151-1164.
- Salminen, A., A. Kauppinen, et al. (2008). "SIRT1 longevity factor suppresses NF-kappaB - driven immune responses: regulation of aging via NF-kappaB acetylation?" BioEssays : news and reviews in molecular, cellular and developmental biology **30**(10): 939-942.
- Segall, M. and F. H. Bach (1976). "Pooled stimulating cells as a "standard stimulator" in mixed lymphocyte culture." Transplantation **22**(2): 79-85.
- Sellner, J., J. Kraus, et al. (2011). "The increasing incidence and prevalence of female multiple sclerosis--a critical analysis of potential environmental factors." Autoimmunity reviews **10**(8): 495-502.

- Slatkin, M. (2009). "Epigenetic inheritance and the missing heritability problem." Genetics **182**(3): 845-850.
- Stoye, D., C. Schubert, et al. (2012). "Zinc aspartate suppresses T cell activation in vitro and relapsing experimental autoimmune encephalomyelitis in SJL/J mice." Biomaterials : an international journal on the role of metal ions in biology, biochemistry, and medicine **25**(3): 529-539.
- Sutherland, D. E. and M. J. Stillman (2011). "The "magic numbers" of metallothionein." Metallomics : integrated biometal science **3**(5): 444-463.
- Takahashi, T., T. Tagami, et al. (2000). "Immunologic self-tolerance maintained by CD25(+)CD4(+) regulatory T cells constitutively expressing cytotoxic T lymphocyte-associated antigen 4." The Journal of experimental medicine **192**(2): 303-310.
- Testi, R., J. H. Phillips, et al. (1989). "T cell activation via Leu-23 (CD69)." Journal of immunology **143**(4): 1123-1128.
- Thorsby, E. and B. A. Lie (2005). "HLA associated genetic predisposition to autoimmune diseases: Genes involved and possible mechanisms." Transplant immunology **14**(3-4): 175-182.
- Tinckam, K. J. and A. Chandraker (2006). "Mechanisms and role of HLA and non-HLA alloantibodies." Clin J Am Soc Nephrol **1**(3): 404-414.
- Tsuda, M., R. W. Kozak, et al. (1987). "Contribution of a p75 interleukin 2 binding peptide to a high-affinity interleukin 2 receptor complex." Proceedings of the National Academy of Sciences of the United States of America **84**(12): 4215-4218.
- Vallee, B. L. and K. H. Falchuk (1993). "The biochemical basis of zinc physiology." Physiological reviews **73**(1): 79-118.
- van den Boogaardt, D. E., P. P. van Miert, et al. (2006). "The ratio of interferon-gamma and interleukin-10 producing donor-specific cells as an in vitro monitoring tool for renal transplant patients." Transplantation **82**(6): 844-848.
- van der Meer, A., W. M. Wissink, et al. (1999). "Interferon-gamma-based mixed lymphocyte culture as a selection tool for allogeneic bone marrow donors other than identical siblings." British journal of haematology **105**(2): 340-348.
- van Loosdregt, J., D. Brunen, et al. (2011). "Rapid temporal control of Foxp3 protein degradation by sirtuin-1." PloS one **6**(4): e19047.
- van Loosdregt, J., Y. Vercoulen, et al. (2010). "Regulation of Treg functionality by acetylation-mediated Foxp3 protein stabilization." Blood **115**(5): 965-974.
- Venken, K., N. Hellings, et al. (2008). "Compromised CD4+ CD25(high) regulatory T-cell function in patients with relapsing-remitting multiple sclerosis is correlated with a reduced frequency of FOXP3-positive cells and reduced FOXP3 expression at the single-cell level." Immunology **123**(1): 79-89.

- Walker, M. R., D. J. Kasproicz, et al. (2003). "Induction of FoxP3 and acquisition of T regulatory activity by stimulated human CD4+CD25- T cells." The Journal of clinical investigation **112**(9): 1437-1443.
- Wang, C. J., E. M. Schmidt, et al. (2011). "Immune regulation by CTLA-4--relevance to autoimmune diabetes in a transgenic mouse model." Diabetes/metabolism research and reviews **27**(8): 946-950.
- Waterhouse, P., J. M. Penninger, et al. (1995). "Lymphoproliferative disorders with early lethality in mice deficient in Ctl4-4." Science **270**(5238): 985-988.
- Wellinghausen, N., M. Martin, et al. (1997). "Zinc inhibits interleukin-1-dependent T cell stimulation." European journal of immunology **27**(10): 2529-2535.
- Wessels, I., H. Haase, et al. (2013). "Zinc deficiency induces production of the proinflammatory cytokines IL-1beta and TNFalpha in promyeloid cells via epigenetic and redox-dependent mechanisms." The Journal of nutritional biochemistry **24**(1): 289-297.
- Wohlfert, E. A., F. C. Nichols, et al. (2007). "Peroxisome proliferator-activated receptor gamma (PPARgamma) and immunoregulation: enhancement of regulatory T cells through PPARgamma-dependent and -independent mechanisms." Journal of immunology **178**(7): 4129-4135.
- Wu, F. Y. and C. W. Wu (1987). "Zinc in DNA replication and transcription." Annual review of nutrition **7**: 251-272.
- Yeh, S. P., Y. M. Liao, et al. (2012). "Kinetics of T helper subsets and associated cytokines correlate well with the clinical activity of graft-versus-host disease." PloS one **7**(9): e44416.
- Yoshizaki, T., S. Schenk, et al. (2010). "SIRT1 inhibits inflammatory pathways in macrophages and modulates insulin sensitivity." American journal of physiology. Endocrinology and metabolism **298**(3): E419-428.
- Yu, M., W. W. Lee, et al. (2011). "Regulation of T cell receptor signaling by activation-induced zinc influx." The Journal of experimental medicine **208**(4): 775-785.
- Zhang, G. X., S. Yu, et al. (2004). "T cell and antibody responses in remitting-relapsing experimental autoimmune encephalomyelitis in (C57BL/6 x SJL) F1 mice." J Neuroimmunol **148**(1-2): 1-10.
- Zhang, G. X., S. Yu, et al. (2004). "T cell and antibody responses in remitting-relapsing experimental autoimmune encephalomyelitis in (C57BL/6 x SJL) F1 mice." Journal of neuroimmunology **148**(1-2): 1-10.
- Zhang, J., S. M. Lee, et al. (2009). "The type III histone deacetylase Sirt1 is essential for maintenance of T cell tolerance in mice." The Journal of clinical investigation **119**(10): 3048-3058.

- Zhang, R., H. Z. Chen, et al. (2010). "SIRT1 suppresses activator protein-1 transcriptional activity and cyclooxygenase-2 expression in macrophages." The Journal of biological chemistry **285**(10): 7097-7110.
- Zheng, S. G., J. Wang, et al. (2007). "IL-2 is essential for TGF-beta to convert naive CD4+CD25-cells to CD25+Foxp3+ regulatory T cells and for expansion of these cells." Journal of immunology **178**(4): 2018-2027.
- Zheng, Y., S. Josefowicz, et al. (2010). "Role of conserved non-coding DNA elements in the Foxp3 gene in regulatory T-cell fate." Nature **463**(7282): 808-812.
- Zozulya, A. L. and H. Wiendl (2008). "The role of regulatory T cells in multiple sclerosis." Nature clinical practice. Neurology **4**(7): 384-398.
- Zuberbier, T., C. Bachert, et al. (2010). "GA(2) LEN/EAACI pocket guide for allergen-specific immunotherapy for allergic rhinitis and asthma." Allergy **65**(12): 1525-1530.

VIII. List of Abbreviations

AAS	atomic absorption spectrophotometry
APC	antigen presenting cell
APS	ammonium persulfate
ATM	adult T cell leukemia-lymphoma
BSA	bovine derum albumin
CFA	complete freuds adjuvant
CNS	central nervous system
CPM	counts per minute
CsA	cyclosporine A
CTL	cytotoxic T cell
CTLA-4	cytotoxic T lymphocyte antigen 4
DSMZ	deutsche Sammlung fuer Microorganismen und Zellkulturen
ELISA	enzyme-linked immunosorbent assay
FACS	fluorescence activated cell sorting
FCS	fetal calf serum
FSC	forward side scatter
GITR	glucocorticoid-induced tumor necrosis factor receptor family related gene
GVHD	graft-versus-host disease
HAT	histone-acetyltransferase
HCT	hematopoietic stem cell transplantation
HDAC	histone deacetylase
HLA	human leukocyte antigen
HRP	horseradish peroxidas
IBD	inflammatory bowel disease
IDDM	insulin-dependent diabetes mellitus
IDO	indoleamine 2,3 dioxygenase
IFN	interferon
IHC	immunohistochemistry
IL	interleukine
IPEX	Immunodysregulation, Polyendocrinopathy, and Enteropathy, X-linked
iTregs	induced regulatory T cells
MDRE	methylation-dependent restriction enzymes
MFI	mean fluorescence intensity
MHC	major histocompatibility complex
MLC	mixed lymphocyte culture
MOG	myelin oligodendrocyte glycoprotein
MS	multiple sclerosis
MSRE	methylation-sensitive restriction enzyme
MT	metallothionein
MTF	metal-responsive transcription factor
NAD ⁺	nicotinamide adenine dinucleotide
NK	natural killer cells
nTregs	natural regulatory T cells
O-AADPr	2'-O-acetyl-ADP-ribose
PAMP	pathogen-associated molecular pattern
PBGD	porphobilinogen deaminase
PBMC	peripheral blood mononuclear cells
PCR	polymerase chain reaction
PI	propidium iodide
PMSF	phenylmethylsulfonylfluorid
PPAR- γ	peroxisome proliferator activated receptor γ

PTEN	phosphatase and tensin homolog
PRR	pattern recognition receptor
RDA	recommended daily allowance
ROR γ t	RAR-related orphan receptor gamma
ROS	reactive oxygen species
RmT	room temperature
SCT	stem cell transplantation
SDS-PAGE	sodium dodecyl sulfate polyacrylamide gel electrophoresis
SEA	Staphylococcus-Enterotoxine A
Sirt	Sirtuin 1
SLE	systemic lupus erythematoses
SSC	side scatter
TCR	T cell receptor
Teffs	effector T cells
TEMED	N,N,N',N'-tetramethylethylenediamine
TGF	transforming growth factor
Th	T helper cell
TMB	3,3',5,5'-tetramethylbenzidine
Tregs	regulatory T cells
TSDR	Treg-specific demethylated region
TSST	toxic shock syndrome toxin
WHO	World Health organisation
Zip	Zrt- and Irt-like proteins
ZnT	zinc transporter

Danksagung

Mein besonderer Dank gilt Herrn Prof. Dr. Lothar Rink für die Möglichkeit, an seinem Institut zu promovieren. Seine ausgezeichnete Betreuung, so wie die vielen Hilfestellungen bei der Planung meiner beruflichen Zukunft, weiß ich sehr zu schätzen.

Herrn Prof. Dr. Jürgen Bernhagen danke ich für die Übernahme des Zweitgutachtens.

Allen Mitarbeiterinnen und Mitarbeitern des Instituts für Immunologie danke ich für die Kollegialität und ständige Hilfsbereitschaft, die zu einer tollen Arbeitsatmosphäre beigetragen haben. Ich bedanke mich bei allen für Anleitungen, Hilfestellungen und aufmunternde Worte.

Dr. Tim Clarner und meiner Kollegin Anne Brieger möchte ich für die gute Zusammenarbeit im EAE-Projekt danken.

Besonderer Dank gilt auch Laura Hausmann und Emma Tassie für ihren Einsatz als Korrekturleser.

Außerdem danke ich meinen Eltern, die mir eine sorgenfreie Doktorarbeitszeit ermöglicht haben. Ihnen und meinen Geschwistern danke ich für die ständige Unterstützung.

Curriculum Vitae

Personal data

Surname	Eva
Forename	Rosenkranz
Date of birth	07/05/1983
City of birth	Düren/ Birkesdorf
Nationality	German

School Education

1989 – 1991	Primary School, Düren-Birkesdorf, Germany
1991 – 1993	Primary School, Merzenich–Golzheim, Germany
1993 – 2002	Secondary School, Städtisches Gymnasium am Wirteltor, Düren, Germany Final degree: Abitur

Studies and Professional Experience

2002 – 2008	Studies of Biology in Aachen, Germany Majors: Molecular Biology; Cellbiology Minors: Immunology, Pharmacology, Plantphysiology Final Degree: Diplom (Dipl.-Biol.)
01/2007– 05/ 2008	Student research assistant, Institute of Immunology, RWTH Aachen, Germany
07/2008– 04/2013	Promotion at the Institute of Immunology, RWTH Aachen, Germany
Since 08/2012	Postdoc Position at the Rowett Institute of Nutrition and Health, Aberdeen, Scotland, GB

Publications:

Articles:

Gruber, K., **Rosenkranz, E.**, Plümäkers, B. and Rink, L. Zinc Deficiency Adversely Influences Interleukin-4 and Interleukin-6 Signaling. (currently submitted at *Journal of Biological Regulators and Homeostatic Agents*)

Wessels, I., **Rosenkranz, E.**, Ventura Ferreira, M., Neuss, S., Zenke, M., Rink, L. and Uciechowski, P. (2012) Activation of IL-1beta and TNFalpha genes is mediated by the establishment of permissive chromatin structures during monopoiesis.(currently published online in *Immunobiology*)

Daaboul, D., **Rosenkranz, E.**, Uciechowski, P. and Rink, L. (2012) Repletion of zinc in zinc-deficient cells strongly up-regulates IL-1beta-induced IL-2 production in T-cells. *Metallomics : integrated biometal science* **4**(10): 1088-1097.

Jansen, J., **Rosenkranz, E.**, Overbeck, S., Warmuth, S., Mocchegiani, E., Giacconi, R., Weiskirchen, R., Karges, W., Rink, L. (2012) Disturbed zinc homeostasis in diabetic patients by in vitro and in vivo analysis of insulinomimetic activity of zinc. *The Journal of nutritional biochemistry* **23**(11): 1458-1466.

Book Chapter:

Eva Rosenkranz, Ananda Prasad and Lothar Rink (2011) "Immunobiology and Hematology of Zinc". In: "Zinc in Human Health" 1st Edition, Amsterdam, IOS Press BV

Zusammenfassung

Die Bedeutung des Spurenelements Zink für das Immunsystem wurde in den letzten Jahren intensiv untersucht. Neben der Wichtigkeit von Zink für eine funktionierende Immunaktivität wurde außerdem die Wirkung von Zinksupplementierung auf Immunreaktionen getestet. Dabei wurde gezeigt, dass Zink in der Lage ist, die allogene Immunreaktion zu mildern. Aufbauend auf diesem Ergebnis wurde im Rahmen der vorliegenden Doktorarbeit die beschriebene Immunmodulation durch Zink genauer erforscht und seine Wirkung auf weitere ungewollte Immunreaktionen untersucht.

Es konnte bestätigt werden, dass Zink die allogene Immunreaktion vermindert. Des Weiteren wurde der verantwortliche Mechanismus für diesen immunmodulierenden Zink-Effekt erschlossen. Dabei wurde festgestellt, dass Zink in der Lage ist den Anteil der regulatorischen T Zellen in der allogenen Immunreaktion zu erhöhen. Da regulatorische T Zellen eine immunsupprimierende Wirkung ausüben, kann die Supplementierung mit Zink zu einer Hemmung der aktivierten T Zellen führen und insgesamt die allogene Immunaktivität herunterregulieren. Als mögliche Ursache für diesen Effekt wurde auf molekularer Ebene die Inhibierung der Histondeacetylase Sirt-1 durch Zink beobachtet. Eine reduzierte Aktivität dieses Enzyms führt in aktivierten T Zellen zu einer erhöhten Foxp3 Stabilität, da der Abbau dieses Moleküls verhindert wird. Da Zink die Aktivität der Sirt-1 hemmt, liegt Foxp3 vermehrt in acetylierter Form vor und erhöht auf diese Weise die Stabilität dieses Transkriptionsfaktors. Ein Anstieg an regulatorischen T Zellen durch Zink während der allogenen Immunantwort ist das Ergebnis.

Bei der allogenen Immunantwort handelt es sich um eine Th1-gesteuerte Immunantwort. Zink war außerdem in der Lage die Th2-spezifische allergische Immunreaktion zu modulieren. Dieses wurde in Immunzellen von Individuen mit Heuschnupfen gezeigt, die *in vitro* mit dem Lieschgrasallergen stimuliert wurden. Auch in diesem System war ein Anstieg an regulatorischen T Zellen zu verzeichnen. Des Weiteren wurde die Wirkung von Zink auf die Th17-dominierte Autoimmunreaktion in einem *in vivo* Tiermodell untersucht. Die Tiere, die täglich mit Zink behandelt wurden zeigten einen deutlich abgemilderten Verlauf der Autoimmunreaktion im Vergleich zu den Kontrolltieren. Auch in diesem Fall war das Ergebnis auf einen erhöhten Anteil an induzierten regulatorischen T Zellen zu beobachten. Diese Ergebnisse bestätigen die Idee, dass Zink unerwünschte Immunantworten ummodulieren kann, indem es regulatorische T Zellen heraufreguliert. Aufgrund seiner fehlenden Toxizität, geringen Nebenwirkungen und den niedrigen Kosten ist die klinische Anwendung von Zink in der Transplantationsmedizin und in der Behandlung von Allergien und Autoimmunkrankheiten daher von großem Interesse.